Article:

Wolfe, S., Murton, J., Bateman, M. orcid.org/0000-0003-1756-6046 et al. (1 more author) (2020) Oriented-lake development in the context of late Quaternary landscape evolution, McKinley Bay Coastal Plain, western Arctic Canada. Quaternary Science Reviews, 242. 106414. ISSN 0277-3791

https://doi.org/10.1016/j.quascirev.2020.106414

Oriented-lake development in the context of late Quaternary landscape evolution, McKinley Bay Coastal Plain, western Arctic Canada

Stephen Wolfe [a] (corresponding author) stephen.wolfe@canada.ca
Julian Murton [b] j.b.murton@sussex.ac.uk
Mark Bateman [c] m.d.bateman@sheffield.ac.uk
and John Barlow [b] john.barlow@sussex.ac.uk
[a] Geological Survey of Canada, Natural Resources Canada, Ottawa, ON, K1A 0E8, CA
[b] Department of Geography, University of Sussex, Brighton, BN1 9RH, UK
[c] Department of Geography, University of Sheffield, Sheffield, S1O 2TN, UK

Declarations of interest: none

Abstract

Oriented lakes—characterized by elongate forms, central basins and shallow littoral shelves—are common features of circum-arctic coastal lowlands. The environmental conditions, geological processes and chronology associated with the development of oriented lakes, however, are little known but essential for understanding how such arctic lowlands evolve. Using combined techniques of field and drill-log stratigraphy and sedimentology, luminescence and radiocarbon dating methods and geomorphic mapping, we reconstruct the landscape evolution leading toward oriented-lake formation on the McKinley Bay Coastal Plain of western Arctic, Canada—a region with over 900 oriented lakes. Most lakes with deep central basins are inherited from a preglacial braidplain (ca. 73–27 ka) and alluvial braided-channel network that extended beyond the glacial limit (ca. 18.6–14.3 ka). Eolian erosion, active during the lateglacial and postglacial period (ca. 12.8–1.9 ka), reworked fluvial deposits.

Eolian processes modified existing basins and created other shallow deflationary basins, as small barchanoid dunes migrated under cold, dry paraglacial conditions between about 12.8 and 10.7 ka. Vegetation cover developed at the onset of the early Holocene climatic optimum ca. 10.7 ka, and parabolic dunes were active between 9.6 and 4.6 ka. Thus, oriented lakes developed in basins conditioned by fluvial and eolian processes. In the absence of much near-surface ground ice, lateral expansion of deep-basin lakes and shallow stabilized deflationary basins predominated during the late Holocene through wind-induced wave and current processes. Overall, this sequence of oriented-lake formation does not support a thaw-lake cycle but, rather, small-basin evolution of a periglacial landscape.

Key words: Late Pleistocene; Holocene; paleogeography; geomorphology, permafrost, periglacial, eolian and fluvial; optical dating; radiocarbon; Arctic North America; Laurentide Ice Sheet; oriented lakes; thermokarst

1. Introduction

Oriented-lake terrains in the tundra zone present some of the most intriguing and distinctive of Arctic landscapes. Examples include the Coastal Plain of northern Alaska (Jorgenson and Shur, 2007; Hinkel et al., 2012), the Kolyma lowlands of northeast Siberia (Morgenstern et al., 2008), the Sachs lowlands of Banks Island (Harry and French, 1983), and the Tuktoyaktuk

Coastlands of the Northwest Territories, Canada (Mackay, 1963). Oriented lakes have long interested permafrost and geomorphological researchers (French, 2017; Harris et al., 2018) and today the topic has greater relevance as there is a growing need to understand more about the sensitivity of terrestrial and aquatic environments in the changing North.

A knowledge gap exists concerning the environmental factors that drive the initiation and long-term growth of oriented lakes. Previous studies of oriented lakes in the Arctic have typically focused on the metrics and mechanisms of orientation, lake expansion and drainage based on annual to decadal observations (Carson and Hussey, 1962; Hinkel et al., 2005; Plug et al., 2008; Côté and Burn, 2002), rather than placing the lake development in a geological framework of landscape evolution over millennial timescales. The latter was partially achieved by Jorgenson and Shur (2007) for the Beaufort Plain of northern Alaska, but that study provided limited details about the stratigraphy and geochronology of the sediments and lacked a geomorphic interpretation of the terrain. Thus, no empirical studies to date have systematically investigated the geological processes, landforms, sediments and timescales required for the initiation and development of oriented lakes. Given the complex range of possible geological processes—including glacial, periglacial, eolian, fluvial, and marine—which may influence oriented-lake formation, the question remains: *what geological processes drove landscape evolution to form oriented lakes?* Oriented lakes in Arctic regions have often been attributed to thaw of ice-rich permafrost, but only limited stratigraphic evidence has been presented to test this hypothesis (Jorgenson and Shur, 2007). Furthermore, as significant environmental change has occurred during the Quaternary Period, we need to determine *when and where were the stratigraphically adjacent sediments deposited and the regional landforms developed before, during and after lake initiation?* Addressing these questions against geological data can provide fresh insight into how Arctic landscapes develop and condition the landforms within them. Stratigraphic observations and geomorphic mapping can provide a geological framework with a relative timescale, and geochronological dating can provide an absolute timescale.

The aim of this paper is to reconstruct the evolution of a lowland landscape in western Arctic Canada in order to elucidate the origin and development of oriented lakes there. The objectives are to: (1) map the extent of oriented-lake basins and associated landforms, (2) report observations of the sediments and stratigraphic sequences, (3) date the landforms and sediments, (4) place the results into a landscape evolution context conformable with the late Quaternary geological history of the region, and (5) evaluate the role of permafrost in landscape evolution and oriented-lake development. Our approach requires step-by-step presentation of a substantial set of data and interpretations of the stratigraphy, sedimentology, geochronology and geomorphology. Key observations and interpretations are presented in the main manuscript, and supporting observations and further details in the Supplementary Materials. We integrate these objectives into a discussion of sedimentation and landscape processes that provides the basis of a conceptual framework from which we consider the initiation and development of the oriented lakes within our study area.

2. Regional setting

2.1 Study area

The study area comprises the McKinley Bay Coastal Plain, Tuktoyaktuk Coastlands, Northwest Territories, Canada (Mackay, 1963; Rampton, 1988). For the purposes of this study, we define the McKinley Bay Coastal Plain according to Mackay (1963; Fig. 37), as the portion of the northeastern end of the Tuktoyaktuk Peninsula that includes oriented-lake terrain (Fig. 1). The plain is approximately 125 km long and 15–35 km wide. It resides within the zone of continuous permafrost, with permafrost locally extending to between 300 and 500 m depth (Pelletier and Medioli, 2014), and with present-day mean annual air temperature (at Tuktoyaktuk) of approximately −10 °C. Mean annual ground temperature is presently about −7 °C under dwarf-shrub tundra in the southwestern part of the Tuktoyaktuk Peninsula (Kokelj et al., 2017), though water bodies such as lakes cause thermal perturbations to the ground thermal regime (Burn, 2002).

In contrast to the surrounding Tuktoyaktuk Coastlands, the McKinley Bay Coastal Plain entirely lacks ground-ice (thaw) slumps and contains abundant oriented lakes (Mackay, 1963). The terrain is of low relief and currently covered by shrub tundra and wetlands. The lowland vegetation is dominated by either cotton-grass (*Eriophorum veginatum*) on drier terrain or by sedge (*Carex* *aquatilis*) in wetlands, with a moss cover (*Sphagnum rubellum, S. squarrosum*) developed on cryic fibrisols with an active layer about 25 to 40 cm thick (Ritchie, 1984). Networks of ice-wedge polygons extend across the lowland terrain and drained former lakes, with individual polygons 5–60 m in diameter. High-centre polygons occur mostly on slightly higher relief terrain and ridges, whereas low-centre polygons abound within drained-lake and low-relief areas. Drained-lake basins commonly contain pingos (Mackay, 1963).

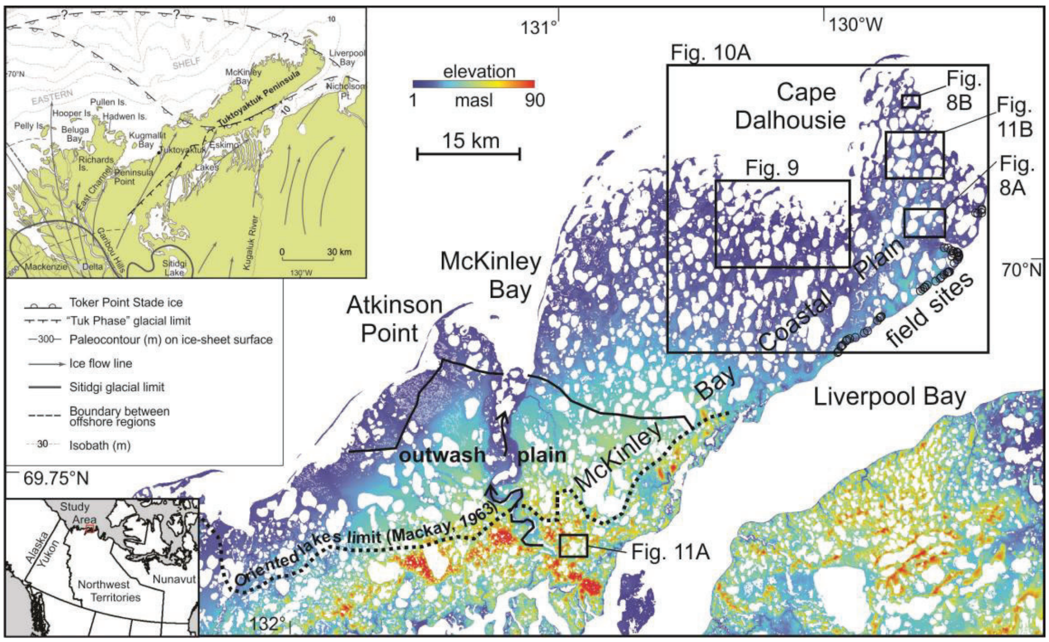

Figure 1. Location map of the Tuktoyaktuk Coastlands (inset) and digital elevation model in metres above sea level (masl) derived from the Arctic-DEM of the McKinley Bay Coastal Plain (see Supplementary Materials S1 and Figure S1-1 for detailed field locations). Solid black line depicts northern limit of the McKinley Bay outwash plain and curving arrows indicate meltwater channel associated with "Tuk phase" glacial limit (Rampton, 1988). Inset map shows two possible glacial limits for the Toker Point Stade ice, one crossing the northeast Tuktoyaktuk Peninsula, an alternative crossing the eastern Beaufort Sea Shelf north of the Tuktoyaktuk Peninsula, indicating uncertainty about the topographic profile of the ice sheet here (Rampton, 1988). Field site locations (black circles) are enlarged in Figure 3B.

The McKinley Bay Coastal Plain contains individual, merged, and drained oriented-lake basins, ranging in area from less than 0.1 km^2 to more than 12 km^2 (Fig. 1). These lakes typically have an elongate form, which has been attributed to wave-induced erosion generated from bi-modal prevailing winds from the ENE and WNW (Côté and Burn, 2002). Most lakes have shallow littoral shelves up to 600 m wide and reportedly "central deep troughs" (Mackay, 1963), although water depths have not been previously documented for these lakes. Further details about the oriented lakes of the area are given by Mackay (1956a, 1963), Côté and Burn (2002) and Plug et al. (2008).

The oriented lakes and drained-lake basins constitute approximately one-half of the McKinley Bay Coastal Plain (Fig. 1), with about one-third presently occupied by water (Plug et al., 2008). Much of the low-relief land surface resides less than 5 m above sea level (masl). Exceptions are areas of hilly terrain reaching 90 masl north of the Eskimo Lakes (Fig. 1). Some oriented lakes south of McKinley Bay occur at elevations up to 40 masl (Fig. 1). Stabilized dunes and associated dune ridges also occur throughout the lowland terrain (Mackay, 1963; Rampton, 1988; Michaud and Begin, 2000) but are absent from higher elevations and hilly terrain.

Lakeshore dunes occur predominately on the western margins of drained and partially drained lakes (Michaud and Begin, 2000). These dunes originate from exposed sandy littoral shelves and blowout depressions that have developed along the formerly wave-eroded shorelines, with wind-deflated sand deposited downwind. Except around recently drained lakes, most lakeshore dunes are stabilized by vegetation. Blowout depressions resulting in low-relief hummocky topography are common along drained and actively deflating shorelines, with sand transported away from the lakeshore. Tundra vegetation effectively inhibits present-day wind erosion, limiting it to exposed lakeshores, with sediment transported within 200 m downwind of these source areas.

Individual lowland dunes are recognizable throughout most of the McKinley Bay Coastal Plain. The stabilized dunes are similar in shape and size, being elongate with 0.5 to 3 m of relief, and typically 200–250 m wide and up to 800 m long. The ridges are aligned east-to-west, with parabolic dune heads that are convex in the downwind direction, oriented toward the west, indicating that sediment-transporting winds were dominantly from the east (Michaud and Begin, 2000).

2.2 Late Quaternary environmental setting

The Tuktoyaktuk Coastlands of the western Arctic (Fig. 1) are the most studied Arctic tundra region in Canada. Their Quaternary history, physiography, surficial geology, vegetation and permafrost conditions are detailed in numerous studies (e.g. Dallimore et al., 1997; Mackay, 1963; Rampton, 1988; Ritchie, 1984; Burn, 1997; Pelletier and Medioli, 2014). Ground ice, stratigraphy, geomorphology and permafrost processes have been extensively investigated (Bateman and Murton, 2006; Kokelj et al., 2009; Mackay and Dallimore, 1992; Murton, 2005, 2009; Murton et al., 2004, 2017), though questions remain regarding the extent and absolute timing of late Quaternary events and Holocene environmental conditions. Below, we summarize key information about the stratigraphy, ground ice and late Quaternary environmental change that provides a conceptual framework essential to this study.

Late Quaternary unconsolidated sediments underlying the Tuktoyaktuk Coastlands include a transitional sequence of marine sands and clays, alluvial and eolian sands, capped by glacial tills and outwash sediments and containing bodies of tabular massive ice (Fig. 2) (Rampton, 1988; Murton, 2009). The lowermost units—the Kendall sediments, characterized by sand interbedded with silt and clay, and the Hooper clay—probably represent deposits from marine transgression and, respectively, a fluctuating shallow sea and high sea level that date to the last (Sangamonian) interglaciation (Murton, 2009). These units are not exposed within the McKinley Bay Coastal Plain but crop out near sea level within the region. Overlying alluvial sands of the Kidluit Formation (Fm) represent braided-river deposits of large pre-Laurentide rivers, including those of the paleo-Porcupine and paleo-Peel-Anderson basins, which flowed into the Arctic Ocean near the location of the modern Mackenzie River. Murton et al. (2017) dated these sands by optically-stimulated luminescence (OSL) to between 76 and 27 ka, with nonfinite ^{14}C ages > 50 ka.

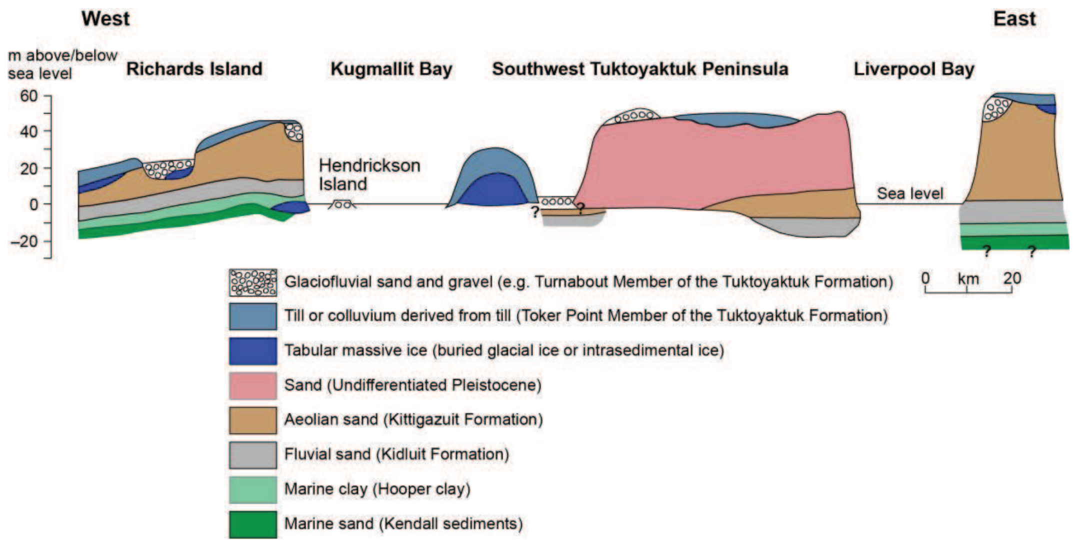

Figure 2. Schematic representation of the late Quaternary stratigraphic succession of the Tuktoyaktuk Coastlands. The section crosses the southwestern region of the Tuktoyaktuk Peninsula, whereas the present study examines the stratigraphy beneath the northeastern region of the peninsula (see Fig. 3). Modified from Rampton (1988).

The overlying Kittigazuit Fm sands—derived from Kidluit Fm sediments—are eolian (Dallimore et al., 1997; Murton et al., 2007, 2017), and probably formed as Laurentide glacial ice further south blocked much of the drainage of the paleo-river system and later terminated with the deglaciation of the Mackenzie Valley. Regionally extensive and thick eolian deposits are observed in two major stratigraphic settings: a thick sand unit characterized by large eolian dune and sand-sheet deposits dating to between ca. 30 and 13 ka, and a sand-sheet unit commonly interbedded with glaciofluvial outwash on Richards Island dating to between 14 and 8 ka (Bateman and Murton, 2006). In addition, Holocene-age eolian deposits are observed along the tops of sandy bluffs, adjacent to shorelines and drained thermokarst lakes along the southern boundary and Liverpool Bay section of the McKinley Bay Coastal Plain (Rampton, 1988), and sand-sheet deposits mantle most of the surface.

Glaciation across much, if not all, of the Tuktoyaktuk Coastlands occurred during the last Pleistocene cold (Wisconsinan) stage, although the exact timing and extent of this Laurentide glaciation remain uncertain. A grey pebbly clay till—the Toker Point Member of the Tuktoyaktuk Fm—extends over much of the coastlands, and uncertainty exists as to the maximum extent of the associated Toker Point Stade ice (Fig. 1). Till is thin to absent on the McKinley Bay Coastal Plain, and Mackay (1963) suggested that this area may have been unglaciated. Rampton (1988) placed the age of widespread glaciation of the Tuktoyaktuk Coastlands as Early Wisconsinan, but without strong chronologic control. According to Murton et al. (2015), glaciation during the Late Wisconsinan reached northern Richards Island, briefly, between 17.5 and 15 ka based upon dating of preglacial and postglacial eolian sands. This is consistent with Mackay and Dallimore's (1992) suggestion that ice advanced to the Tuktoyaktuk area between about 17 and 15 ka. Exposures on Richards Island, southern Liverpool Bay and Eskimo Lakes reveal glaciotectonically deformed preglacial sediments, till and ground ice, indicating that permafrost was likely preserved before, during and after glaciation of these areas beneath a cold-based ice margin (Murton et al., 2004; 2005). Rampton (1988) further identified a later "Tuk phase" north of Eskimo Lakes and a younger still Sitidgi glacial limit north of Sitidgi Lake (Fig. 1).

The Cape Dalhousie Sands underlie much of the McKinley Bay Coastal Plain, beneath a cap of eolian sand-sheet deposits. The Cape Dalhousie Sands have been ascribed by Rampton (1988) to a glaciofluvial outwash plain during the Toker Point Stade, and therefore assigned to the Tuktoyaktuk Fm. However, Bateman and Murton (2006) suggested that the Cape Dalhousie Sands might underlie the Kittigazuit Fm, suggesting that they may correlate with the older Kidluit Fm. Thus, uncertainty exists as to the nature and age of these sediments.

Ground ice is abundant in permafrost of the Tuktoyaktuk Coastlands, particularly at depths of a few metres to a few tens of metres within or beneath silt- or clay-rich stratigraphic units. Excess-ice types at a scale relevant to the formation of thermokarst basins comprise massive ice, ice wedges and multiple ice lenses (Murton, 2013). Tabular bodies of massive ice are common in glaciated terrain, representing buried basal ice from the Laurentide Ice Sheet or non-glacial intrasedimental ice and tend to be associated stratigraphically with tills or glaciotectonites (Fig. 2; Murton, 2005). Ice wedges are widespread in clay, silt and sand, and multiple ice lenses in frost-susceptible substrates. Summaries of ground ice in the region are given by Mackay (1963), Rampton (1988) and Murton (2009).

The lithostratigraphic succession summarized above is simplified, and specific stratigraphic sequences may vary from it. In particular, a major unit of sand several tens of metres thick and generally grey in colour has been identified by Rampton (1988) on the southwestern part of the Tuktoyaktuk Peninsula (Fig. 2). Its origin, age and paleoenvironmental significance are not known.

Furthermore, glaciotectonic processes resulting from passage of the Laurentide Ice Sheet across the region have disturbed some stratigraphic successions. For example, some show an inverted stratigraphy, whereas others contain a frozen glaciotectonite formed by mixing and erosion of different lithostratigraphic units (Murton et al., 2004).

Environmental and climatic change during the last 30 ka in the Tuktoyaktuk Coastlands has been complex. Dry conditions likely prevailed between 30 and 17.5 ka (Bateman and Murton, 2006), when the Cordilleran Ice Sheet may have deflected the jet stream south (Edwards et al., 2001) and blocked the passage of moist Pacific air to the northeast (Dyke et al., 2002). Slow climatic warming is thought to have commenced at ca. 18.3 cal ka BP, followed by rapid warming between ca. 14.0 and 11.5 cal ka BP with vegetation cover south of Tuktoyaktuk (60° 03' N; 133° 27' W) predominantly sedge-marsh to dwarf-birch (*Betula glandulosa*) dominated tundra, and herb tundra on drier sites (Ritchie, 1984). The mean July air temperature by ca. 11.5 cal ka BP was about 3–5 °C higher than the modern value. The basal sediments of numerous thermokarst-lake basins date to 11.5–10.2 cal ka BP, with a widespread thaw unconformity at about 8.9 cal ka BP representing an active layer about 2.5 times thicker than present (Burn, 1997). A slow cooling trend began at ca. 8.9 cal ka BP but probably with warmer-than-modern conditions until ca. 5.2 cal ka BP. Between one and two thirds of the amount of summer cooling felt along the Beaufort Sea coast since the early Holocene may be due to coastal recession (Burn, 1997). As the coast receded southward, the present Tuktoyaktuk Coastlands experienced an increased frequency of onshore winds blowing off a cold sea, resulting in lower summer air temperatures. The early Holocene warm interval witnessed a rise in spruce (*Picea*) with a coniferous forest advance until ca. 6.3 cal ka BP, followed by a transitional forest and dwarf shrub-tundra tundra under alder (*Alnus*) and birch. Vegetation cover in the last 3.8 cal ka BP has been similar to that today.

3 Methods

3.1 Stratigraphy and sedimentology

3.1.1 Field logs

Observations of 53 field exposures were made along 30 km of shoreline (Fig. 1 and S1-1; see Table S1 for details), including logging and measuring of section heights, sedimentary properties and thickness of individual stratigraphic units. Detailed descriptions and measurements were made at six field sites (sections 2.11; 2.14; 05-01; 05-02; 05-05; 18-13), noting stratigraphic units and contacts and collecting samples for geochronological analysis. These observations were supplemented by five additional sites (sections 2.9, 2.10, 2.12, 2.13, 05-03) reported earlier by Bateman and Murton (2006) and Bateman et al. (2010). Most units were placed into the regional lithostratigraphic framework for the area as developed by Rampton (1988) and summarized by Murton (2009).

3.1.2 Shothole logs

Subsurface conditions were examined using data from 1098 shothole logs drilled on the northeastern section of the McKinley Bay Coastal Plain (Côté et al., 2003). Shothole log data used in this study included the presence or absence of surface ice, water, or soil; lake-ice occurrence and thickness; water depths; and sediment stratigraphy and ground ice. We noted shothole positions and their location on land, lake or sea ice, which was either landfast or floating on water. The combined measurements of surface ice thickness—which probably included hard snow where recorded ice thicknesses exceeded 2.4 m—and water depth were used to determine the lake-basin depths, as these factors affect the drilling depth required for shotholes to obtain reliable seismic results.

The stratigraphic logs are considered less reliable than the data discussed above, as shothole drillers are not trained in formal stratigraphic techniques and nomenclature, and the material is logged at varying degrees of resolution and accuracy (Smith, 2015). After analyzing the shothole logs, we determined that the records of sand and silt could not be consistently differentiated by shothole loggers (see Supplementary Materials S2 for details) and so we combined these sediments into a single sedimentological unit of sand or silt. Similarly, recorded observations of sandstone and shale probably referred to frozen sand or frozen silt or clay, respectively, rather than rock, as shotholes were drilled through unconsolidated sediments within permafrost (Mackay, 1971). In contrast, records indicating clay could be distinguished from sand and silt, enabling us to reduce the analytical data to records of combined sand or silt, and of clay. This differentiation of sediment types using shothole logs in the Tuktoyaktuk Coastlands is similar to that made by Mackay (1971) and Mackay and Dallimore (1992). Finally, we noted the depth of any ground ice recorded in the shotholes.

3.2 Geochronology

3.2.1 Optically stimulated luminescence (OSL) sampling and dating

Samples for OSL were collected from cleared-back sedimentary exposures using opaque PVC tubes. Samples were prepared to obtain clean quartz fractions as per Bateman and Catt (1996). When tested using infra-red light, no prepared sample showed signs of feldspar contamination. All samples were measured using a Risø reader, green light stimulation and luminescence filtered through a Hoya U-340 filter. Paleodose (De) values were determined using the single aliquot regeneration (SAR) procedure (Murray and Wintle, 2000) with an experimentally derived preheat of 240 °C for 10 s and 5 regeneration points. This included a replicate of the first regeneration point (known as recycling) used to check that the sensitivity correction was adequate. Previously published samples from the region Bateman and Murton (2006) were based on aliquot level measurements with multiple replicates per sample. Aliquots were rejected from further analysis if they exhibited poor luminescence characteristics or poor recycling (beyond 1.0 ± 0.1). During analysis, further aliquots were considered as outliers if they fell beyond 2 standard deviations of the mean. Repeated De measurements of samples showed most had good reproducibility indicative of sediment which had been fully exposed to sunlight prior to burial. Reported De values are therefore based on the mean of replicates with 1 standard error. OSL samples published by Bateman et al. (2010) and new results presented here were based on single-grain level measurements, which in most cases showed more replicate variability. As a result, reported De values are based on the Finite Mixture Model of Galbraith and Green (1990). Dose rates for all samples were derived from in-situ gamma spectrometry measurements attenuated for grain-size and density (Table 2). Past moisture used present-day values with ± 5% uncertainties to allow for past fluctuations. The cosmic ray dose-rate was calculated based on Prescott and Hutton (1994). Final ages are in calendar years from the time of sampling (Table 2).

3.2.2 Radiocarbon sampling and dating

Eight samples for radiocarbon dating were collected from detrital organic layers within eolian and lacustrine sediments to date localized sand sheets and lake basins and to supplement the OSL dating of these units. Nine samples were also collected for the purpose of defining basal ages of well-identified Holocene humic organics overlying eolian sand sheets. Ages derived from these samples were used to assess the onset of organic matter accumulation on terrestrial surfaces and the stabilization of eolian deposits. Two detrital wood fragments from sediments identified as Cape Dalhousie Sands were also sampled and dated as confirmation of these older deposits. Sixteen ages were obtained by accelerator mass spectrometry (AMS) dating, and three analyses (Beta – 195573, SRR-6928 and SRR-6929) by standard radiometric dating (liquid scintillation counting). Ages reported by Bateman and Murton (2006) were dated at the Beta Analytic Radiocarbon Dating Laboratory (Beta), Miami, USA, and the NERC Radiocarbon Laboratory at the Scottish University Environmental Research Centre (SUERC) in East Kilbride, Glasgow, Scotland. New ages reported in this study were determined at the A.E. Lalonde AMS Laboratory (OUC) in Ottawa, Canada. AMS ages were calibrated with the CALIB 7.1 program, using the IntCal13 calibration dataset (Stuiver et al., 2019). All radiocarbon ages are reported to 2 standard deviations. For convenience, ages referred to in text represent the median probabilities of the calibrated ages.

3.3 Geomorphic mapping

We used the open source Government of Canada CanVec waterbody layer to determine the percent area occupied by lakes. We mapped surficial features within the McKinley Bay Coastal Plain using a combination of Landsat and WorldView-2 (WV2) imagery in Google Earth. Stabilized lowland area dune ridges and active and stabilized lakeshore dunes were mapped to assess the spatial extent of eolian activity. Lake basins and drainage features were mapped by identifying the general strike of each oriented-lake basin and defining stream networks and channels connecting basins to establish the relation between past and present hydrology. Finally, unmodified lowland terrain, former lake basins, and present-day confined, partially drained, and breached lakes (i.e. those open to marine waters) were mapped to support shothole bathymetric and stratigraphic analysis.

4 Results

4.1 Stratigraphy and sedimentology

4.1.1 Section summaries

Section observations along 30 km of the northern shoreline of Liverpool Bay reveal distinctive areas from south to north, as summarized in Figure 3. In the south, Kittigazuit Fm sands are capped by glacial till and outwash sediments on upland terrain, whereas a lowland plain exposes Kittizaguit Fm with sand wedges and, rarely, Kidluit Fm overlain by eolian sheet sands. This lowland transitions northeastward into upland terrain comprising mainly Kittigazuit Fm capped with glaciofluvial outwash and eolian sheet sands. The northern half of the McKinley Bay Coastal Plain comprises lowland terrain that exposes Cape Dalhousie Sands with sand wedges capped by sandy lacustrine sediments, eolian sheet sands and thick humic organics.

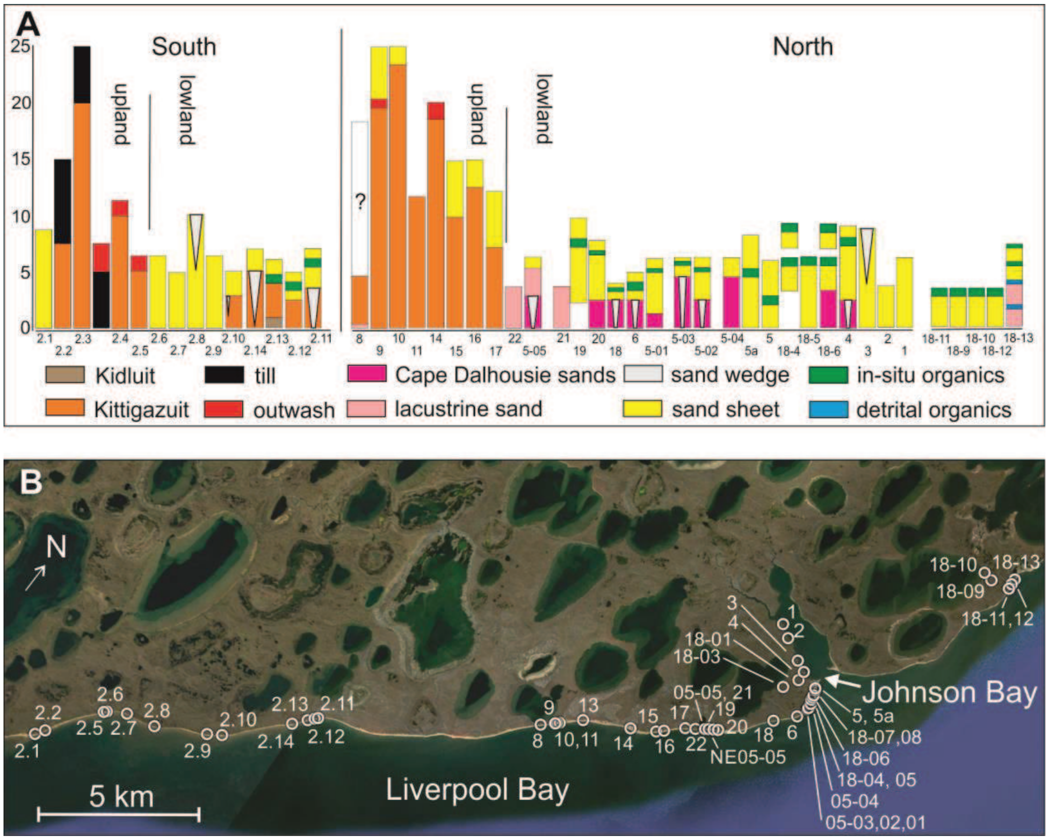

Figure 3. Locations and summary of stratigraphic sections observed along the northern shoreline of Liverpool Bay. A) Sections sorted from south to north (horizontal distance not to scale). B) Section locations (image source Google Earth). See Supplementary Materials S1 for summary notes.

4.1.2 Stratigraphic unit descriptions

Nine primary stratigraphic units and several secondary features and contacts were observed in the McKinley Bay Coastal Plain. Their main characteristics are summarized below, within the general stratigraphic framework developed by Rampton (1988), and details are given in Table 1.

Table 1. Description of stratigraphic units and features on the McKinley Bay Coastal Plain.

INSERT TABLE 1 HERE (NOTE – IT IS AT THE END OF THE PAPER)

(1) Kidluit Fm sand is exposed rarely in the McKinley Bay Coastal Plain, below Kittigazuit Fm sand. One exposure was examined (Fig. S1-5; section 2.13), which had earlier been interpreted by Bateman and Murton (2006) as Cape Dalhousie Sands. However, as the sediment at the base—beneath brown Kittigazuit Fm sand—is a light grey, wavy, horizontally laminated sand, characteristic of Kidluit Fm (Murton et al., 2017), we re-assign it to the Kidluit Fm. This formation also contains sand veins and at least one small ice-wedge pseudomorph.

(2) Kittigazuit Fm sands are exposed in the southernmost portion of the McKinley Bay Coastal Plain beneath uplands capped by glacial till or outwash sediments, and lowlands where they are truncated and overlain by eolian sand sheets (Fig. 4 and S1-2; sections 2.11 and 2.14, respectively; and sections 2.10, 2.12, 2.13 in Bateman and Murton, 2006; Fig. S1-5 and S1-6). Some upland sections expose more than 20 m of Kittigazuit Fm, whereas lowlands expose typically 3 m or less. These eolian sands typically host sand veins and sand wedges, up to 1.5 m wide (Fig. 4), where strata are commonly upturned adjacent to sand-wedge contacts. Within these exposures, the Kittigazuit Fm and sand wedges are typically truncated by an erosional contact overlain by a single-grained granule–pebble layer.

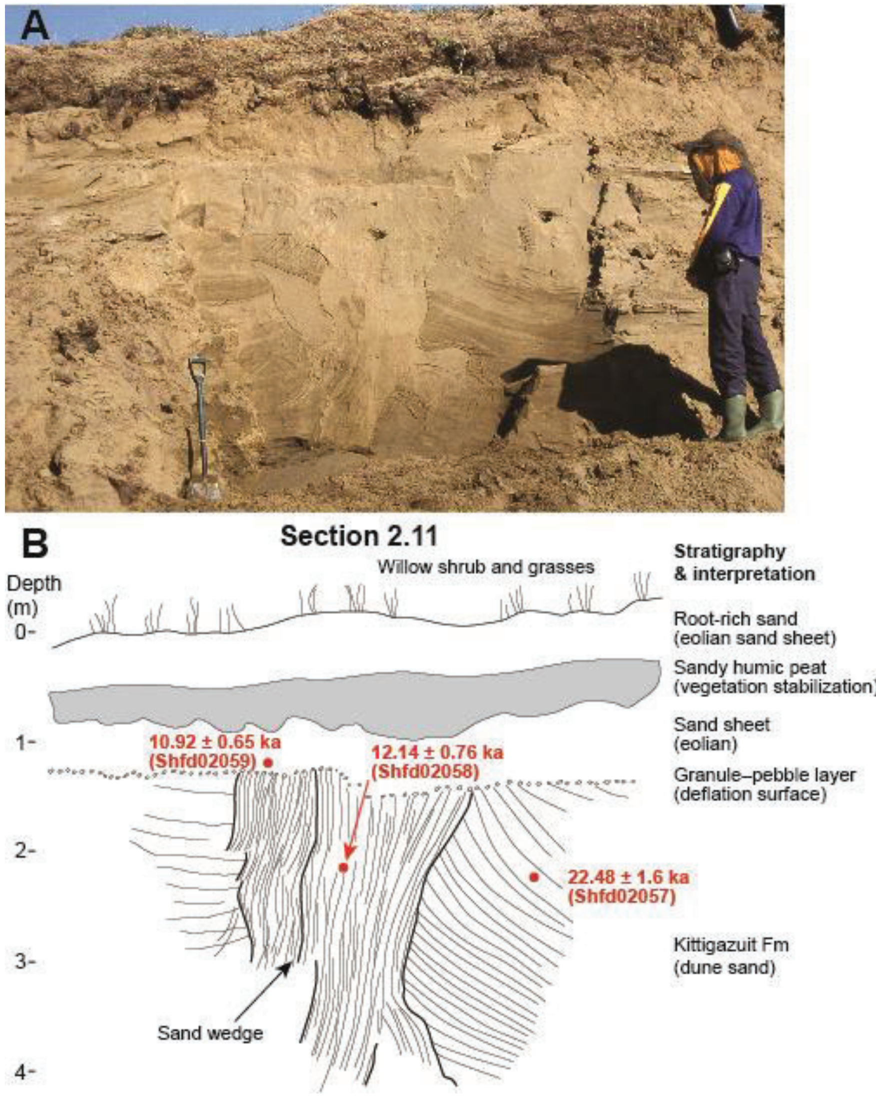

Figure 4. Photograph (A) and sketch (B) showing vertical section exposing Kittigazuit Fm sand truncated along the top by an erosional surface and overlain by an eolian sand sheet, section 2.11. Upturned host strata are adjacent to the sand wedge. OSL sample locations, ages, and lab codes are indicated, with complete results reported in Table 2.

(3) Cape Dalhousie Sands underlie much of the McKinley Bay Coastal Plain (Rampton, 1988). In the northern half of the sections, sediments ascribed to Cape Dalhousie Sands are exposed beneath lowland terrain (Fig. 3). These sands are generally poorly sorted and coarse-grained, but not cobble-rich (Table 1). They include both planar parallel lamination and foresets characteristic of

fluvial channel deposits. They also contain wood fragments and coal that appear to be reworked. At many exposures (Fig. 5, 6 and S1-6; sections 05-02, 05-05 and 05-03; Bateman et al., 2010) the Cape Dalhousie Sands host sand wedges commonly 3.0 m wide, with steeply upturned to overturned strata adjacent to them (Fig. 5). As with the Kittigazuit Fm, the sediments are truncated at the top by an erosional surface overlain by a pebble lag. These observations suggest that the sand wedges are antisyngenetic (Murton and Bateman, 2007), having formed as wind deflated the surface downward. Significantly, Cape Dalhousie Sands and Kittigazuit Fm were not observed together in any stratigraphic section (Fig. 3). At one location (Fig. S1-3; 05-01) Cape Dalhousie Sands appear to have been glaciotectonically deformed, as foresets are overturned where they are overlain by a pebbly silt with evidence of a sheared horizon, similar to that observed by Murton et al. (2015) on Hadwen Island.

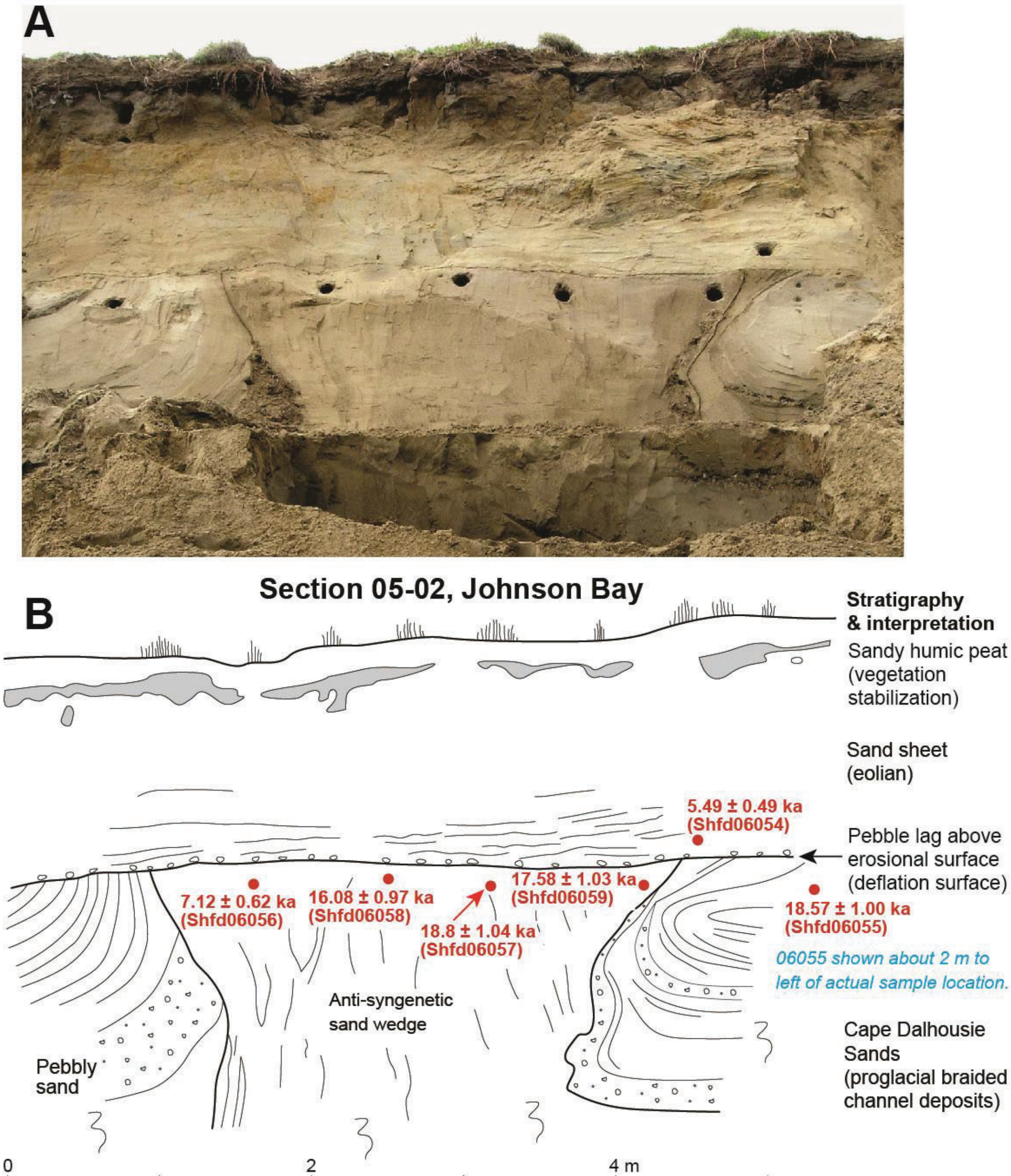

Figure 5. Photograph (A) and sketch (B) of vertical sections through Cape Dalhousie Sands hosting sand wedges and truncated by upper erosional surface overlain by eolian sand-sheet deposits (sand unit A) with pebble lag above an erosional surface, section 05-02. OSL sample locations, ages, and lab codes are indicated, with complete results reported in Table 2.

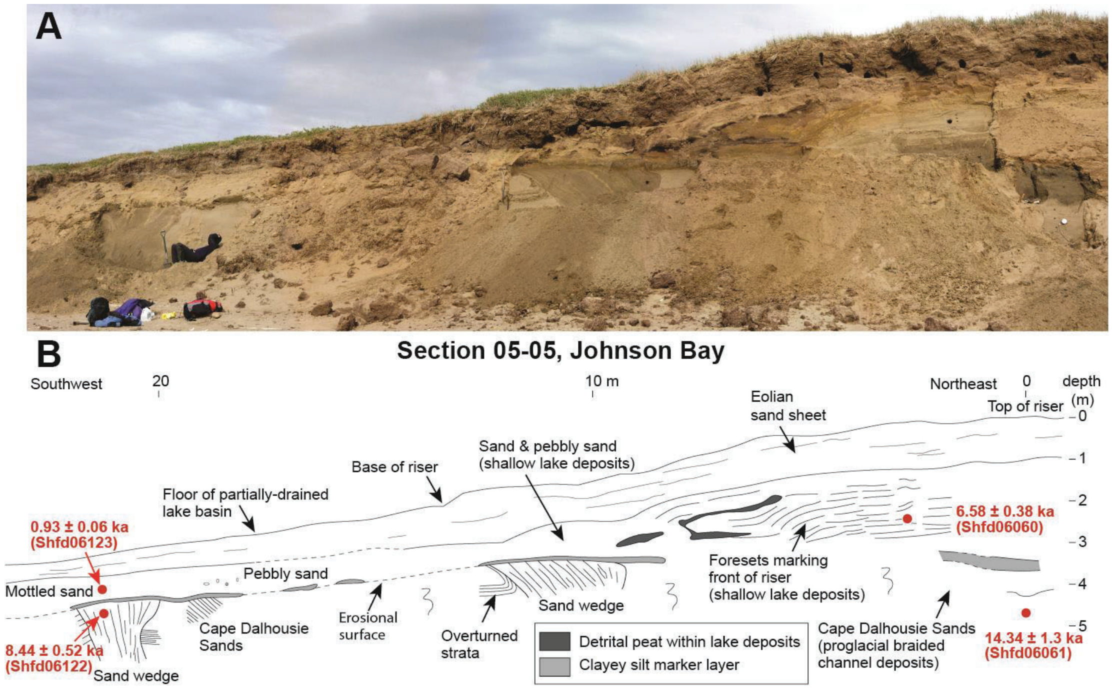

Figure 6. Photograph (A) and sketch (B) of sandy and pebbly lacustrine sediments (sand unit B) with a clayey silt layer above an erosional surface, and thicker sandy foresets marking a former riser in shallow lake deposits, section 05-05. OSL sample locations, ages, and lab codes are indicated, with complete results reported in Table 2.

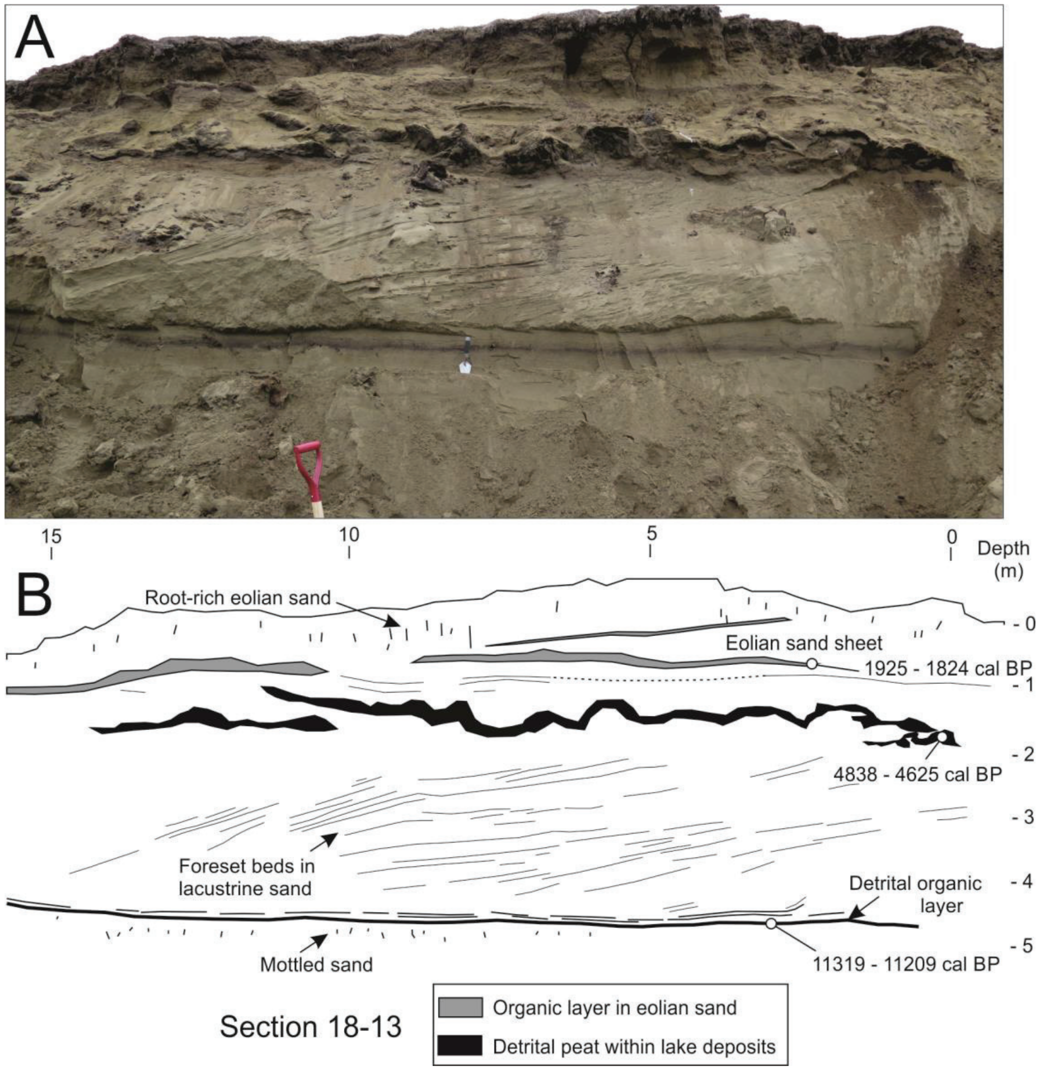

Figure 7. Photograph (A) and sketch (B) of vertical section showing shallow lake deposits (sand unit B) and upper eolian sand-sheet unit, section 18-13. AMS ages are indicated (see Table 3 for details).

(4) Diamicton interpreted as Toker Point till and overlying Kittigazuit Fm sand is exposed in the southernmost sections in upland terrain (Fig. 3). These exposures lie along the limit of the Toker Point Stade mapped by Rampton (1988) and appear to represent a glacial ice-marginal position.

(5) Outwash sediments, observed as rounded gravel and cobble deposits, are exposed only in the southern portion of the study upland terrain, where they are underlain by Toker Point till or Kittigazuit Fm sand (Fig. 3).

(6) A lower sand unit A commonly overlies Kittigazuit Fm sand or Cape Dalhousie Sands and sand wedges. An erosional contact at the base of the unit is overlain by a granule–pebble layer containing wind-polished pebbles (Fig. 4 and 5). The unit contains strata characteristic of both dry and moist eolian sand-sheet surfaces (Ruegg, 1983; Schwan, 1988) with and without vegetation cover (Table 1).

(7) A humic organic layer 0.3–1.0 m thick occurs primarily in the northern part of the McKinley Bay Coastal Plain area within lowland terrain, as observed at most sections. This organic layer overlies the lower eolian sand-sheet unit.

(8) A lower sand unit B, noted at two locations, occurs in lowland terrain within drained-lake basins. At section 05-05, 0.5-m thick mottled sand to pebbly sand with a discontinuous clay–silt layer overlies Cape Dalhousie Sands with an erosional surface marking the contact with the underlying sediments (Fig. 6). This unit is interpreted as shallow lake deposits, as they also contain detrital organic layers and foresets up to 2.5 m thick marking the front of a former shallow littoral shelf (i.e. riser) of the lake basin. Similar lacustrine deposits occur in section 18-13 (Fig. 7).

(9) An upper eolian sand-sheet unit directly underlies the land surface and is commonly root-rich. Eolian sand-sheet deposits are extensive in the area, except where till, outwash or lacustrine sediments occur (e.g. sections 05-05 and 18-13; Fig. 6 and 7).

4.2 Geochronology

4.2.1 OSL ages

OSL ages from 29 samples within seven stratigraphic units were obtained in the area, comprising 15 previously published ages (Bateman and Murton, 2006; Bateman et al., 2010) and 14 new ages (Table 2). These ages are reported below in relation to the stratigraphic units, from oldest to youngest.

One OSL age from the Kidluit Fm returned an age of 62.6 ± 3.44 ka (Bateman and Murton, 2006), and falls within the range of 72–27 ka for the Kidluit Fm dated regionally (Murton et al., 2017). Four previously published OSL ages from the Kittigazuit Fm on the McKinley Bay Coastal Plain returned ages of 43.4–14.5 ka (Table 2), and one new sample returned an age (22.48 ± 1.6 ka) within this range from sand whose strata had been upturned by an epigenetic sand wedge (Fig. 4). Three OSL ages from Cape Dalhousie Sands returned ages between 18.6 and 14.3 ka, including one previously published value (Bateman et al., 2010) and two new ages. Significantly, these ages are contemporary with the depositional period of the Kittigazuit Fm. Nine OSL ages from sand wedges range between 18.8 and 5.3 ka. One sample from a sand wedge hosted by the Kittigazuit Fm returned an age of 12.14 ± 0.76 ka (Fig. 4B; section 2.11). The remaining OSL ages were from sand wedges hosted by Cape Dalhousie Sands. Ages from within individual sand wedges ranged over a considerable time period. At section 05-03 three samples from one antisyngenetic sand wedge returned ages of 17.9 ± 1.1, 8.53 ± 0.78 and 5.32 ± 0.42 (Fig. S1-7B; Bateman et al., 2010). At section 05-02 four samples from another antisyngenetic sand wedge returned ages of 18.8 ± 1.04, 17.58 ± 1.03, 16.08 ± 0.97, and 7.12 ± 0.62 (Fig. 5B). One additional sand wedge sample returned an age of 8.44 ± 0.52 (Fig. 6B). Collectively, these sand-wedge ages indicate that the wedges were, at least, intermittently active between the end of the Last Glacial Maximum and the mid Holocene, and this sand-wedge activity may correlate with specific periods of hemispheric cooling (Bateman et al., 2010).

Nine OSL samples from the eolian sand-sheet deposits (lower sand unit A) overlying Kittigazuit Fm, Cape Dalhousie Sands and sand wedges returned ages ranging from 12.55 to 4.37 ka. One section (2.9; Fig. S1-3) returned a sequence of five ages upwards through the profile of 12.55 ± 0.64, 12.10 ± 0.67, 12.11 ± 0.67, 9.44 ± 0.51 and 8.18 ± 0.48 ka (Bateman and Murton, 2006). At all other sites, an erosional contact—typically overlain by a pebble lag—occurred at the top of the underlying sediments. The ages of the sand-sheet deposits directly overlying the erosional contact from each section were 10.92 ± 0.65, 10.68 ± 0.61, 5.49 ± 0.49, 4.37 ± 0.44 ka, respectively. These ages indicate that eolian sand-sheet activity occurred, at least intermittently, throughout much of the early to mid Holocene.

Two OSL ages from lacustrine sand (lower sand unit B), in a shallow lake basin, are 6.58 ± 0.38 and 0.93 ± 0.06 ka (section 05-05, Fig. 6B). Although limited in number, they confirm that lake sedimentation and expansion occurred at least during the mid to late Holocene.

4.2.2 Radiocarbon ages

Radiocarbon ages relevant to the study were obtained from samples collected within three stratigraphic units containing organic materials. Two wood samples from Cape Dalhousie Sands returned ages of >45600 ^{14}C BP (Table 3). As the OSL ages from these sands are between 18.6 and 14.3 ka, we suggest that the wood is re-transported from older deposits such as the Kidluit Fm.

Radiocarbon dating of organic materials within eolian sand sheets (lower sand unit A) at two sites reported by Bateman and Murton (2006) returned several ages between 12.8 and 11.6 cal ka BP, comparable to the OSL ages from the same section (Table 3; Fig. S1-3). In addition, two samples from lacustrine sand (lower sand unit B) returned ages bracketing deposition between 11.3 and 4.7 cal ka BP (Fig. 7), suggesting that some lake basins have been present for much of the Holocene. We note, however, that both samples are detrital in nature, and therefore they may be older than the depositional age of the host sedimentary unit.

A humic organic layer covers much of the McKinley Bay Coastal Plain, except within recently drained lake basins, modern lakeshores and active eolian surfaces. Nine AMS samples from the base of this organic layer were collected from interdune plains (including a recently drained small pond) and from areas of stabilized dunes on eolian plains. Five basal ages from interdune areas ranged from 10.7 to 8.9 cal ka BP, indicating development of a vegetation cover beginning in the early Holocene. Four basal ages from organic layers interstratified with eolian sands and mantling small eolian dunes were generally younger, ranging from 9.6 to 4.7 cal ka BP. Finally, two AMS ages from surface eolian sands both returned ages of about 1.9 cal ka BP (Table 3).

Table 2. OSL-related data for sand deposits on the McKinley Bay Coastal Plain.

Section	Lat °N; Long °W	Stratigraphic unit	Lab. code	Depth (m)	PaleodoseDe (Gy)	Dose Rate (Gy/ka)	Age (ka)
2.9	69.9148; 129.8775	Sand sheet	Shfd02049	0.95	15.72 ± 0.49 [b,d]	1.920 ±0.097	8.18 ±0.48[1]
		Sand sheet	Shfd02050	2.25	17.76 ± 0.35 [b,d]	1.862 ±0.094	9.44 ±0.51[1]
		Sand sheet	Shfd02053	3.25	22.86 ± 0.37 [b,d]	1.886 ±0.094	12.11 ±0.67[1]
		Sand sheet	Shfd02051	3.95	21.75 ± 0.43 [b,d]	1.795 ±0.092	12.10 ±0.67[1]
		Sand sheet	Shfd02052	4.85	23.47± 0.32 [b,d]	1.870 ±0.092	12.55 ±0.64[1]
2.10	69.9169; 129.8662	Sand sheet	Shfd02055	4.1	19.10 ± 0.41 [b,d]	1.788 ±0.094	10.68 ± 0.61[1]
		Kittigazuit Fm (dunes)	Shfd02054	4.6	27.73 ± 0.54 [b,d]	1.907 ±0.097	14.54 ± 0.79[1]
		Kittigazuit Fm (dunes)	Shfd02056	5.8	38.4 ± 0.32 [b,d]	2.18 ± 0.11	17.6 ± 1.0[1]
2.11	69.9353; 129.8101	Kittigazuit Fm (dunes)	Shfd02057	2.4	46.51 ± 2.30 [a,d]	2.07 ± 0.11	22.48 ± 1.6
		Sand wedge	Shfd02058	2.25	22.60 ± 0.80 [a,d]	1.86 ± 0.097	12.14 ± 0.76
		Sand sheet above sand wedge	Shfd02059	1.25	22.96 ± 0.73 [a,d]	2.10 ± 0.105	10.92 ± 0.65
2.13	69.9335; 129.8156	Kidluit Fm	Shfd02060	4.1	105.2 ± 2.2 [b,d]	1.680 ± 0.086	62.6 ± 3.44[1]
		Kittigazuit Fm (sand sheet)	Shfd02061	3.9	76.2 ± 1.6 [b,d]	1.755 ± 0.089	43.4 ± 2.4[1]
		Kittigazuit Fm (dunes)	Shfd02062	1.57	61.0 ± 1.1 [b,d]	2.06 ± 0.11	29.6 ± 1.6[1]
05-02	70.0099; 129.4971	Sand sheet	Shfd06054	2.25	9.16 ± 0.68 [a,c]	1.67 ± 0.084	5.49 ± 0.49
		Cape Dalhousie Sands	Shfd06055	2.6	28.0 ± 0.94 [a,c]	1.50 ± 0.074	18.57 ± 1.00
		Sand wedge	Shfd06056	2.65	11.38 ± 0.86 [a,c]	1.60 ± 0.081	7.12 ± 0.62
		Sand wedge	Shfd06057	2.65	32.61 ± 1.30 [a,c]	1.74 ± 0.088	18.8 ± 1.04
		Sand wedge	Shfd06058	2.55	26.59 ± 1.14 [a,c]	1.65 ± 0.083	16.08 ± 0.97
		Sand wedge	Shfd06059	2.55	28.38 ± 1.15 [a,d]	1.62 ± 0.080	17.58 ± 1.03
05-03	70.0099; 129.4971	Sand sheet	Shfd06067	2.1	7.34 ±0.64 [a,c]	1.68 ± 0.083	4.37 ± 0.44[2]
		Cape Dalhousie Sands	Shfd06068	2.7	25.0 ± 1.03 [a,c]	1.68 ± 0.086	14.90 ± 1.05[2]
		Sand wedge	Shfd06069	2.65	28.0 ± 1.03 [a,c]	1.57 ± 0.078	17.9 ± 1.1[2]
		Sand wedge	Shfd06070	2.7	7.91 ± 0.49* [a,c]	1.49 ± 0.074	5.32 ± 0.42[2]
		Sand wedge	Shfd06071	5.1	13.40 ± 1.0 [a,c]	1.57 ± 0.082	8.53 ± 0.78[2]
05-05	69.9905; 129.5544	Riser of former shallow littoral shelf	Shfd06060	2	10.84 ± 0.34 [b,c]	1.65 ± 0.080	6.58 ± 0.38[2]
		Cape Dalhousie Sands	Shfd06061	4.4	19.53 ± 1.41 [a,c]	1.36 ± 0.074	14.34 ± 1.3
		Sand wedge	Shfd06122	1.7	13.72 ± 0.52[a,c]	1.63 ± 0.080	8.44 ± 0.52
		Shallow-lake deposit	Shfd06123	1	1.47 ± 0.06 [b,d]	1.58 ± 0.074	0.93 ± 0.06

[a] Measurements at the single-grain level, [b] measurements at the single-aliquot level, [c] De based on finite mixture modelling, [d] De based on mean of De replicates.
[1] Reported in Bateman and Murton (2006). [2] Reported in Bateman *et al.* (2010).

Table 3. Radiocarbon ages of organic material on the McKinley Bay Coastal Plain.

Section	Lat °N; Long °W	Setting	Sample description	Material dated	Lab. code	Depth (m)	^{14}C age yr BP ± std dev.	Cal. age yr BP (95.4 % (2σ) [a]	Median Prob.
Humic layer deposits (Table S1d)									
18-05	70.01276; 129.49818	Interdune plain	In situ basal organics	Bulk sed.	OUC-7409	0.70	8750±31	9893-9601 (1)	9729
18-06	70.01331; 129.49876	Interdune plain	In situ basal organics	Bulk sed.	OUC-7410	0.70	8012±32	9008-8771 (1)	8886
18-09	70.06574; 129.43286	Interdune plain	In situ basal organics	Bulk sed.	OUC-7413	0.55	9447±28	10635-10587 (0.22) 10750-10640 (0.78)	10683
18-12	70.06783; 129.41803	Interdune plain	In situ basal organics	Twig	OUC-7416	0.80	9349±30	10449-10444 (0.004) 10664-10496 (0.996)	10566
18-01	70.01505; 129.51544	Eolian plain	In situ basal organics	Bulk sed.	OUC-7406	0.45	5549±28	6398-6295 (1)	6344
18-03	70.01128; 129.52246	Eolian plain	In situ basal organics	Bulk sed.	OUC-7407	0.30	4212±26	4675-4646 (0.11) 4761-4694 (0.50) 4848-4803 (0.39	4746
18-10	70.06641; 129.44060	Eolian plain	In situ basal organics	Bulk sed.	OUC-7414	0.50	8708±31	9746-9550 (0.99) 9761-9753 (0.01)	9645
18-11	70.06644; 129.41782	Eolian plain	In situ basal organics	Bulk sed.	OUC-7415	0.70	5181±28	5955-5907 (0.69) 5990-5957 (0.31)	5936
18-04	70.01259; 129.49863	Drained pond	In situ basal organics	Bulk sed.	OUC-7408	0.30	9031±37	10244-10174 (1)	10212
Eolian and lacustrine sands (Fig. 7; section 18-13)									
18-13.1	70.06947; 129.41801	Lacustrine sand	Detrital organic layer	Wood	OUC-7417	4.00	9860±33	11319-11209 (1)	11251
18-13.2	70.06947; 129.41801	Lacustrine sand	Detrital organic layer	Bulk sed.	OUC-7418	2.00	4192±26	4762-4625 (0.75) 4838-4796 (0.25)	4733
18-13.3	70.06947; 129.41801	Eolian sand	Detrital organic layer	Bulk sed.	OUC-7419	1.00	1930±22	1925-1824 (1)	1879
Cape Dalhousie Sands (Table S1d)									
18-07	70.01390; 129.49892	Subsurface exposure	Detrital wood	Wood	OUC-7411	2.50	>46500	n/a	n/a
18-08	70.01390; 129.49892	Subsurface exposure	Detrital wood	Wood	OUC-7412	3.00	>46500	n/a	n/a
Eolian sand-sheet deposits (Bateman and Murton, 2006; sections 2.9 and 2.12)									
2.9-1	69.91486; 129.87755	Eolian plain	In situ sandy humic organic layer	Bulk sed.	Beta – 195573[a]	0.25	2020±60	1843–1831 (0.01) [b] 2134–1864 (0.99) [b]	1979
2.9-2	69.91486; 129.87755	Eolian plain	In situ wood	Wood	SRR-6928	4.25	10949±70	12992–12709 (1) [b]	12817
2.9-3	69.91486; 129.87755	Eolian plain	In situ wood	Wood	SRR-6929	3.75	10578±80 [c]	12284–12236 (0.02) 12340–12301 (0.01) 12715–12377 (0.96)	12548
2.9-3	69.91486; 129.87755	Eolian plain	In situ wood	Wood	SUERC-1934	3.75	10609±59 [c]	12494–12425 (0.12) 12702–12517 (0.88)	12595
2.12-1	69.934789; 129.81194	Eolian plain	Detrital Wood	Wood	SUERC-1687	1.40	10074±59	11836–11332 (0.94) 11959–11869 (0.06)	11630

All ages were obtained by accelerator mass spectrometry (AMS) dating, except from three analyses (Beta – 195573, SRR-6928 and SRR-6929), which were obtained by standard radiometric dating (liquid scintillation counting)

[a] Calibrated by CALIB 7.1 using IntCal13 calibration dataset (Stuiver et al., 2019); 95.4 % (2σ) cal age ranges BP (relative area under distribution)

[b] Relative area under distribution

[c] Two assays on same wood fragment using standard radiometric dating (SRR-6929) and AMS dating (SUERC-1934)

4.3 Shothole data analysis

The locations of shotholes, water depths and a summary of stratigraphic logs are provided in Supplementary Materials S2. Below, we summarize observations of water depths, stratigraphy and ground ice.

4.3.1 Water-body depths

Given the absence of lake-depth data in the region, shothole data provide useful information. Shothole data were examined from confined lake basins, drained-lake basins and marine settings to compare recorded ice thicknesses and water depths (Table 4; see Supplementary Materials S2 for details).

Most basin depths, whether within the marine nearshore or beneath lakes, are less than 5.0 m, and littoral shelves are less than 1.8 m deep with the ice frozen to the bed (Fig. S2-2). Shotholes drilled beneath breached lakes indicated the shallowest water depths, with a maximum (ice + water) depth of 5.2 m (Table 4). The marine nearshore recorded water depths beneath the ice ranged from 0.3 to 6.1 m, and a maximum (ice + water) depth of 7.9 m. The greatest depths occurred beneath undrained lakes, with a maximum combined ice and water depth of 9.1 m occurring in three separate lakes. Two were adjacent oriented lakes, with dimensions of 1800 by 1300 m, and 1500 by 1000 m, respectively, with shallow littoral shelves up to 300 m wide. The third was a small non-oriented lake within a 400 by 600 m basin. Additionally, one hole drilled beneath a small stream connecting two lakes encountered a depth of 6.4 m (1.8 m ice + 4.6 m water). Despite the occurrence of a few deep basins, most central basins within the undrained lakes are relatively shallow (2.0–5.0 m).

Table 4. Range in depth of ice and water, and maximum depth of ice and water, encountered in 1098 shotholes, sorted by water body type.

Water body	Ice (m)	Water (m)	Maximum (m) ice + water*	Number of holes
marine nearshore	0.6–2.7‡	0.3–6.1	7.9	312
undrained lakes	1.2–4.6‡	0.3–7.3	9.1	225
breached lakes	0.9–3.0‡	0.3–3.4	5.2	107
stream	1.8	4.6	6.4	1

‡ where ice thickness exceeds 2.4 m it is assumed to include snow cover
* maximum depths include 1.8 m of recorded ice plus recorded water depth

4.3.2 Stratigraphy and ground ice

Unlike other areas of the Tuktoyaktuk Coastlands, gravel and boulders that may be interpreted as glacial outwash or till were not recorded in these shotholes. Sandy sediments, however, are not only prevalent at the surface but are the predominant subsurface material on the northeastern McKinley Bay Coastal Plain. Combined shothole observations of sand or silt occurred in 95% of shotholes (Table 5) and were most common beneath drained basins. This likely relates to the continuity of Kittigazuit Fm or Cape Dalhousie Sands and underlying Kidluit Fm, and possibly Kendall sediments, beneath the area, as well as to modern deposition of sandy materials in the marine nearshore and on shallow littoral shelves of oriented lakes.

In contrast, clay is less common in the northeastern McKinley Bay Coastal Plain area (26% of shotholes; Table 5, Fig. S2-4). Shotholes drilled on land confirm the occurrence of clay at depth throughout the area, in similar abundance beneath land, drained-lake basins, breached lakes, and the marine nearshore, but less common (21%) beneath confined lakes. Although typically underlying the sands, in 5% of shotholes clay was the only sediment recorded. The clays could be Hooper clay, which is presumed to be regionally extensive (Rampton, 1988; Murton, 2009). The occurrence of shotholes encountering only clay (i.e. no sand or silt) within lake basins and the marine nearshore indicates potential deposition of clay at the surface with perhaps only a thin veneer of sand and silt. It is possible that re-deposition of clays could occur with thermokarst activity and slumping beneath water bodies. However, 99% of shotholes drilled beneath drained lake basins encountered sand, which indicates that the shallow littoral shelves of oriented lakes are composed primarily of sand and that the lake basins also infill primarily with sand.

Table 5. Number and percent (in brackets) of shotholes recording sand or silt, and clay, sorted by terrain or water-body type. Note that 16 of 1098 shotholes contained no stratigraphic record.

Terrain or water body	**Sand or silt**	**Clay**	**Clay only**	**Number of holes**	**No record**
all	1025 (95)	282 (26)	57 (5)	1082	16
lowland	283 (94)	77 (26)	14 (6)	300	0
drained basins	152 (99.3)	39 (25)	1 (0.7)	153	0
confined lakes	215 (98)	47 (21)	5 (2)	220	5
breached lakes	91 (88)	30 (29)	12 (12)	103	5
marine	282 (92)	89 (29)	25 (8)	306	6

Ground ice was noted in only 10 of 1098 boreholes, at four locations in the area (see Supplementary Materials S2 for details). This included a small, shallow drained-lake basin with ground ice at 10 to 20 m depth, and ice occurring between 7 and 40 m at the other locations. These observations indicate that near-surface excess ground ice is rare on the northeastern peninsula.

4.4 Geomorphic mapping

Detailed maps of eolian dunes, lake basins and drainages (channels and streams) are provided in Supplementary Materials S3. Below, we present specific results relevant to the landscape evolution of the area.

4.4.1 Eolian dunes

Two prominent dune types occur on the McKinley Bay Coastal Plain: lakeshore dunes and parabolic dunes (Fig. 8A). Both active and stabilized lakeshore dunes occur around the margins of mostly drained or partially drained lakes, whereas all of the parabolic dunes are stabilized and occupy the intervening lowland terrain. The stabilized parabolic dunes differ from the lakeshore dunes in several significant ways. First, the lakeshore dunes represent the accumulation of sediment from a fixed source and have migrated no more than 200 m from lake shorelines. In contrast sediment supplying parabolic dunes has been transported further due to higher supply rates and/or longer development times, and the parabolic dunes are up to 800 m long. Second, the oriented-lake shorelines truncate many of the parabolic dunes (see Fig. 8), indicating that lake expansion post-dates dune stabilization. Third, whereas the lakeshore dunes have distinctive upwind source areas, the stabilized parabolic dunes do not. The absence of blowout features upwind of the parabolic dunes suggests that the upwind surfaces may have been largely devoid of vegetation, which would otherwise have preserved blowout hollows. This helps explain why the parabolic dunes, although longer than the lakeshore dunes, are still only a few hundred to several hundred metres long. The formation of a vegetation cover likely promoted dune stabilization and dune ridge preservation. Without the stabilizing effect of vegetation cover, earlier dune features would not have been preserved.

An examination of parabolic dune orientations found only slight difference across the McKinley Bay Coastal Plain, when divided into two sectors (see Supplementary Materials S3 for details). The mean dune orientation is approximately 267.6° in the eastern sector (based on 1623 observations), and in the western sector it is 269.2° (1638 observations) (Fig. S3-3). This small difference of 1.6° is statistically significant under a two-tail t-test at 0.01 level of significance. Overall, the dune orientations in both sectors indicate net sediment transport toward the west during dune activity.

Two generations of lowland dunes are evident. The shapes of the lowland dune ridges are typically indicative of stabilized parabolic dunes, as the preserved dune crest ridges are convex in the downwind (westward) direction (Fig. 8A). However, sequences of preserved residual dune ridges on the eastward ends (i.e. in the upwind direction) of the parabolic dunes are concave toward the west (Fig. 8B). Residual dune ridges preserve the shape of the stoss (upwind) side of the dunes as they migrate downwind (Wolfe and Hugenholtz, 2009). In these cases, the ridges signify a change in form from barchanoid dunes to parabolic dunes prior to stabilization. Although active barchan dunes do not presently occur in Canada, they have previously occurred under cold, dry (non-permafrost) conditions in southern Canada (Wolfe and Hugenholtz, 2009), and examples of active barchanoid dunes in modern permafrost environments include those in the Victoria Valley, Antarctica; and Kobuk Valley, Alaska (Dijkmans and Koster, 1990; Bourke et al., 2009).

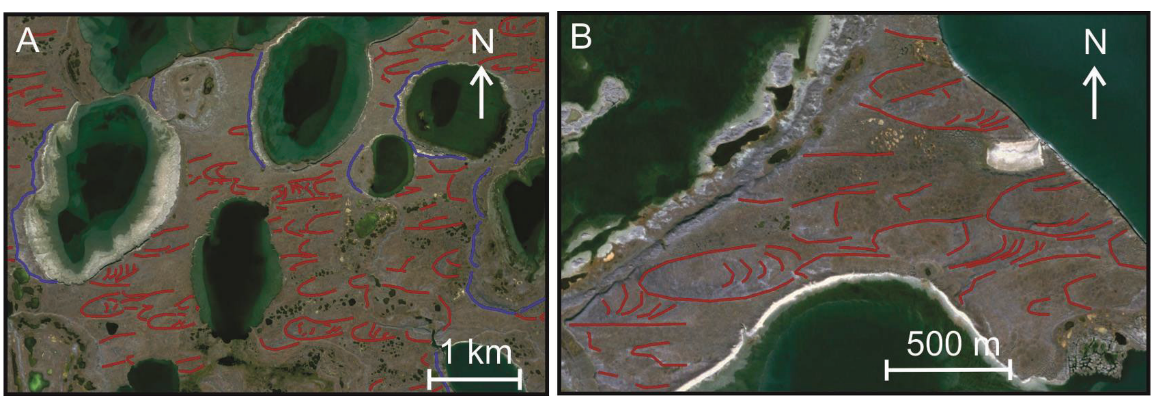

Figure 8. Surficial eolian dunes. A) Source-bordering lakeshore dunes (blue lines) and stabilized lowland dune ridges (red lines). B) Stabilized lowland dune ridges with residual dune ridges indicative of barchanoid dunes. Note truncation of stabilized dune ridges by lake shorelines. Lowland dune lengths in both A and B are indicative of a period of transition from unvegetated dunes to dunes fully stabilized by vegetation. Image source Google Earth.

4.4.2 Lake basins and streams

Water-filled lake basins occupy approximately 40% of the area between McKinley Bay and the northeastern tip of the Tuktoyaktuk Peninsula (Fig. S3-4). Two scales of landform alignment are apparent from mapping of lake basins and streams in a portion of the McKinley Bay Coastal Plain (Fig. 9) (see Supplementary Materials S3 for details). First, the lake basins individually are strongly oriented, with average trends previously reported as 6° (i.e. N 6° E; Mackay, 1963) and as 7° (Côté and Burn, 2002), respectively. Mackay (1963) found an eastward, clockwise, shift in the axial trend based on analysis of 88 lakes: from 2° in the west (27 lakes) to 5° in the centre (30 lakes) and 11° in the east (31 lakes). We examined lake azimuths in two sectors to compare to those reported by Mackay (1963), obtaining mean axial trends of 5.5° in the western sector (based on 687 observations) and 21° in the eastern sector (220 observations) (Fig. S3-4 and S3-5). The difference of 15.5° is statistically significant under a two-tail t-test at 0.01 level of significance, confirming an eastward, clockwise, shift in the axial trend of lake basins.

Second, the lake basins collectively are arranged in a parallel northward-trending alignment. That is, the central portion of the lakes tend to be aligned in parallel succession, rather than being random or offset. Figure 9 also illustrates the streams and channel network between drained and undrained lakes, indicating a degree of connectivity, despite the low slope and relief.

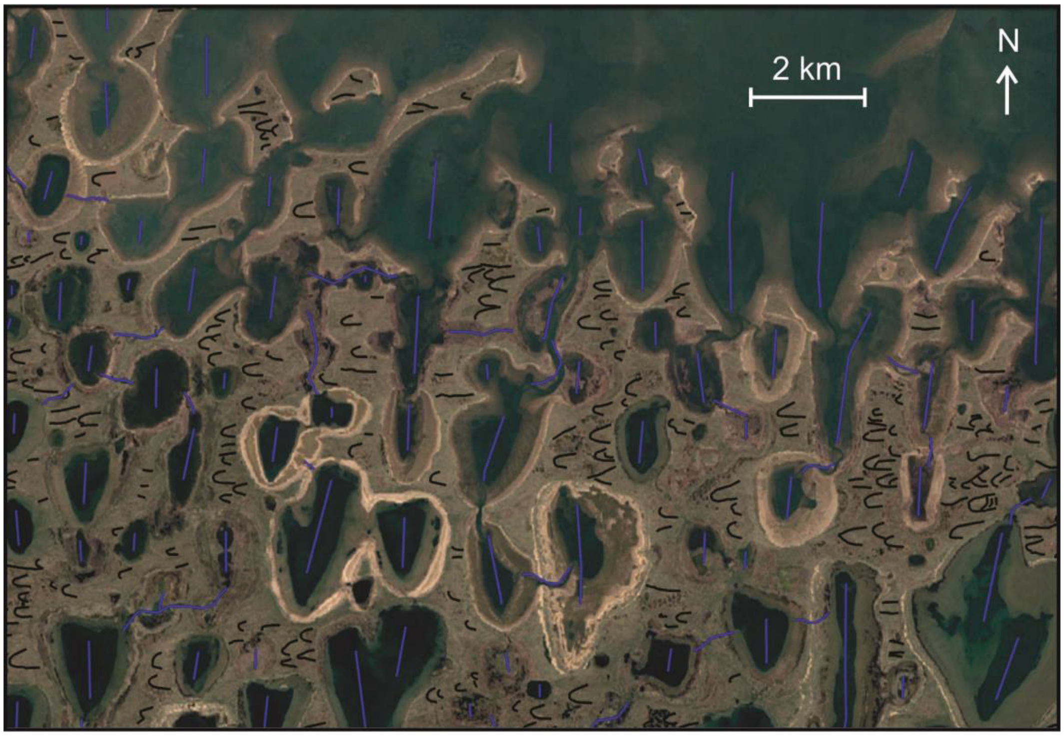

Figure 9. Example of lake-basin orientations (straight blue lines) and streams (irregular blue lines) and stabilized lowland dune ridges (black line). Image source Google Earth.

5. Discussion

5.1 Sedimentation and landscape processes

A conceptual framework in which to place the initiation and development of the oriented lakes of the McKinley Bay Coastal Plain requires an understanding of late Quaternary geological processes and glacial limits. We consider these in terms of (1) preglacial and proglacial processes, (2) glacial processes and limit, and (3) postglacial processes.

5.1.1 Preglacial and proglacial processes

Neither Hooper clay nor Kendall sediments were observed within stratigraphic sections ~4–25 m high in the McKinley Bay Coastal Plain, though they likely underlie the region, as noted by observations of clay in the shothole logs. Although Kidluit Fm sand was identified at only one exposure (Fig. S1-5), these sediments also likely underlie much of the area as they are observed regionally both onshore and offshore (Rampton, 1988; Murton et al., 2017). In fact, the Kidluit Fm is thought to be the major source of sand, reworked by wind, for the overlying Kittigazuit Fm (Dallimore et al., 1997). Consequently, the McKinley Bay Coastal Plain likely represented part of a more extensive paleo-river braidplain prior to drainage diversion caused by glacial advance in the south (Murton, 2009). Sedimentation may have occurred here throughout much of the early to mid Wisconsinan, as the age of 62.6 ± 3.44 ka obtained on Kidluit Fm sediments in the area resides within the earlier age range obtained regionally (Murton et al., 2017).

The Kittigazuit Fm was observed only in the southern portion of the McKinley Bay Coastal Plain, where in most instances it was capped by till and outwash sediments attributed to the Toker Point Stade. The Kittigazuit Fm is regionally dated to between 43 and 13 ka (Bateman and Murton, 2006) and on the McKinley Bay Coastal Plain is dated to between 43.4 and 14.5 ka. Eolian activity, in the form of large dune construction, likely occurred over abandoned portions of the Kidluit Fm braidplain as regional flow declined and transitioned to a glacial discharge streamflow, exposing Kidluit Fm sands to eolian processes.

The Cape Dalhousie Sands underlie lowland terrain in the northern half of the McKinley Bay Coastal Plain and have been interpreted by Rampton (1988) as glaciofluvial outwash deposited during the Toker Point Stade. We have dated the sands to between 18.6 and 14.3 ka, which is partly in the age range of 17.5–15 ka for the glacial limit on Richards Island. Overall, the Cape Dalhousie Sands are generally coarser grained and more gravel-rich than the Kidluit Fm. We suggest that the McKinley Bay Coastal Plain area occupied by oriented lakes was characterized by braided channels that likely carried glacial outwash, as seasonal glacial meltwater, northward across the former braidplain of the preglacial river system. Although it could be argued that Kittigazuit Fm sands were subsequently eroded from the area, either by glacial advance or fluvial activity, this appears unlikely as remnants of them would likely remain. Rather, the Cape Dalhousie Sands and the Kittigazuit Fm were contemporaneous, as their ages and those of sand wedges within them overlap. Kittigazuit Fm deposition occurred on the abandoned portions of the regional braidplain, whereas glacial outwash sedimentation continued in this area, depositing the Cape Dalhousie Sands. Eolian processes were active in both areas, with large dunes characteristic of the Kittigazuit Fm occurring in areas of higher sediment supply. Antisyngenetic sand wedges within the Cape Dalhousie Sands, dating to between 18.8 and 16.1 ka, attest to eolian deflation over terrestrially exposed areas at this time. The absence of thicker eolian sediments over the Cape Dalhousie Sands is likely due to a limited sediment supply, caused by a cap of lag deposits on the terrestrial surface, and by active water-filled channels in low-lying areas.

5.1.2 Glacial processes and limit

The Toker Point Stade limit is well defined south of the McKinley Bay Coastal Plain and appears to represent the late Wisconsinan glacial limit on the Tuktoyaktuk Peninsula. Highly deformed preglacial sediments and ground ice underlie a glacial diamicton extensively within the Toker Point Stade glacial limit along Liverpool Bay, Nicholson Island and the Eskimo Lakes regions (Mackay, 1956b, 1963; Murton et al., 2004, 2005). Toker Point Till and outwash sediments, probably the Turnabout Member (Rampton, 1988), occur along the southern boundary of the McKinley Bay Coastal Plain within the upland area underlain by Kittigazuit Fm sands (Fig. 3). However, no diamicton is observed in the lowland terrain in the northern half of the McKinley Bay Coastal Plain. Rampton (1988, Figure 56) mapped extensive outwash plains, including the Cape Dalhousie Sands, across the northeastern Tuktoyaktuk Coastlands and valley trains north of the Toker Point Stade limit (Fig. 1). This suggests that when glacial ice was at this limit, meltwaters drained northward across McKinley Bay Coastal Plain.

The McKinley Bay Coastal Plain may have been unglaciated during the last ice advance (Mackay, 1963, p.22). Evidence includes an absence of recognizable glacial features north of the inferred glacial limits and very few erratics along the shorelines and at Atkinson Point (Fig. 1). Two, independent lines of evidence, however, suggest that thin ice likely did advance a short distance beyond the well-defined glacial limit of the Toker Point Stade. The first, reported by Mackay (1963, Figure 4), is the transition in channel width across the glaciofluvial outwash plain north of the Toker Point limit between Eskimo Lakes and McKinley Bay (Fig. S4-1). This channel, which disappears to the south at the Toker Point Stade limit, is defined by a narrow (ca. 500 m wide) glacially-modified winding channel within hilly terrain, which transitions northward at about 69.73° N into a broad (≤7 km wide) channel with multiple terraces across flat terrain. This transition is only about 5 km north of the Toker Point limit as mapped by Rampton (1987) (see Supplementary Materials S4 for details). The second line of evidence is the deformed uppermost strata of the Cape Dalhousie Sands, overlain by a pebbly silty sand and erosional surface observed at section 05-01 (Fig. S1-2) in this study. Similar deformation occurs in Kittigazuit Fm sands overlain by Toker Point till on Hadwen Island (Murton et al., 2015). On the McKinley Bay Coastal Plain, an overlying till unit appears absent, with the contact defined by a thin pebbly silty sand layer with convoluted lamination. These overturned strata suggest that the Cape Dalhousie Sands were glaciotectonically deformed, possibly by thin ice with little or no till. Given the OSL ages of 18.6 to 14.3 ka from Cape Dalhousie Sands, this suggests that if glacier ice advanced over the McKinley Bay Coastal Plain, then it occurred within this time period. This site is only ~10 km north of the inferred Toker Point Stade limit at Liverpool Bay, and the absence of an overlying diamicton and outwash sediments suggests that glacial ice cover here was thin.

If glacial ice did not extend across the entire McKinley Bay Coastal Plain during the last glacial advance, the question arises as to why permafrost thickness here is less than on Richards Island. Permafrost beneath the McKinley Bay Coastal Plain is thinner (300–500 m) than beneath Richards Island (600–

700 m), yet geological evidence suggests that much of Richards Island also remained ice-free until between about 17.5 and 15 ka (Murton et al., 2015). We suggest that during most of the last glacial interval the Richards Island area was covered by Kittigazuit Fm dunes, which occupied the abandoned braidplain of the Kidluit Fm. Cold arid conditions across the abandoned plain on Richards Island promoted permafrost aggradation to depths of 700 m. In contrast, inundation by persistent seasonal meltwater flow across the active braided-channel network on the McKinley Bay Coastal Plain may have inhibited deep permafrost aggradation during this same period. In contrast, permafrost thickness to the south, within the limit of the Toker Point Stade, is typically less than 300 m where it is was extensively covered by glacial ice.

5.1.3 Postglacial processes

Extensive eolian deflation across the McKinley Bay Coastal Plain is indicated by antisyngenetic sand wedges, the erosional contact with wind-polished pebbles, and overlying eolian sand sheets. Such wedges grow downward beneath land surfaces lowering by denudation. Eolian activity occurred between 12.8 and 4.4 ka, with eolian activity truncating sand wedges occurring between 10.9 and 5.3 ka, based on OSL ages. During the early part of this period (ca. 12.8 to 10.9 ka) eolian erosion occurred on a mostly unvegetated landscape of exposed alluvial sediments. Sand wedges remained active as alluvial deposits were deflated, and abandoned fluvial channels were filled in by eolian sheet sands, whereas wider and deeper alluvial channel sections remained open as isolated basins. Sediment-transporting winds were primarily from the east.

Small deflationary basins and low-lying terrain also formed through eolian erosion. Dune forms at this time were probably low-relief barchans, migrating westward over a predominantly dry and unvegetated surface. Barchan dune formation likely occurred under a cold, arid climate with bare sand but a restricted supply—caused by a shallow permafrost table and/or a pebbly substrate—limiting the dune size. The limitations on sand supply, likely caused by development of a coarse-sediment lag deposit (Fig. 4 and 5), probably restricted the size of the dunes more than did the permafrost table.

Increasing surface moisture and vegetation cover during the early Holocene caused a change in dune type from barchanoid to parabolic across the former alluvial surfaces. Vegetation cover, represented by a humic organic layer, began to establish as early as 10.7 cal ka BP, and covered much of the lowland surfaces by 8.9 cal ka BP. Sediment-transporting winds at this time were from the east, driving dune migration toward the west (267° to 269°), as indicated by stabilized dune ridges. Parabolic dunes continued to migrate across the area until about 4.6 cal ka BP. As Holocene winds persisted under an increasingly bimodal (ENE and WNW) regime, wave action and currents drove lake expansion and lake orientation, which eroded the vegetated shorelines and created shallow littoral shelves along the lake perimeters (Mackay, 1963; Côté and Burn, 2002). Nevertheless, sediment-transporting winds from the east have remained dominant until present, as evidenced by contemporary westward-migrating lakeshore dunes and an absence of shoreline dunes on the eastern lakeshores.

Postglacial eolian activity occurred almost entirely on terrain lacking earlier high-energy outwash activity. Although eolian dunes occur extensively on much of the McKinley Bay Coastal Plain, they are absent on outwash deposits south of McKinley Bay, where a large valley train extends north of the Toker Point Stade limit, except for one localized area (See Supplementary Materials S3 for details). The persistence of eolian activity between about 12.8 and 4.4 ka suggests that areas subjected to late-stage high-energy glaciofluvial outwash deposition were not subsequently conducive to dune construction.

5.2 Origin of primary basins

To evaluate the origin of the primary basins, we first briefly consider their morphology and how it compares with that of other tundra lakes developed in late Quaternary sedimentary sequences in the Tuktoyaktuk Coastlands.

The oriented lakes of the McKinley Bay Coastal Plain generally consist of "deep central troughs" partially surrounded by shallow submerged littoral shelves (Mackay, 1963, pp.46–55). Shothole data indicate that most closed-basin oriented lakes in the area typically have central basins that range between 2.0 and 5.0 m in depth, but reach a maximum depth (ice thickness + water depth) of about 9 m. Rampton (unpublished data) measured the water depth of the central basin of one oriented lake to range between 7 and 9 m, and the shallow littoral shelf between 60 and 120 cm deep. These shelves are typically 100–400 m wide along the long axis of the oriented lakes, but narrow or disappear near the ends of the lakes. As indicated by the shothole data, these shallow shelves freeze to the lake bottom in winter (Burn, 2002). Permafrost is likely preserved in these areas, whereas taliks occur in the sediments beneath the central basins. This assumption is supported by observations of water depths in 12 tundra lakes on Richards Island from Burn (2002), which range from 2.1 to 13 m, with shallow littoral shelves of < 1 m. There, the shelves are underlain by permafrost, with a talik beneath the central pool. Those lakes occur within ice-rich morainic terrain, and about one quarter of the lakes have taliks that penetrate the permafrost beneath the deep central pools (Burn, 2002). Shothole data reveal maximum recorded water depths of 16 m on Richards Island, compared to 9 m on northeastern McKinley Bay Coastal Plain (Fig. S2-3). It appears that the oriented lakes in the McKinley Bay Coastal Plain have central basins that are shallower than the tundra lakes within moraine deposits on the Tuktoyaktuk Coastlands. As well, the upper tens of metres of permafrost on the Tuktoyakuk Peninsula are generally sandy and ice-poor (Fig. S2-4), which raises the question as to whether these lakes on the coastal plain, therefore, have an origin independent of thermokarst processes.

Recently, Jorgenson and Shur (2006) re-evaluated the mechanisms of initiation and expansion of oriented lakes in northern Alaska, proposing an alternative to the “thaw-lake cycle”. They proposed that thermokarst processes caused by the degradation of ground ice were not the primary mechanism to form these lakes. Rather, the original lakes and basins formed from the initial flooding of depressions in low-lying areas across the undulating surface and that many of the deep lakes today are simply remnants of these older lakes. This proposal, although supported by that fact that the area studied contained insufficient ground ice to form thaw lakes, did not discuss how the nature of these incipient depressions, or earlier landscape processes, may have promoted their formation.

5.2.1 Non-thaw-lake basin origin

Several lines of evidence indicate that the oriented lakes of the McKinley Bay Coastal Plain also did not originate and evolve as thaw lakes from the melting of underlying excess ice:

(i) Paucity of near-surface massive ground ice or icy layers.

Mackay (1971) examined 4150 seismic shotholes logs in the Tuktoyaktuk Coastlands, of which 263 (6%) recorded massive ice, with a mean thickness of about 13 m, and 26% of the shothole logs recorded layers of sand and ice. Commonly these massive ice layers underlie an upper layer of sandy clay and boulders (interpreted as till) and overlie a lower layer of sand. In the McKinley Bay Coastal Plain, however, only 10 of 1098 (0.9%) shothole logs recorded any ice, indicating that massive ice and icy layers are rare in near-surface sediments.

(ii) An absence of thaw slumps associated with ice-rich sediments.

The present-day terrain associated with massive icy and icy sediments in near-surface sediments is hummocky or undulating, either as a result of glacial landscape-forming processes or Holocene thermokarst processes (Rampton, 1984). Thaw slumps are commonly associated with this terrain and are co-located with lake basins (Kokelj et al., 2009). In contrast, such slumps are entirely absent from the oriented-lakes region of the McKinley Bay Coastal Plain (Mackay, 1963).

(iii) Surficial sediments not conducive to thaw subsidence.

Unlike most of the Tuktoyaktuk Coastlands, the stratigraphy in the McKinley Bay Coastal Plain is dominated by an upper layer of sand or silt (as noted in 95% of the shotholes) and an absence of clay and boulders (which might represent till). Most shotholes recording clay note it below the sand/silt unit or otherwise primarily in shotholes in marine or breached lake settings. Compared to stratigraphy containing icy sediments (Mackay and Dallimore, 1992), this area is uncharacteristic in terms of its sandy near-surface stratigraphy. Similarly, surficial sediments noted in the field reveal a dominance of eolian sand sheets underlain by eolian and alluvial sands with intervening sand wedges. Almost none of the exposed sediments are thaw-sensitive and none show signs of post-depositional thaw subsidence.

(iv) No organic terrain or ice wedges in the early Holocene to initiate thaw subsidence or lake expansion.

Given the absence of massive ice and icy sediments and the predominance of thaw-stable (sandy) near-surface sediments, an alternative origin for thaw lake basins may be the thawing of ice wedges (Jorgenson et al., 2015) to form initial small thermokarst ponds (Billings and Peterson, 1980; Jorgenson and Shur, 2007). In the study area, the earliest basal age of the humic organic layer dates to about 10.7 cal ka BP. Thus, postglacial ice-wedge development in the

McKinley Bay Coastal Plain was likely initiated at this time, or later, with ice-wedge growth occurring during the Holocene. In this regard, initiation of thaw lakes induced by ice-wedge degradation should be more prevalent into the late Holocene as wedge-ice volume increases with time. However, field evidence from section WDA18-13 (Fig. 7) indicates that lacustrine basins existed as early as 11.3 cal ka BP, suggesting that lakes and basins existed when near-surface ice-wedge volumes were low.

(v) Lake basins unresponsive to historic warming.

Thaw-slump activity in the Mackenzie Delta region has increased from 1950–1973 to 1973–2004, probably due to increased annual and summer air temperatures (Lantz and Kokelj, 2008). As noted above, most slumps in the region are associated with lakes, and increased slumping has promoted lake enlargement, talik expansion and thawing of deeper ground ice (West and Plug, 2008). In contrast, Plug et al. (2008) found that the tundra lakes on the McKinley Bay Coastal Plain changed very little overall between 1978 and 2001, further supported by observations of Olthof et al. (2015) for the period of 1991 to 2001. Observed changes in lake area were primarily correlated to short-term antecedent cumulative precipitation, with no long-term trends that relate to warming or changes in the evaporation / precipitation balance. These observations led Plug et al. (2008) to suggest that, among other possible causes, few of these lakes may be of thermokarst origin.

5.2.2 Formation of initial depressions

Without evidence for a thermokarst subsidence origin of these lake basins, we examine past landscape and permafrost processes that may have promoted the formation of initial depressions and the formation of central lake basins.

As noted earlier, the McKinley Bay Coastal Plain is widely underlain by Cape Dalhousie Sands, interpreted here as an alluvial plain supplied with seasonal glacial meltwater, and that occupied the earlier preglacial braidplain of the Kidluit Fm alluvial system. Flow was generally northward, away from the meltwater source and across the broad coastal plain. However, the observed clockwise shift from west to east in northward alignment of oriented lakes in the area is unexplained (Fig. S3-4). We suggest that this shift—from 5° to 21° (Mackay, 1963, Côté and Burn, 2002; and this study)—may reflect trends in regional drainage alignment, as does the parallel arrangement of the central portion of these lake basins (Fig. 10A). In addition, whereas present-day streams may be enhanced by thermal erosion along ice wedges, permitting lake drainage or partial drainage, incised streams connecting both drained and undrained lakes may also represent part of the former drainage network.

These observed patterns closely follow the drainage alignments of other Arctic river braidplains, for example that of the second level terrace of the Lena River Delta, northern Yakutia, Russia (Fig. 10B; Morgenstern et al., 2008). Although its origin has been debated, this terrace is interpreted by Are and Reimnitz (2000) to a have formed by alluvial deposition, and is interpreted by Schwamborn et al. (2002) as a highly energetic periglacial braided river channel network deposited in the early Holocene. The terrace is 20 to 22 m above sea level, composed of freshwater sand deposits with oriented-lake basins containing 1 to 2-m-deep shelves and 10 to 35-m-deep central basins. Schwamborn et al. (2002) suggested that periglacial outwash sedimentation occurred during early summer peak discharge of the Lena River. The resulting forms included river channels, sandbars and oxbow lakes (Schirrmeister et al., 2011) across an area that, today, comprises deep-basin oriented lakes. The surficial terrain contains ice wedges but is otherwise ice-poor, and the thawing of ice-wedge terrain cannot account for the deep lake basins (Grigoriev, 1993 in Are and Reimnitz, 2000). Morphologically, the McKinley Bay Coastal Plain closely resembles an Arctic alluvial plain like the Lena River delta, and the underlying Cape Dalhousie Sands support this interpretation.

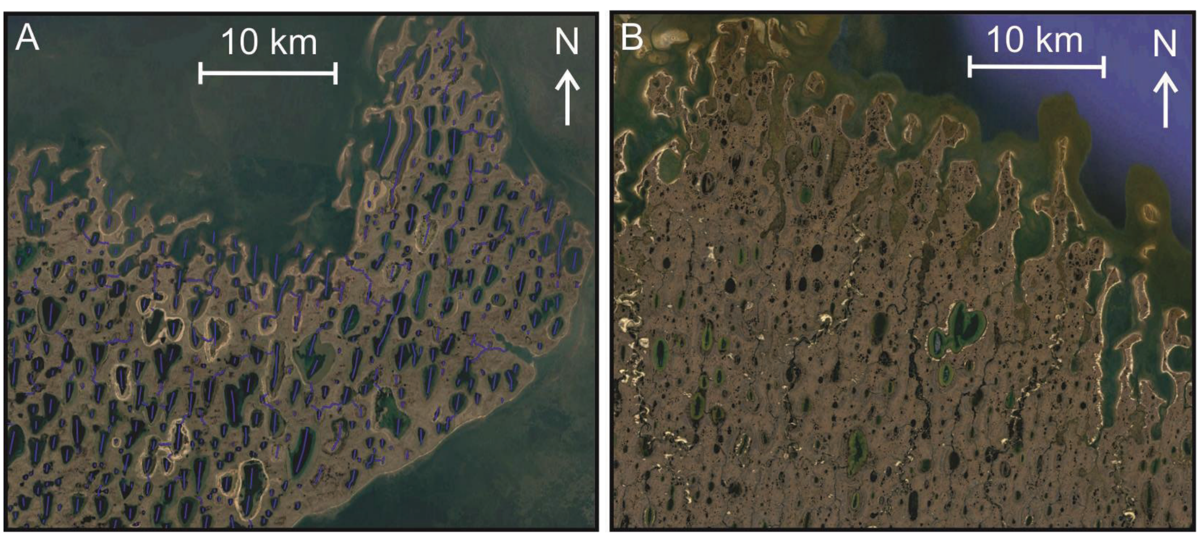

Figure 10. Comparison of drainage patterns of A) the northeastern McKinley Bay Coastal Plain and B) the second level terrace of the Lena River Delta. Blue lines in A show lake orientations and streams. Image source Google Earth.

We hypothesize that the process of deep-basin formation in the McKinley Bay Coastal Plain was associated with alluvial processes operating within a periglacial setting. The alignment of lakes with deep central basins along apparent stream channels suggests that these two features are connected by a common process. Although the exact mechanism of channel deepening is not known, deepening may have occurred during seasonal high-energy flow (Schirrmeister et al. 2011) or during early-season discharge when surface ice or icings were present to facilitate channel scour (Woo, 2012). In this regard, and in close proximity to the glacial limit, the McKinley Bay Coastal Plain closely resembles a sandar or, as French (2007) suggested, a periglacial sandar.

If the oriented lakes of the McKinley Bay Coastal Plain originated within river channels discharging water across a broad braidplain, then it is significant that the oriented lakes today represent discrete basins that are not all clearly connected. Exposures within the area indicate that it is widely mantled with eolian deposits, and that eolian erosion and deposition have significantly altered the surface expression of the underlying Cape Dalhousie Sands. The eolian sand-sheet deposits are 2 to 10 m thick, and typically about 5 m (Fig. 3), blanketing the underlying fluvial deposits. OSL and AMS dating of eolian sediments, truncated sand wedges and organic materials indicate that eolian processes operated extensively between at least about 12.8 and 5.3 ka. As such, eolian activity reworked the surface and eolian sands filled abandoned portions of the former fluvial channel network.

5.2.3 Basin widening and central basins

Dyke and Evans (2003) questioned why in the Tuktoyaktuk Coastlands "shallow lakes occurring in non-moraine terrain are wind-aligned whereas deeper kettle-like lakes on morainic terrain are not". Tundra lakes on morainic terrain in the Tuktoyaktuk Coastlands contain ice-rich thaw-sensitive sediments in the near surface (Fig. 11A). The primary mechanism of lake expansion of these lakes is by melting and slumping of ice and sediments along the lake perimeter (Murton, 1996), described by Kokelj et al. (2009) as the polycyclic behaviour of tundra thaw slumps. Climatic warming has increased the rate of retrogressive thaw slumping and, in turn, lake expansion (Lantz and Kokelj, 2008). These lakes are not wind-aligned, as wind-induced currents and wave erosion do not play a significant role in their expansion. Rather, lake shape is defined by the location and abundance of thawing near-surface ice-rich sediments. In ice-rich terrain, tundra lake basins include both central basins, where deep taliks have developed, and lake-perimeter basins, where subadjacent ice-rich permafrost has thawed along the lake margins (Kokelj et al., 2009). Whereas lakes with both of these basin types occur on glaciated terrain on the Tuktoyaktuk Peninsula (Fig. 11A), only lakes with central basins occur on the McKinley Bay Coastal Plain (Fig. 11B). Additionally, the cohesive nature of fine-grained till—which is extensive in regions of massive ice in the Tuktoyaktuk Coastlands—limits or prevents wave and current reworking of sand and development of littoral shelves and oriented-lake basins. Where sediment enters the lake it is typically associated with deep holes that formed due to ice-meltout (driving conditions for more slumping), and negating terrace development (S. Kokelj, pers. comm. 2019). In contrast, the oriented lakes of the McKinley Bay Coastal Plain contain little to no excess ice in the near surface, with the exception of ice wedges which are, in general, of equal abundance around lake perimeters. With the absence of ice-rich, thaw-sensitive sediments in the near surface, wind-induced processes are the primary mechanism of lake expansion (Mackay, 1963; Côté and Burn, 2002), resulting in extensive shallow littoral shelves around lake perimeters (Fig. 11B). Thus, lake expansion is driven, not by warming-induced thaw, but by high-water stages causing shoreline erosion. Historically, these stages have been driven primarily by cumulative precipitation (Plug et al., 2008).

In summary, oriented lakes in the McKinley Bay Coastal Plain are thought to have initiated within pre-existing depressions. These lakes have their primary origins as portions of abandoned river channels and have been further modified and enlarged by wind-induced processes. Thaw subsidence through the formation of taliks penetrating permafrost is unlikely to have contributed significantly to Holocene basin deepening due to an absence of near-surface ice. Given the abundance of thaw-stable sandy sediments in the near surface, basin subsidence might only be initiated by thawing of deeper thaw-sensitive sediments. However, Burn (2002) estimated that steady-state talik conditions may be reached within thaw lakes in about 3000 years, whereas most basins here have been in place for at least 11000 years.

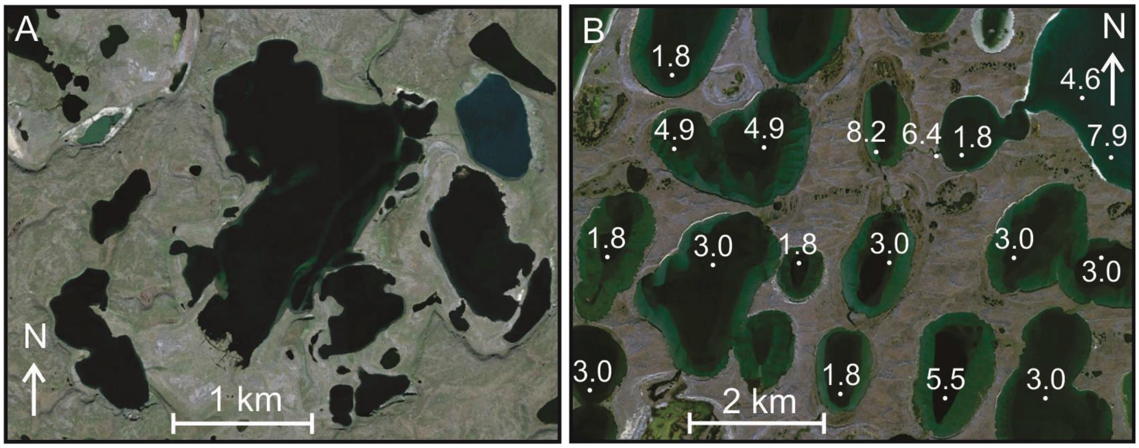

Figure 11. Comparison of tundra lakes and oriented lakes of the northeastern Tuktoyaktuk Peninsula. A) Tundra lakes with active lake-marginal thaw slumps, deep central basins and deep lake-marginal basins, south of McKinley Bay. B) Oriented lakes showing shallow littoral shelves (green) and central basins (black) with maximum lake depths in metres as recorded by shothole logs, south of Cape Dalhousie on the McKinley Bay Coastal Plain. Image source Google Earth.

5.2.4 Development of shallow littoral shelves

The development of shallow littoral shelves in oriented arctic lakes has been attributed to both deposition and subsidence (Black, 1969). Depositional features of shelves include offshore sediment thickening (Carson and Hussey, 1962), subaqueous dunes and ripples (cf. Mackay, 1963, p.50), and foreset-bedded sand (<1.5 m thick; Hopkins and Kidd, 1988). The sand is probably supplied mainly by bank erosion during lake growth and deposited by wind-driven currents (Hinkel et al., 2012). On the Tuktoykatuk Peninsula shoreline erosion predominates during high-water stages related to increased precipitation (Plug et al., 2008), which may diminish wave action with depth. During low-water stages, wind-induced currents can transport sand farther into the centre. This process results in basin shallowing over time, as sand infills the central basins.

An additional (or alternative) process by which shelves may form is thermokarst subsidence (Mackay, 1963; Sellmann et al., 1975, fig. 10). Subsidence of the lake floor may occur beneath those parts of lakes that do not freeze to the bottom in winter (>~2 m depth) and that are underlain by excess ice. In such areas the mean annual lake bottom temperature exceeds 0°C, causing thaw of the underlying permafrost (Brewer, 1958; Brown et al., 1964) and thus, through thermokarst subsidence, to accentuate the depth of the central trough of growing oriented lakes (Mackay, 1963). By contrast, the shallow shelves may freeze to the bottom, permitting the preservation of underlying excess ice. Eventually, however, the ice beneath the shelves may melt because of thaw from water perennially >0°C in the deeper part of the central trough (Sellmann et al., 1975), i.e. lateral expansion of the lake talik. Burn (2005) measured a maximum water depth of 16 m in 'Todd Lake' (informal name), an elongated lake 1.6 km long and up to 800 m wide, with well-developed sandy littoral benches, on tundra in north–central Richards Island. Beneath the central, deep pool a talik penetrates completely through the permafrost, whereas beneath the littoral benches, covered by <1 m of water, an active layer ~1.4 m deep overlies permafrost (Burn, 2002).

Our observations from a truncated partially drained oriented lake basin are consistent with a purely depositional origin for shallow littoral shelves in the McKinley Bay Coastal Plain. First, the early stages of shelf formation cannot relate to thermokarst subsidence because, as discussed above, there is little or no evidence for excess ice in near-surface permafrost when the lakes formed.

Second, the prominent foresets in section JB05-05 (Fig. 6) are unequivocally depositional features, which we interpret to have formed on the riser at the front of a shallow sublittoral shelf, prior to partial drainage of the basin. Similar foresets from another section in the area are shown in Fig. 7.

We hypothesize that the break of slope between the littoral shelves and the deeper central basins relates, at least in part, to the depth of maximum storm wave base during the ice-free season, when maximum transport of sand must occur within the lake basins. This process would be effective during high-water to low-water stages. During winter, when the shallow shelves tend to freeze to the lake bottom, the shelves would be coldest during low-water stages, which and may allow permafrost to grow inward toward the central basin.

5.3 Role of permafrost in landscape evolution and lake development

Permafrost has had a limited role in landscape evolution of the McKinley Bay Coastal Plain, largely because the sandy surficial permafrost tends to be ice-poor, with little potential for geomorphic disturbance due to frost heave or thaw subsidence. The main influence of permafrost has probably been on the thermal regime of the ice margin of the Laurentide Ice Sheet, where coupling between the ice sheet and submarginal permafrost influenced ice movement and limits and, by implication, ice-marginal sedimentation and deformation with characteristic stratigraphy and glaciotectonic structures (Murton el al., 2004). Beyond the glacial limit, the presence of permafrost influenced the morphologies, sedimentary sequences and stream patterns of the periglacial fluvial systems (Vandenberghe and Woo, 2002), giving rise to characteristic braidplain morphologies.

The influence of permafrost on eolian activity may have been to limit sand supply, giving rise to smaller barchanoid and parabolic dunes on the McKinley Bay Coastal Plain, although eolian processes are not necessarily inhibited within permafrost environments, as noted by the thicker eolian sequences that characterize the Kittigazuit Fm. Antisyngenetic sand wedges and pebble lags provide clear evidence of eolian erosion within the periglacial environment. Finally, in terms of the oriented lakes, the main role of permafrost has been on the structure and slope of littoral terraces, which are partly a function of frozen sand.

5.4 Summary of landscape evolution

We summarize the landscape evolution of the oriented-lakes terrain of the McKinley Bay Coastal Plain as follows. The preglacial landscape was dominated by a large alluvial braidplain, likely that of the paleo-Peel–Anderson river as represented by the Kidluit Fm dating to between 73 and 27 ka. As glacial ice advanced northward portions of the braidplain were abandoned and became occupied by eolian dunes of the Kittigazuit Fm between 43 and 14.5 ka. The McKinley Bay Coastal Plain, however, remained occupied by a braided-channel plain carrying seasonal meltwater northward. This area remained mostly unglaciated during the late Wisconsinan, experiencing deposition of the Cape Dalhousie Sands (dated to at least 18.6 to 14.3 ka) within an unvegetated periglacial landscape. Antisyngenetic sand wedges formed between 18.8 and 16.1 ka on exposed terrestrial surfaces undergoing eolian deflation. Glacial ice advanced to its late Wisconsinan (Toker Point Stade) limit, reaching the southern portion of the area and thin ice advanced at least a few kilometres northward of the mapped limit, reaching the Johnson Bay area (Figs. 1 and 3b).

With fluvial abandonment, eolian processes dominated, eroding the Cape Dalhousie alluvial sand deposits and truncating active sand wedges. Existing basins were modified, and other small basins were formed by eolian erosion and re-deposition. Small barchanoid dunes migrated across much of the coastal plain, except where lateglacial meltwater flowed in the McKinley Bay area. Sediment-transporting winds were from the east, and eolian sand filled many of the abandoned river channels. Incipient lake basins formed as early as 11.3 ka within deeper portions of the former fluvial channel system.

In the early Holocene, cold and dry paraglacial conditions transitioned into warmer and moister postglacial environments, as evidenced by formation of an organic layer (AMS ages) beginning at 10.7 ka, corresponding with the onset of the early Holocene climatic optimum. At this time, unvegetated barchanoid sand dunes transitioned into small vegetation-stabilized parabolic dunes that continued to migrate westward between 10.7 and 4.6 ka. Where bare sand remained, sand wedges continued to form between 10.9 and 5.3 ka, whereas in other areas sand sheets accumulated. In the absence of near-surface ground ice, lateral lake expansion particularly during high-water stages occurred by wind-dominated erosional processes, forming shallow littoral shelves that were further modified during low-water stages. This sequence of oriented-lake formation, therefore, does not support a thaw-lake cycle but, rather, the small-basin evolution of an inherited periglacial landscape.

6 Conclusions

We draw the following conclusions about oriented lakes in the McKinley Bay Coastal Plain:

1. A thermokarst subsidence origin for the initiation of the oriented lakes is discounted because of the absence or limited occurrence of excess ice in the near-surface sandy sediments. Thus, it is inappropriate to invoke a thaw-lake cycle inferred from some oriented lakes in ice-rich permafrost terrain underlain by frost-susceptible silt–clay in some other Arctic regions.

2. The oriented lakes initiated and developed in basins conditioned largely by fluvial and eolian processes operating during the last ~20,000 years. The basins initiated in river channels abandoned during Laurentide deglaciation and partially infilled with eolian sand sheets during the lateglacial and early Holocene. The oriented lakes are products of a small-basin evolution of an ice-poor sandy periglacial landscape.

3. Lateral expansion of deep-basin lakes and shallow stabilized deflationary basins predominated during the late Holocene through wind-induced wave and current processes. Lake expansion may be more effectively driven by cumulative precipitation that enhances wind-driven wave erosion, rather than increased temperature inducing thaw.

4. Wind-induced lake currents transport sand onto depositional bedforms represented by shallow littoral shelves, probably resulting in basin shallowing over time.

5. The oriented lakes of the McKinley Bay Coastal Plain differ fundamentally from tundra lakes elsewhere in Tuktoyaktuk Coastlands, where near-surface ice plays a significant role in lake-basin expansion and deepening. This highlights the distinctions between juxtaposed ice-rich glaciated terrain and ice-poor proglacial terrain.

7 Acknowledgements

JBM and MDB acknowledge financial support from The Royal Society, The Quaternary Research Association and the British Society for Geomorphology, and in-kind support for radiocarbon dating by the Natural Environmental Research Council. Logistical support was provided by the Aurora Research Institute (Inuvik) and the Polar Continental Shelf Project. Field assistance was provided by Fred Wolki, Della Murton, Enoch Pokiak and Peter Morse. Rob Ashurst is thanked for preparing all the samples for OSL dating. Comments on the manuscript by an anonymous reviewer, Peter Morse, Steve Kokelj and Xiaoping Yang are gratefully acknowledged. This paper is a contribution to Natural Resource Canada, Climate Change Geoscience Program and is contribution number 20190136.

8 References

Are, F. and Reimnitz, E., 2000. An overview of the Lena River Delta setting: tectonics, geomorphology, and hydrology. Journal of Coastal Research 16, 1083-1093.

Bateman, M.D. and Murton, J.B., 2006. The chronostratigraphy of Late Pleistocene glacial and periglacial aeolian activity in the Tuktoyaktuk Coastlands, NWT, Canada. Quat. Sci. Rev. 25, 2552-2568. DOI: 10.1016/j.quascirev.2005.07.023

Bateman, M.D., Murton, J.B. and Boulter, C., 2010. The source of De variability in periglacial sand wedges: Depositional processes versus measurement issues. Quat. Geochronol. 5, 250-256.

Bateman, M.D. and Catt, J.A., 1996. An absolute chronology for the raised beach and associated deposits at Sewerby, East Yorkshire, England. J. Quat. Sci. 11, 389-395.

Billings, W.D. and Peterson, K.M., 1980. Vegetational change and ice wedge polygons through the thaw lake cycle in Arctic Alaska. Arct. Alp. Res. 12, 413-432.

Black, R.F., 1969. Thaw depressions and thaw lakes: a review. Biuletyn Peryglacjalny 19, 131–150.

Bourke, M.C., Ewing, R.C., Finnegan, D. and McGowan, H.A., 2009. Sand dune movement in the Victoria Valley, Antarctica. Geomorphol. 109, 148-160.

Brewer, M.C., 1958. The thermal regime of an arctic lake. Transactions, American Geophysical Union 39, 278–284.

Brown, W.G., Johnston, G.H. and Brown, R.J.E., 1964. Comparison of observed and calculated ground temperatures with permafrost distribution under a northern lake. Can. Geotech. J. 1, 147–154.

Burn, C.R., 1997. Cryostratigraphy, paleogeography, and climate change during the early Holocene warm interval, western Arctic coast, Canada. Canadian Journal of Earth Sciences 34, 912–935.

Burn, C.R. 2002. Tundra lakes and permafrost, Richards Island, western Arctic coast, Canada. Can. J. Earth Sci. 39, 1281–1298.

Burn, C.R., 2005. Lake-bottom thermal regimes, western Arctic coast, Canada. Permafrost Periglacial Processes, 16, 355–367.

Carson, C.E. and Hussey, K.M., 1962. The oriented lakes of Arctic Alaska. J. Geol. 70, 417–439.

Côté, M.M. and Burn, C.R., 2002. The oriented lakes of Tuktoyaktuk Peninsula, western Arctic coast, Canada: a GIS based analysis. Permafrost Periglacial Processes 13, 61-70.

Côté MM, Wright JF, Duchesne C, Dallimore, SR., 2003. Surficial materials and ground ice information from seismic shotholes in the Mackenzie - Beaufort region, Yukon and Northwest Territories: digital compilation. Geological Survey of Canada, Open File 4490. doi: 10.4095/214840

Dallimore, S.R., Wolfe, S.A., Matthews, J.V. Jr., Vincent, J-S., 1997. Mid-Wisconsinan eolian deposits of the Kittigazuit Formation, Tuktoyaktuk Coastlands, Northwest Territories, Canada. Can. J. Earth Sci. 34, 1421–1441.

Dijkmans, J.W. and Koster, E.A., 1990. Morphological development of dunes in a subarctic environment, central Kobuk Valley, northwestern Alaska. Geogr. Ann. Ser. A Phys. Geogr. 72, 193-109.

Dyke, A.S., Andrews, J.T., Clark, P.U., England, J.H., Miller, G.H., Shaw, J., Veillette, J.J., 2002. The Laurentide and Innuitian Ice Sheets during the Last Glacial Maximum. Quat. Sci. Rev. 21, 9-31.

Dyke, A.S. and Evans D.J.A., 2003. Ice-Marginal Terrestrial Landsystems Northern Laurentide and Innuitian Ice Sheet Margins. *In:* Glacial Landsystems. Hodder Arnold, London. 532 p.

Edwards, M.E., Mock, C.J., Finney, B.P., Barber, V.A., Bartlein, P.J., 2001. Potential analogues for palaeoclimatic variations in eastern interior Alaska during the past 14,000 yr: atmospheric circulation controls of regional temperature and moisture responses. Quat. Sci. Rev. 20, 189-202

French, H.M. 2007. *The Periglacial Environment*. 3rd ed. Chichester, UK: Wiley.

French, H.M. 2017. *The Periglacial Environment*. 4th ed. Hoboken, New Jersey: Wiley Blackwell.

Galbraith, R.F., Green, P.F., 1990. Estimating the Component Ages in a Finite Mixture. Nucl. Tracks Radiat. Meas. 17, 197-206.

Grigoriev, M.N., 1993. Cryomorphogenesis in the Lena Delta: Yakutsk: Permafrost Institute Press, 176 p. (in Russian).

Harris, S.A., Brouchov, A. and Guodong, C., 2018. Geocryology. Characteristics and use of frozen ground and permafrost landforms. Boca Raton, Florida: CRC Press/Balkema.

Harry, D.G. and French, H.M., 1983. The orientation and evolution of thaw lakes, southwest Banks Island, Canadian Arctic. In Proceedings, fourth international conference on permafrost (Vol. 1, pp. 456-461). Washington, DC: National Academy of Science.

Hinkel, K.M., Frohn, R.C., Nelson, F.E., Eisner, W.R., and Beck, R.A., 2005. Morphometric and spatial analysis of thaw lakes and drained thaw lake basins in the western Arctic Coastal Plain, Alaska. Permafrost Periglacial Processes 16: 327-341. DOI: 10.1002/ppp.532

Hinkel, K.M., Sheng, Y., Lenters, J.D., Lyons, E.A., Beck, R.A., Eisner, W.R., and Wang, J., 2012. Thermokarst lakes on the Arctic Coastal Plain of Alaska: geomorphic controls on bathymetry. Permafrost Periglacial Processes 23: 218-230. DOI: 10.1002/ppp.1744

Hopkins, D.M. and Kidd, J.G., 1988. Thaw lake sediments and sedimentary environments. In: *Permafrost, Fifth International Conference, Proceedings*, vol. **1**, pp. 790–795. Tapir, Trondheim.

Jorgenson, M.T. and Shur, Y., 2007. Evolution of lake basins in northern Alaska and discussion of the thaw lake cycle. Journal of Geophysical Research 112, F2. DOI: 10.1029/2006JF000531

Jorgenson, M.T., Kanevskiy, M., Shur, Y., Moskalenko, N., Brown, D.R.N., Wickland, K., Striegl, R. and Koch, J., 2015. Role of ground ice dynamics and ecological feedbacks in recent ice wedge degradation and stabilization. J. Geophys. Res. Earth Surf. 120(11), pp.2280-2297. DOI: 10.1002/2015JF003602

Kokelj, S.V., Lantz, T.C., Kanigan, J., Smith, S.L. and Coutts, R., 2009. Origin and polycyclic behavior of tundra thaw slumps, Mackenzie Delta region, Northwest Territories, Canada. Permafrost Periglacial Processes 20: 173-184. DOI: 10.1002/ppp.642

Kokelj, S.V., Palmer, M.J., Lantz, T.C. and Burn, C.R., 2017. Ground temperatures and permafrost warming from forest to tundra, Tuktoyaktuk Coastlands and Anderson Plain. Permafrost Periglacial Processes 28, 543-551. DOI: 10.1002/ppp.1934

Lantz, T.C. and Kokelj, S.V., 2008. Increasing rates of retrogressive thaw slump activity in the Mackenzie Delta region, NWT, Canada. Geophys. Res. Lett. 35. DOI: 10.1029/2007GL032433

Mackay, J.R., 1956a. Notes on oriented lakes of the Liverpool Bay area, Northwest Territories. Revue Canadienne de Géographie 10, 169–173.

Mackay, J.R., 1956b. Deformation by glacier ice at Nicholson Peninsula, N.W.T., Canada. Arctic 9, 218-228.

Mackay, J.R., 1963. The Mackenzie Delta Area, N.W.T. Memoir. Geographical Branch, Mines and Technical Surveys, Ottawa. 202 p

Mackay, J.R., 1971. The origin of massive icy beds in permafrost, western Arctic coast, Canada. Can. J. Earth Sci. 8, 397-422.

Mackay, J.R., 1979. Pingos of the Tuktoyaktuk Peninsula Area, Northwest Territories. Géographie physique et Quaternaire 33, 3-61. DOI: 10.7202/1000322ar

Mackay J.R. and Dallimore, S.R., 1992. Massive ice of the Tuktoyaktuk area, western Arctic coast. Can. Jour. Earth Sci. 29, 1235-1249.

Michaud, Y. and Bégin C., 2000. Past environmental change recorded in dune fields. In: The Physical Environment of the Mackenzie Valley, Northwest Territories: A Base Line for the Assessment of Environmental Change, Dyke LD, Brooks GR (eds). Bulletin 547. Geological Survey of Canada, Ottawa, 79–87.

Morgenstern, A., Grosse, G. and Schirrmeister, L., 2008. Genetic, morphological and statistical characterization of lakes in the permafrost-dominated Lena Delta. In: Proceedings of the 9th International Conference on Permafrost, Fairbanks, Alaska, 29 June – 3 July. Edited by Kane, D.L. and Hinkel, K.M., Institute of Northern Engineering, University of Alaska Fairbanks, 1239-1244.

Murray, A.S. and Wintle, A.G., 2000. Luminescence dating of quartz using an improved single-aliquot regenerative-dose protocol. Radiat. Meas. 32, 57-73.

Murton, J.B., 1996. Thermokarst-lake-basin sediments, Tuktoyaktuk Coastlands, Western Arctic Canada. Sedimentology 43, 737–760.

Murton, J.B., 2005. Ground ice stratigraphy and formation at North Head, Tuktoyaktuk Coastlands, western Arctic Canada: a product of glacier-permafrost interactions. Permafrost Periglacial Processes 16, 31-50. DOI: 10.1002/ppp.513

Murton, J.B., 2009. Stratigraphy and palaeoenvironments of Richards Island and the eastern Beaufort Continental Shelf during the last glacial-interglacial cycle. Permafrost Periglacial Processes 20, 107-126. DOI: 10.1002/ppp.647

Murton, J.B., 2013. Ground ice and cryostratigraphy. In: Shroder, J.F. (Editor-in-Chief), Giardino, R. & Harbor, J. (volume eds) Treatise on Geomorphology, Volume 8, Glacial and Periglacial Geomorphology. Academic Press, San Diego, 173–201.

Murton, J.B., Frechen, M. and Maddy, D., 2007. Luminescence dating of Mid- to Late Wisconsinan aeolian sand as a constraint on the last advance of the Laurentide Ice Sheet across the Tuktoyaktuk Coastlands, western Arctic Canada. Can. J. Earth Sci. 44, 857–869.

Murton, J.B., Waller, R.I., Hart, J.K., Whiteman, C., Pollard, W.H. and Clark, I.D., 2004. Stratigraphy and glaciotectonic structures of permafrost beneath the northwest margin of the Laurentide ice sheet, Tuktoyaktuk Coastlands, Canada, J. Glaciol. 50, 399-412.

Murton, J.B., Waller, R.I., Hart, J.K., Whiteman, C., Pollard, W.H. and Clark, I.D., 2005. Basal ice facies and supraglacial melt-out till of the Laurentide Ice Sheet, Tuktoyaktuk Coastlands, western Arctic Canada, Quat. Sci. Rev. 24, 681-708.

Murton, J.B., Bateman, A.M., Waller, R., and Whiteman, C., 2015. Late Wisconsin glaciation of Hadwen and Summer islands, Tuktoyaktuk Coastlands, NWT, Canada. In Proceedings of a Symposium to Commemorate the Contributions of J. Ross Mackay (1915-2014) to Permafrost Science in Canada, 7th Canadian Permafrost Conference, Burn CR (ed), 20-23 September 2015: Quebec City, Canada, 43-48.

Murton, J.B., Bateman, M.D., Telka, A.M., Waller, R., Whiteman, C. and Kuzmina, S., 2017. Early to mid Wisconsin fluvial deposits and palaeoenvironment of the Kidluit Formation, Tuktoyaktuk Coastlands, western arctic Canada. Permafrost Periglacial Processes 28, 523-533. DOI: 10.1002/ppp.1946

Olthof, I., Fraser, R.H. and Schmitt, C., 2015. Landsat-based mapping of thermokarst lake dynamics on the Tuktoyaktuk Coastal Plain, Northwest Territories, Canada since 1985. Remote Sens. Environ. 168, 194-204. DOI: 10.1016/j.rse.2015.07.001

Pelletier, B.R. and Medioli, B.E., 2014. Environmental atlas of the Beaufort coastlands. Geological Survey of Canada, Open File 7619. 271p.

Prescott, J.R. and Hutton, J.T., 1994. Cosmic ray contributions to dose rates for luminescence and ESR dating: large depths and long-term time variations. Radiat. Meas. 23, 497-500.

Plug, L.J., Walls, C. and Scott, B.M., 2008. Tundra lake changes from 1978 to 2001 on the Tuktoyaktuk Peninsula, western Canadian Arctic. Geophys. Res. Lett. 35, L03502. DOI: 10.1029/2007GL032303, 2008

Rampton, V.R., 1987. Surficial Geology, Tuktoyaktuk Coastlands, Northwest Territories. Geological Survey of Canada, Map 1647A.

Rampton, V.R., 1988. Quaternary Geology of the Tuktoyaktuk Coastlands, Northwest Territories. Geological Survey of Canada, Memoir 413. Ottawa. 198 p.

Ritchie, J.C., 1984. Past and Present Vegetation of the Far Northwest of Canada. University of Toronto Press. 251 p.

Ruegg, G. H. J., 1983. Periglacial eolian evenly laminated sandy deposits in the late Pleistocene of NW Europe, a facies unrecorded in modern sedimentological handbooks. *In* Brookfield, M. E. & Ahlbrandt, T. S. (eds.): *Eolian Sediments and Processes. Developments in Sedimentology 38*, 455–482 Elsevier, Amsterdam.

Schirrmeister, L., Grosse, G., Schwamborn, G., Andreev, A.A., Meyer, H., Kunitsky, V.V., Kuznetsova, T.V., Dorozhkina, M.V., Pavlova, E.Y., Bobrov, A.A. and Oezen, D., 2003. Late Quaternary history of the accumulation plain north of the

Chekanovsky Ridge (Lena Delta, Russia): a multidisciplinary approach. Polar Geogr. 27, 277-319.

Schwamborn, G., Rachold, V. and Grigoriev, M.N., 2002. Late Quaternary sedimentation history of the Lena Delta. Quat. Int. 89, 119-134.

Schwan, J., 1988. The structure and genesis of Weichselian to early Holocene aeolian sand sheets in western Europe. Sediment. Geol. 55, 197–232.

Sellmann, P.V., Brown, J., Lewellen, R.I., McKim, H. and Merry, C., 1975. *The classification and geomorphic implications of thaw lakes on the Arctic Coastal Plain, Alaska.* Cold Regions Research and Engineering Laboratory, Research Report 344. Hanover, New Hampshire.

Smith, I.R., 2015. Seismic shothole drillers' lithostratigraphic logs: unearthing a wealth of regional geoscience information in northwestern Canada. GeoResJ 6, 21-19.

Stuiver, M., Reimer, P.J., and Reimer, R.W., 2019, CALIB 7.1 [WWW program] at http://calib.org, accessed 2019-5-1

Vandenberghe, J. and Woo, M.K., 2002. Modern and ancient periglacial river types. Prog. Phys. Geogr. 26, 479-506.

Wolfe, S.A. and Hugenholtz, C.H., 2009. Barchan dunes stabilized under recent climate warming on the northern Great Plains. Geology 37, 1039-1042.

Woo, M.-K., 2012. Permafrost Hydrology. Berlin Heidelberg: Springer-Verlag.

Supplementary Materials

S1 Stratigraphic sections

S1.1 Stratigraphic section notes

Table S1a. 2001 Camp 1 section notes

Section #	Lat / Long	2001 Camp 1 section notes
1	70.025227; 129.549585	Eolian sand sheet (> 3 m thick); ~3–6 m high bluff
2	70.022767; 129.540210	Eolian sand sheet (>2 m); ~2–3 m high bluff
3	70.019195; 129.524284	Sand wedge in sand sheet; ~8 m high bluff
4	70.017690; 129.515864	Sand wedge in Cape Dalhousie Sands beneath eolian sand sheet (~5 m) beneath peat beneath eolian sand (1 m); ~8.5 m high bluff
5	70.015611; 129.501452	Eolian sand sheet (>2 m) beneath sandy humic peat (20–50 cm; buried palaeosol?) beneath eolian sand sheet (3–4 m)
5a	70.015411; 129.500445	Eolian sand sheet (>4.7 m) beneath peat (0.45 m) beneath eolian sand sheet (2.5 m)
6	70.006640; 129.501344	Sand wedge in Cape Dalhousie Sands beneath eolian sand sheet (1.3 m) beneath peat (3–20 cm) beneath eolian sand sheet (40 cm); ~5 m high bluff
8	69.967009; 129.663856	Dune ridge (~5 m thick sand) above mottled silty sand at least 25 cm thick at base of sequence, apparently massive; ~18 m high bluff
9	69.969350; 129.655112	Kittigazuit Fm (>20 m) capped by gravel lag and eolian sand sheet (2.2 m); ~25 m high bluff
10	69.969772; 129.653751	Kittigazuit Fm foresets (24° to 060°); Kittigazuit Fm extends to within 1.5 m of ground surface; ~25 m high bluff
11	69.970325; 129.651977	Large cross-sets in Kittigazuit Fm (42° to 156°)
13	69.974239; 129.638487	Igneous boulder >61 cm long (erratic)
14	69.979639; 129.603758	Pebble–cobble lag above Kittigazuit Fm; striated boulder on beach; ~20 m high bluff
15	69.982647; 129.585514	Sand-poor ice and convolute lamination beneath sand sheet (puzzling section); ~15 m high bluff
16	69.983860; 129.581327	Kittigazuit Fm sand beneath sand sheet; ~15 m high bluff
17	69.987643; 129.568456	Sand with interbedded clay near base of 10–12 m high bluff
18	70.002129; 129.515056	Sand wedge in Cape Dalhousie Sands (>1.5 m) beneath eolian sand (~1 m) beneath peat (20–30 cm) beneath eolian sand sheet (~40 cm)
19	69.990860; 129.552939	Eolian sand sheet (~5 m) beneath peat (2–28 cm) beneath sand (1.5 m); plateau ~9 m asl
20	69.992115; 129.546121	Cape Dalhousie Sands (>2.1 m) beneath eolian sand sheet (4.5 m) beneath peat (30 cm) beneath eolian sand sheet (60 cm)
21	69.990338; 129.555234	Sandy foresets of former riser of shallow littoral shelf in partially drained oriented lake basin
22	69.989180; 129.560217	Former riser at southwest margin of same partially drained oriented lake basin as section 21

Table S1b. 2001 Camp 2 section notes

Section #	Lat °N / Long °W	2001 Camp 2 section notes
2.1	69.889613; 129.985853	Eolian sand sheet (> 8 m thick); ~12 m high bluff
2.2	69.892208; 129.981196	Pebbles and cobbles on bluff; slumping; ~15 m high bluff

2.3	69.896625; 129.972642	Sand beneath diamicton (Toker Point till or reworked till) beneath horizontally bedded sand (few m); numerous boulders (?till derived) on beach ~20–25 m high bluff
2.4	69.898708; 129.968229	Kittigazuit Fm (~12 m) beneath gravel (1 m; outwash)
2.5	69.904915; 129.951088	Kittigazuit Fm beneath gravel
2.6	69.905442; 129.949379	Horizontally bedded sand (6 m) (sand sheet)
2.7	69.908144; 129.936091	Sand sheet: silty fine sand (2 m) with horizontal alternating bedding and root rich (in situ, fibrous to woody) beneath fine sand (2 m). Interpreted as a wet eolian sand sheet (alternating fine sand and silty sand), as in European coversand
2.8	69.908987; 129.913841	Sand wedge (10 cm wide, >70 cm high) in horizontally stratified sand
2.9	69.914827; 129.878912	Eolian sand sheet (>5 m thick); 5 OSL ages; ~5–6 m high bluff
2.10	69.917097; 129.866298	Fluvio–eolian deposits beneath eolian sand sheet; sand veins and wedges; ~6 m high bluff
2.11	69.929963; 129.825332	Sand wedge in Kittigazuit Fm (>6 m) beneath granule–pebble layer beneath sand (40 cm) beneath peat (30 cm) beneath eolian sand sheet (60 cm); 3 OSL ages; ~7 m high bluffs
2.12	69.933409; 129.816004	Kittigazuit Fm foresets dip at 18° to 056° beneath eolian sand sheet (80 cm) beneath peat (30–40 cm) beneath eolian sand sheet (40 cm)
2.13	69.934394; 129.813406	Kidluit Fm beneath Kittigazuit Fm; 3 OSL ages; ~6 m high bluff
2.14	69.934721; 129.812478	Kittigazuit Fm beneath eolian sand sheet; multiple levels of sand veins and wedges; ~7 m high bluff

Table S1c. 2005 section notes

Section #JB	Lat / Long	2005 section notes
05-01	70.009516; 129.497268	Cape Dalhousie Sands (>1 m) beneath eolian sand sheet (4 m) beneath peat (~30 cm) beneath eolian sand sheet (50–70 cm); ~6 m high bluff
05-02	70.010231; 129.496930	Sand wedge in Cape Dalhousie Sands beneath sand sheet (~1.5 m); 6 OSL ages; ~6 m high bluff
05-03	70.010147; 129.496965	Sand wedge in Cape Dalhousie Sands beneath sand sheet (~1.5 m); 3 OSL ages; 6 m high bluff
05-04	70.011582; 129.497174	Approximate location; glacially deformed Cape Dalhousie Sands beneath eolian sand sheet (1.8 m); ~6 m high bluff
05-05	69.990267; 129.555570	Sand wedges in Cape Dalhousie Sands beneath lake sands (~0.5–2.5 m; including foresets of riser) beneath eolian sand sheet (1 m); ~6–7 m high bluff.
NE05-05	69.991537; 129.549204	Eolian sand sheet (alternating fine sand and silty fine sand) with in situ woody roots

Table S1d. 2018 Section Notes

Section #WDA	Lat / Long	2005 section notes
18-1	70.01505; 129.51544	45 cm peat layer (OUC-7406) over frozen well-sorted brown eolian sand
18-3	70.01128; 129.52246	30 cm peat layer (OUC-7407) over well-sorted grey-brown eolian sand
18-4	70.01259; 129.49863	30 cm peat layer (OUC-7408) over well-sorted grey eolian sand
18-5	70.01276; 129.49818	70 cm peat layer (OUC-7409) over grey sand eolian underlain by oxidized orange sand
18-6	70.01331; 129.49876	70 cm peat layer (OUC-7410) over grey sand eolian underlain by oxidized orange sand, with clean brown sand at 100 cm
18-7	70.01390; 129.49892	50 cm peat layer over bedded Cape Dalhousie Sands with occ. pebbles and wood (OUC-7411), and locally upturned by a sand wedge
18-8	70.01390; 129.49892	50 cm peat layer over oxidized 50 cm eolian sand over 3 m bedded Cape Dalhousie Sands with climbing ripples and containing detrital wood (OUC-7412), locally upturned by sand wedge

18-9	70.06574; 129.43286	55 cm peat layer (OUC-7413) over well-sorted grey-brown eolian sand to 2 m
18-10	70.06641; 129.44060	50 cm peat (OUC-7414) and sand layers over well-sorted grey-brown mottled eolian sand
18-11	70.06644; 129.41782	1 m grass roots and grey-brown eolian sand over 70 cm peat layer (OUC-7415) over 1 m well-sorted brown eolian sand
18-12	70.06783; 129.41803	80 cm peat layer (OUC-7416) over 30-50 cam well-sorted brown eolian sand
18-13	70.06947; 129.41801	20 cm organic cover over 2 m eolian sand with buried organic layers (OUC-7419); undulating detrital organic layer at 2 m (OUC-7418) underlain by well-sorted sands with foresets with thin detrital organic layer at 4 m (OUC-7417), underlain by mottled to grey eolian sand to 7 m depth

Detailed stratigraphic section descriptions

New sections in this study

Section 2.14 (69.9308°; –129.8225°) is ~7 m high, exposing Kittigazuit Fm sand (>2.5 m thick) beneath eolian sheet sand (3 m), a peat layer (0.2 m) and capped by root-rich eolian sand (0.5 m) (Fig. S1-1). The Kittigazuit Fm sand contains foresets with measured dips of 20° toward 244° (WSW) and 10° toward 084° (N). Multiple levels of sand veins, sand wedges, composite-wedge pseudomorphs and ice-vein pseudomorphs occur within the Kittigazuit Fm and overlying sand sheet. Two prominent erosional surfaces occur within the Kittigazuit Fm, and one along its top.

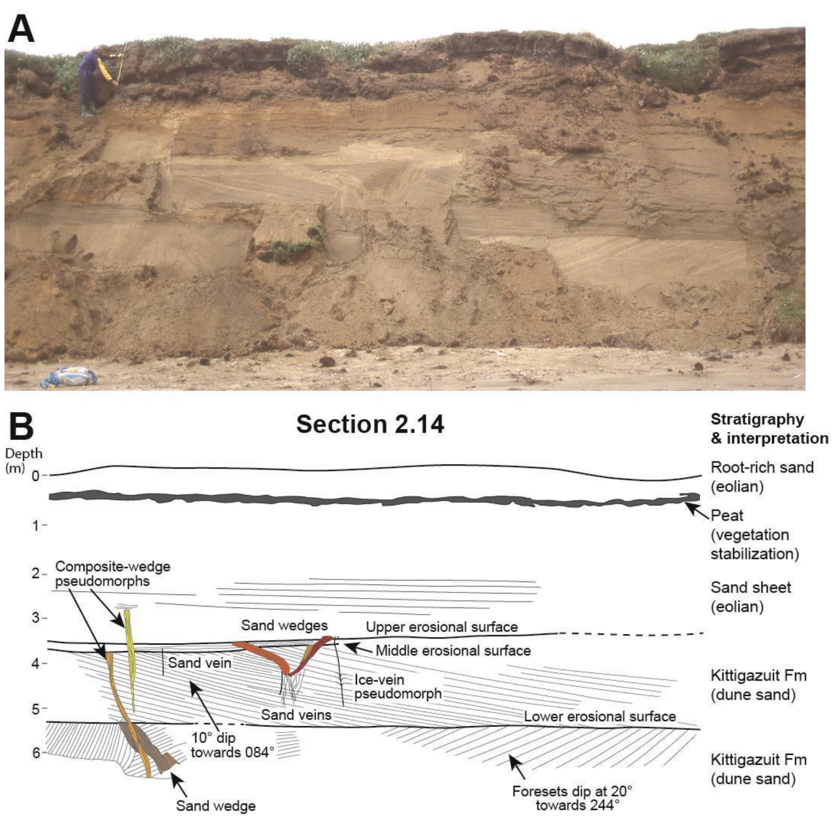

Figure S1-1. Photograph (A) and sketch (B) showing vertical section exposing Kittigazuit Fm sand truncated along the top by an erosional surface and overlain by eolian sand sheet deposits at section 2.14, illustrating composite wedges and veins within Kittigazuit Fm with a range of dip directions. OSL sample locations, dates, and lab codes are indicated, with complete results reported in Table 2.

Section 2.11 (69.9353°; –129.8101°) is 4 m high, exposing sub-horizontally laminated Kittigazuit Fm sands (>3 m) overlain by sheet sand (40 cm), sandy humic peat (0.3 m) and root-rich eolian sand (0.6 m) covered by willow shrubs and grasses (Fig. 4). The Kittigazuit Fm sand hosts a sand wedge (≤1.5 m wide) with adjacent upturned strata attributed to wedge growth. The top of the wedge and the Kittigazuit Fm is truncated by an erosional surface overlain by a granule–pebble layer.

Section 05-05 (69.9905°; –129.5544°) is 7 m high and 22 m long, exposing Cape Dalhousie Sands (CDS; >2 m) beneath a discontinuous clay–silt layer (0.3 m) or mottled sand to pebbly sand (0.5 m) and a capped by root-rich eolian sand (1 m) with a surface cover of grasses (Fig. 6). The CDS contain sand wedges with adjacent upturned strata attributed to wedge growth. The tops of the wedges are truncated by an erosional surface. The overlying mottled sand and pebbly sand are interpreted as shallow-water lake deposits because they also contain detrital peat layers and foresets that mark the front of a former riser of a shallow littoral shelf within the partially drained oriented lake-basin.

Section 05-01 (70.009631°; –129.497206°) is 6 m high, exposing Cape Dalhousie Sands (>1 m) beneath an eolian sand sheet (4 m) overlain by a sandy organic layer (0.3 m) and capped by root-rich eolian sand (0.5–0.7 m) (Fig. S1-2). Foresets in the CDS are overturned near their tops and truncated at their tops by an erosional surface that is overlain by a pebbly silty sand (2–10 cm); the overturning is attributed to glaciotectonic overriding by glacial ice. The overlying sand sheet has a lower half comprising wavy horizontal silty sand and fine sand (interpreted as a wet eolian deposit) and an upper half of poorly stratified fine sand (interpreted as a dry eolian deposit).

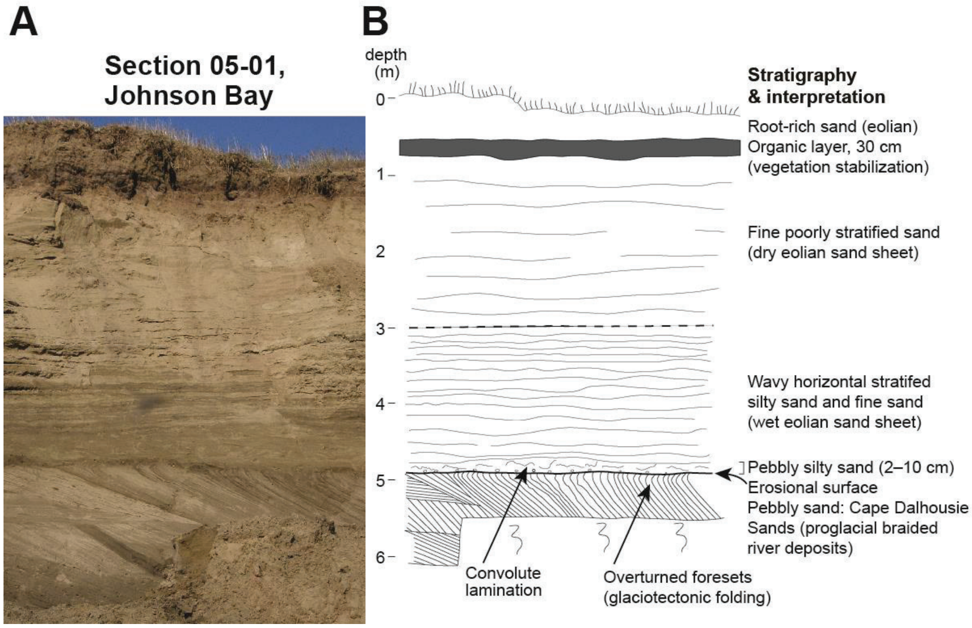

Figure S1-2. Photograph (A) and sketch (B) of vertical section showing Cape Dalhousie Sands with an upper erosional surface at section 05-01. The tops of foresets in the Cape Dalhousie Sands are overturned directly below the contact. Above the contact is a thin pebbly silty sand layer with convoluted lamination. The upper 5 m of the section comprise eolian sand sheets, deposited under wet and dry conditions, and an organic cap with a surface sheet sand cover.

Section 05-02 (70.0099°; –129.4971°) is 6 m high, exposing Cape Dalhousie Sands (>2 m) beneath an eolian sand sheet (1.5 m), a sandy organic layer (0.1–0.2 m) and capped by root-rich eolian sand (0.2 m) (Fig. 5). The CDS host a sand wedge (≤3.5 m wide) with adjacent upturned to overturned strata in the CDS attributable to wedge growth. Both the wedge and the CDS are truncated along their top by an erosional surface overlain by a pebble lag. The wedge is interpreted as antisyngenetic in origin. The overlying sand sheet consists of wavy to horizontal alternating silty sand and fine sand (interpreted as a wet eolian deposit).

Section 18-01 (70.06947°; –129.41801°) is 7 m high, exposing sandy lacustrine sediments (2 m) underlain and overlain by horizontal, flat to wavy, layers of organic detritus (Fig. 7). The upper detrital organic layer is overlain by eolian sheet sands with at least two organic horizons and capped with root-rich sands and a surface cover of grasses.

Referenced sections (Bateman and Murton, 2006; 2010):

Section 2.9 (69.9148°; –129.8775°) is 5.5 m high, exposing eolian sand-sheet deposits (>5 m) capped by a sandy organic layer (0.2 m) and root-rich eolian sand, with a surface cover of *Dryas* sp. and grass (Fig. S1-3). The sand sheet is horizontally to subhorizontally stratified, with vegetation-rich and vegetation-poor strata. Stratification includes wavy to crinkly, and pinstripe lamination (eolian wind ripples) (Bateman and Murton, 2006).

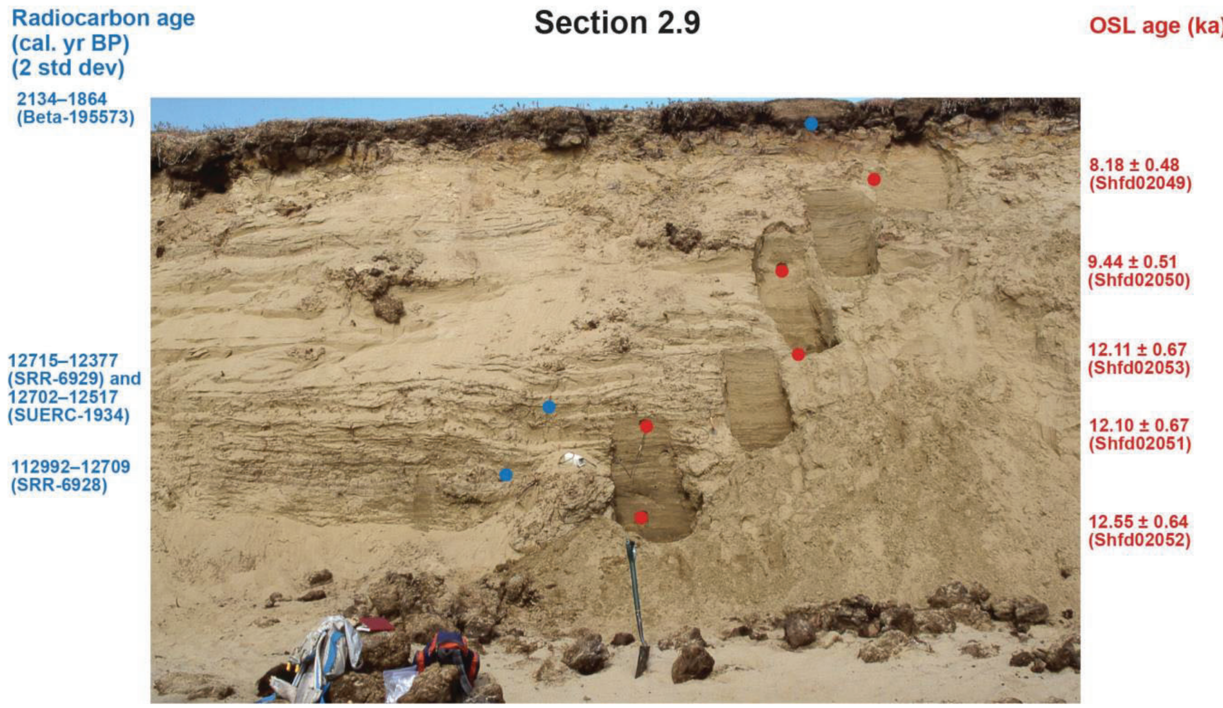

Figure S1-3. Eolian sand-sheet deposits capped by sandy organic layer at section 2.9, showing OSL and radiocarbon ages (see Tables 2 and 3 for details). Spade for scale.

Section 2.10 (69.9169°; –129.8662°) is 6 m high, exposing Kittigazuit Fm sand (>2.5 m) overlain by eolian sand-sheet deposits (2.5 m), a sandy organic layer (0.2 m) and capped by root-rich eolian sand (0.4 m) (Fig. S1-4). Foresets in the Kittigazuit Fm dip at 6° toward 077° (E) and contain sand veins and sand wedges. The tops of some sand veins and the top of the Kittigazuit Fm are truncated by an erosional contact overlain by a pebble lag (Bateman and Murton, 2006).

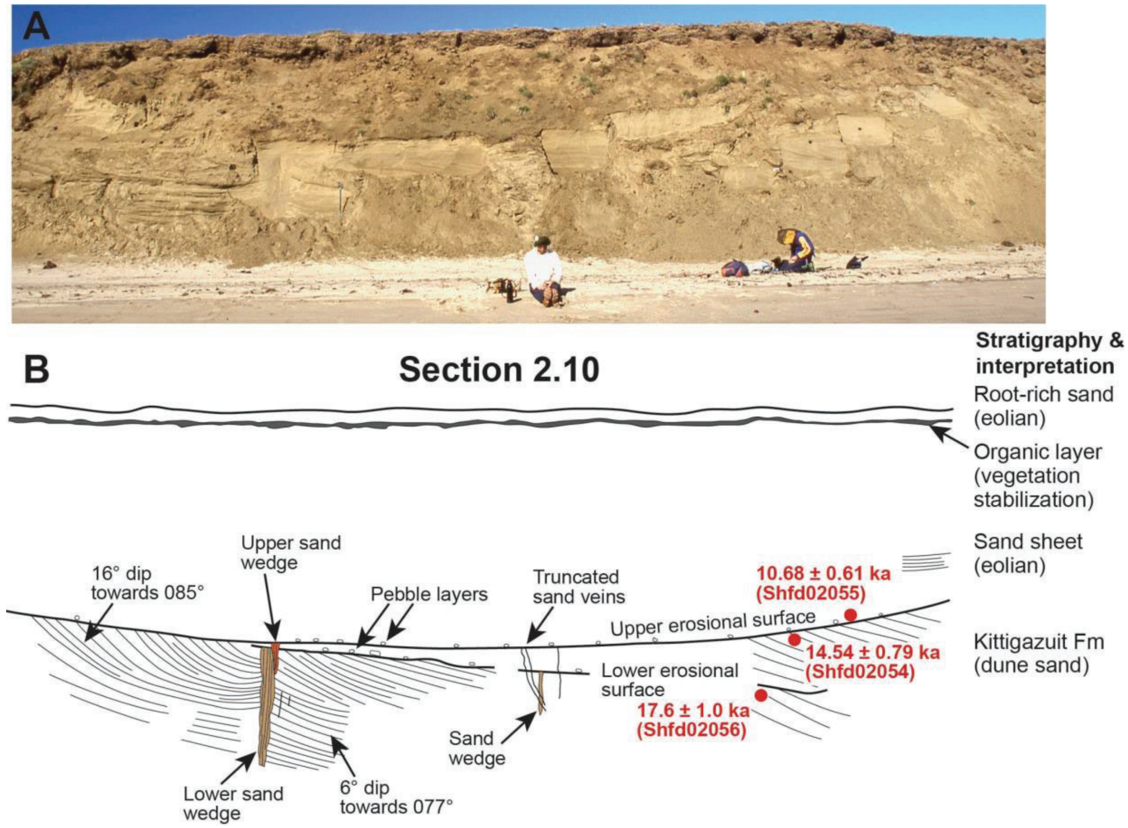

Figure S1-4. Photograph (A) and sketch (B) of vertical section through dune sand of the Kittigazuit Fm overlain by eolian sand-sheet deposits, section 2.10. OSL ages indicated (see Table 2 for details).

Section 2.12 (69.9347°; –129.8119°) is 3.5 m high, exposing Kittigazuit Fm sand (>2 m) beneath an eolian sand sheet (0.8 m), sandy peat (0.3 m) and capped by root-rich eolian sand (0.4 m). The Kittigazuit Fm contains foresets dipping at 18° toward 056° (NE) and is truncated along the top by an erosional surface overlain by a granule–pebble lag (Bateman and Murton, 2006).

Section 2.13 (69.9335°; –129.8156°) is 6 m high, exposing Kidluit Fm sand (>1 m) overlain by Kittigazuit Fm sand (3.3 m), a sandy humic organic layer (0.3 m) and root-rich eolian sand (0.4 m) (Fig. S1-5). The Kidluit Fm sand is light grey in colour, well stratified, with horizontal to inclined strata (foresets dip at 15° toward 287° (W)) and contains sand veins. The tops of the Kidluit Fm and the sand veins are truncated by an erosional surface overlain by occasional granules, small pebbles and wood fragments. Foresets in the Kittigazuit Fm dip at 38° toward 185° (S), 30° toward 174° (S) and 38° toward 188° (S) (Bateman and Murton, 2006).

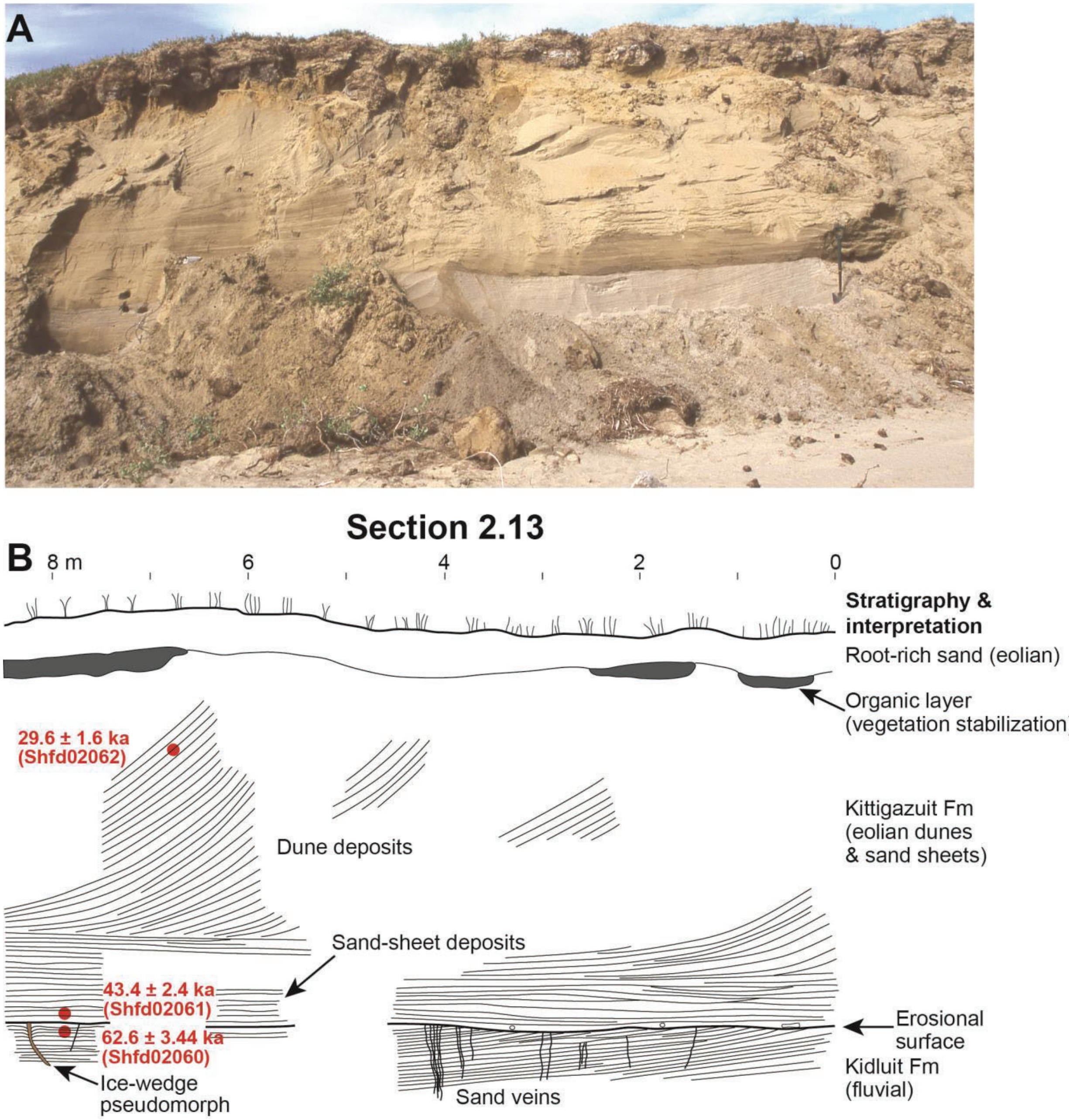

Figure S1-5. Photograph (A) and sketch (B) of vertical section through grey sand of the Kidluit Fm overlain by brown sand of the Kittigazuit Fm, section 2.13. OSL ages indicated (see Table 2 for details.

Section 05-03 (70.0099°; –129.4971°) is 6 m high, exposing Cape Dalhousie Sands (>4 m) overlain by eolian sand-sheet deposits (1.5 m), sandy humic organic layer (0.2 m) and capped by eolian root-rich sand (0.2–0.3 m) (Fig. S1-6). The CDS are pebbly in places and contain a sand wedge (≤3 m wide) with adjacent upturned strata attributed to wedge growth. The tops of the wedge and the CDS are truncated by an erosional surface. The wedge is interpreted as antisyngenetic in origin. The overlying sand sheet comprises a lower part of wavy horizontal silty sand (wet eolian) and an upper part of poorly stratified fine sand (dry eolian) (Bateman et al., 2010).

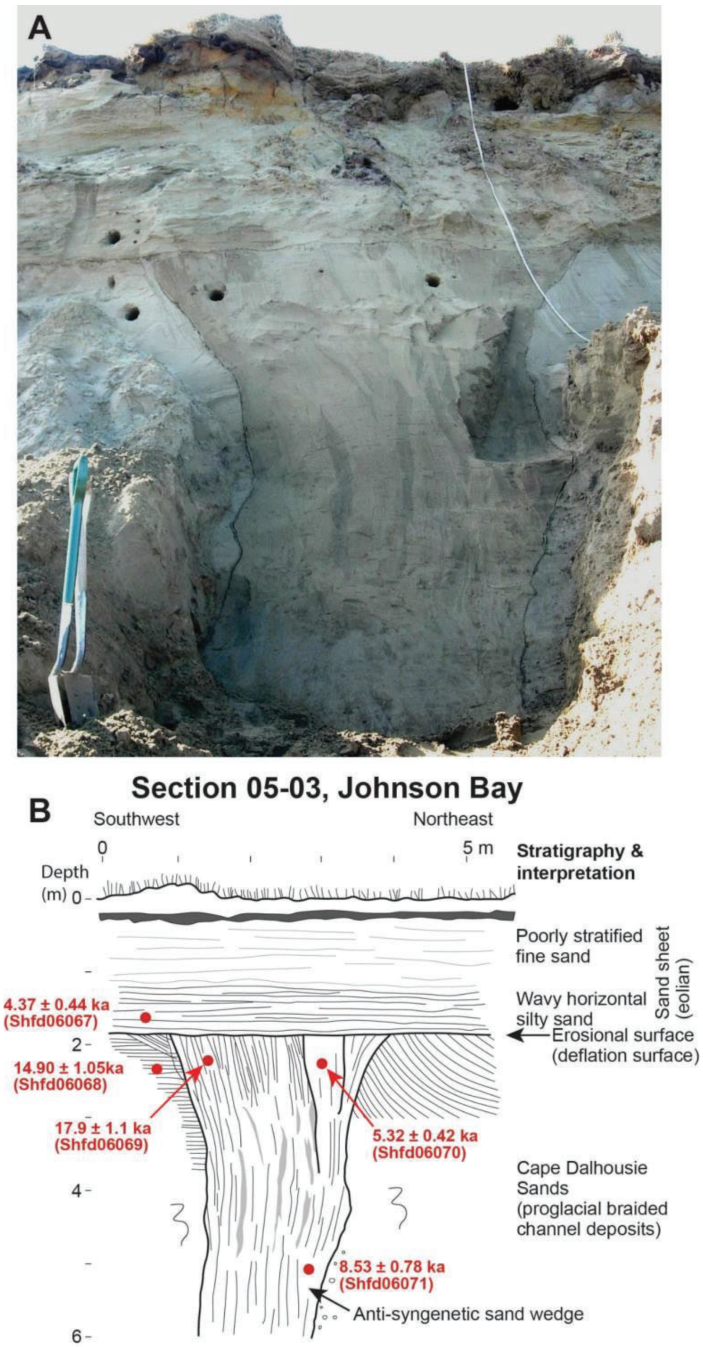

Figure S1-6. Photograph (A) and sketch (B) of vertical section through anti-syngenetic sand wedge in Cape Dalhousie Sands overlain by eolian sand sheet. OSL ages indicated (see Table 2 for details).

S2. Shothole Data

The shotholes were drilled to depths typically between 15 and 60 m during winter in the 1970s and 1980s for the purpose of seismic surveys. The surveys traversed land, inland water bodies and the marine nearshore. The stratigraphic logging tended to be rudimentary, commonly without defined depths for materials encountered, and with a range of vocabulary to describe the materials (Smith, 2015).

Shothole locations for the northeastern McKinley Bay Coastal Plain are shown in Fig. S2-1. The shotholes were sub-divided into five categories based on terrain type and water bodies: (1) *Lowland* terrain represents land areas that show no evidence of past lake inundation, and contain preserved eolian sand dunes, organic polygonal terrain and occasional wetlands. (2) *Drained lake basin* terrain is land that was previously submerged by lakes but is now terrestrially exposed due to drainage. (3) *Confined lakes* are water bodies, including oriented lakes and smaller ponds, that are not drained or breached by coastal erosion. (4) *Breached lakes* are connected to marine environments, and may be subjected to coastal erosion, surges and sediment deposition. (5) *Marine nearshore* indicates shotholes drilled offshore but close to the McKinley Bay Coastal Plain.

Water depths

Surface ice conditions and water depths across the study area are shown in Fig. S2-2 and summarized in Table S2-1 according to depth ranges and settings. Maximum depths occur in undrained lakes, with three water bodies reaching depths of 9.1 m (Fig. S2-2).

Location	**No ice**	**Ice only**	**Ice + 0.3 to 1.8 m water**	**Ice + >1.8 to 3 m water**	**Ice + >3 to 6 m water**	**Ice + > 6 m water**	**Total**
land	440 (99.8)	1 (0.2)					441
undrained lakes	96 (41.6)	78 (33.8)	39 (16.9)	9 (3.9)	2 (0.8)	7 (3.0)	231
drained lakes	43 (82.7)	9 (17.3)					52
marine & breached lakes	112 (30.0)	155 (41.6)	68 (18.2)	27 (7.2)	11 (2.9)		373
stream					1 (100)		1

Table S2-1. Near-surface ice and water-depth data for 1098 shotholes in the study area. The number of shotholes is shown and the percent (in brackets) in each depth class.

Burn (2002) investigated 12 lakes on Richards Island, ranging from 2.1 to 13.1 maximum depth from spot soundings. To assess if water depths differ between Richards Island and the oriented lakes on the McKinley Bay Coastal

Plain, we compared shothole data from these two areas. Surface ice thickness and water depths recorded from 387 shotholes on the northeastern McKinley Bay Coastal Plain (Fig. S2-2) were compared to 369 shotholes drilled over water bodies on Richards Island. Figure S2-3 shows the shot hole arrays and the total depths measured in both areas. In both areas, approximately 49% of the depths were between 1 and 2 m, which likely represents the shallow littoral shelves around perimeters of lakes. On Richards Island, depths reach a maximum of 16 m, with approximately 4% exceeding 9 m. On the NE McKinley Bay Coastal Plain water depths reach a maximum of 9 m. In addition, a secondary peak in water depths occurs between 3 and 4 m, suggesting that many of these lakes may reach maximum depths that are shallower than on Richards Island.

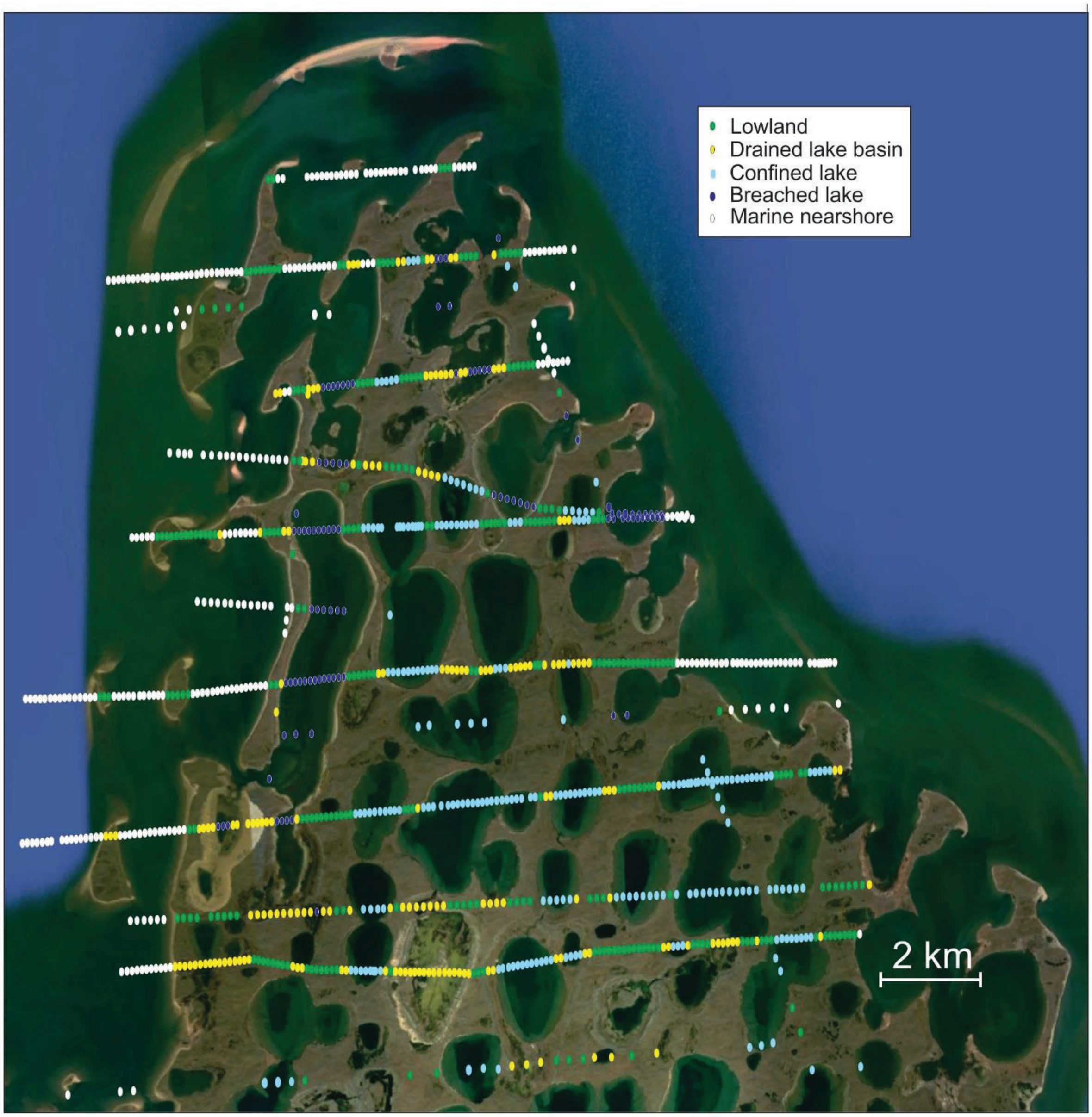

Figure S2-1. Shothole locations on the northeastern McKinley Bay Coastal Plain, classified according to terrain type and water bodies. Image source Google Earth.

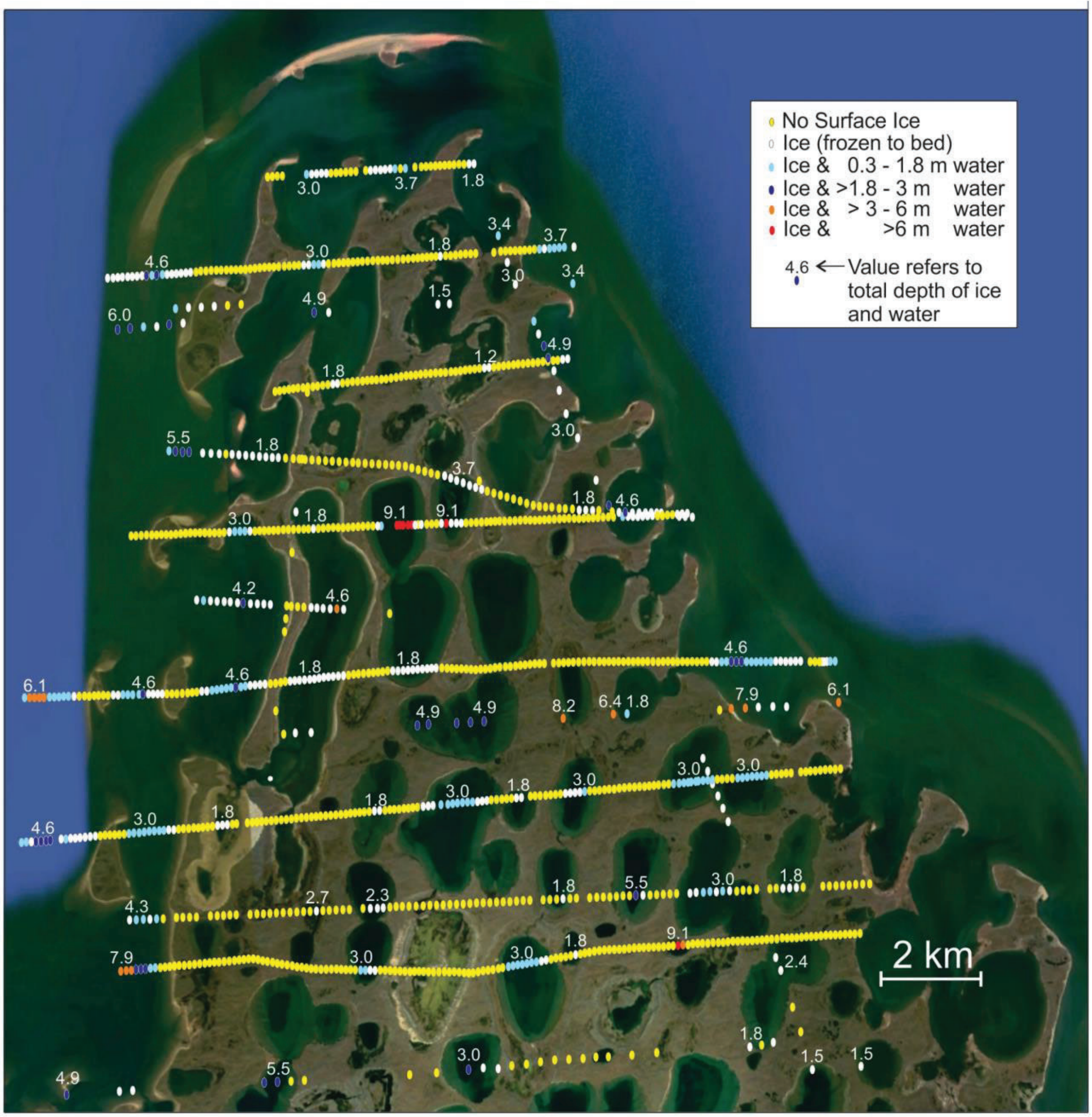

Figure S2-2. Surface ice occurrence and water depths recorded in shotholes on the northeastern McKinley Bay Coastal Plain. Image source Google Earth.

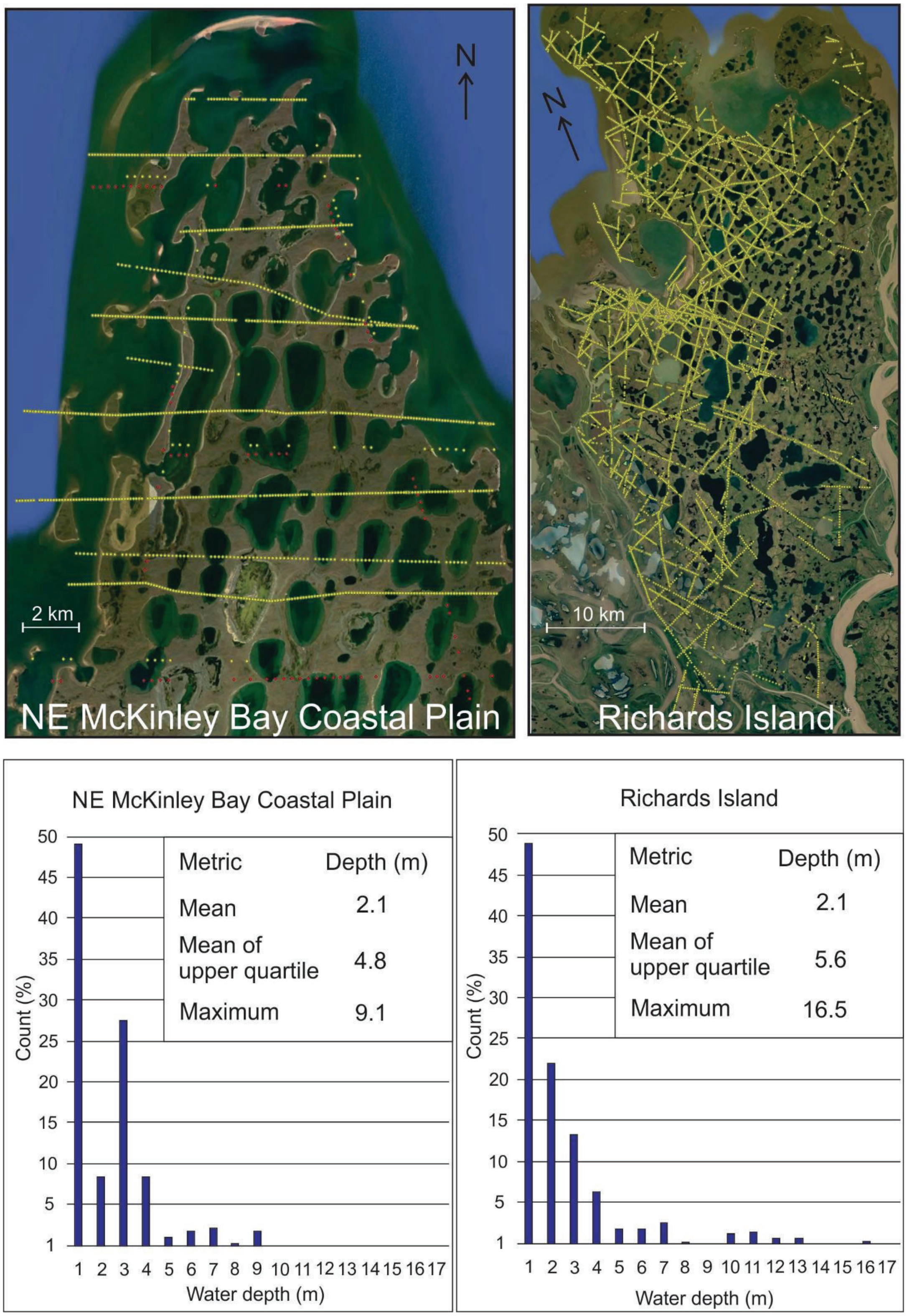

Figure S2-3. Water depths recorded in shotholes on Richards Island and the northeastern McKinley Bay Coastal Plain. Image sources Google Earth.

Sediments

Sediments recorded in shotholes are distinguished as sand (aka 'sandstone'), silt and clay (aka 'shale') (Fig. S2-4). Note that the figure illustrates the occurrence of materials, but not their relative depths, as many shotholes do not record the depths of the stratigraphic sequence. Sand was the most common sediment recorded in the shotholes, but silt was also predominant in a few seismic transects (Fig. S2-4). Examination of the data suggests, in fact, that these two sediments are likely interchangeable due to logger bias in interpreting the sediments, with silt being synonymous with sand. For analysis we, therefore, combined sand and silt into one class and clay into another to compare their relative occurrence.

Ground ice

Ground ice was noted in only three locations (Fig. S2-4), and where these occurred we examined the stratigraphy in more detail, noting the actual ground ice and sediment depths, where recorded (Fig. S2-4 insets A, B and C). The insets show the stratigraphy and depths as recorded in the shothole logs. In Figure S2-4A, the shotholes traversed land and a small, shallow drained basin. Sand and silt were recorded in all logs with clay beneath it in the basin. Ground ice was recorded in two holes to a depth of 20 m in a mixed stratigraphy of sand, silt and clay, and was underlain by a unit of clay. At another location (Fig. S2-4B) shotholes traversed land, with ice recorded at 12 to 30 m in two holes in association with sand and silt. At a third location (Fig. S2-4C) ice was encountered in four holes, typically between 4.5 and 7.5 m depth within silt and sand. These observations confirm the presence of ground ice on the peninsula. Although the origin of the ground ice is unknown, the continuity and depths of ice suggest it is probably not near-surface wedge ice.

Figure S2-4. Sediments and ground ice recorded in shotholes on the northeastern McKinley Bay Coastal Plain. Note that shotholes in the main figure record only observations of material type, and not actual depths or stratigraphic order. Insets A, B, and C indicate material types and depths recorded in shotholes. Image source Google Earth.

S3. Geomorphic Mapping

Eolian deposits

Surficial sand dune ridges mapped across the northeastern McKinley Bay Coastal Plain are shown in Fig. S3-1. Lakeshore dune ridges (n=161; outlined in blue) fringe lake basins and represent eolian erosion and redeposition from a proximal source. They extend downwind from the source areas for distances of up to only 200 m. Other ridges (outlined in white) are more numerous and are located across the lowland terrain in areas that have not been occupied by lake basins. These dune ridges represent stabilized parabolic dune remnants. Unlike the source-bordering lakeshore dunes, the stabilized parabolic dunes do not appear to have clear upwind source area. Rather, these dunes tend to be several hundred metres long (up to 800 m) and either disappear upwind or form enclosed arcuate dune ridges that form large enclosed ellipses. We mapped 3265 lowland dune ridges, representing more than 2500 individual dunes. These are concentrated in the northeastern end of the McKinley Bay Coastal Plain and are generally absent from that part of the study area south of McKinley Bay.

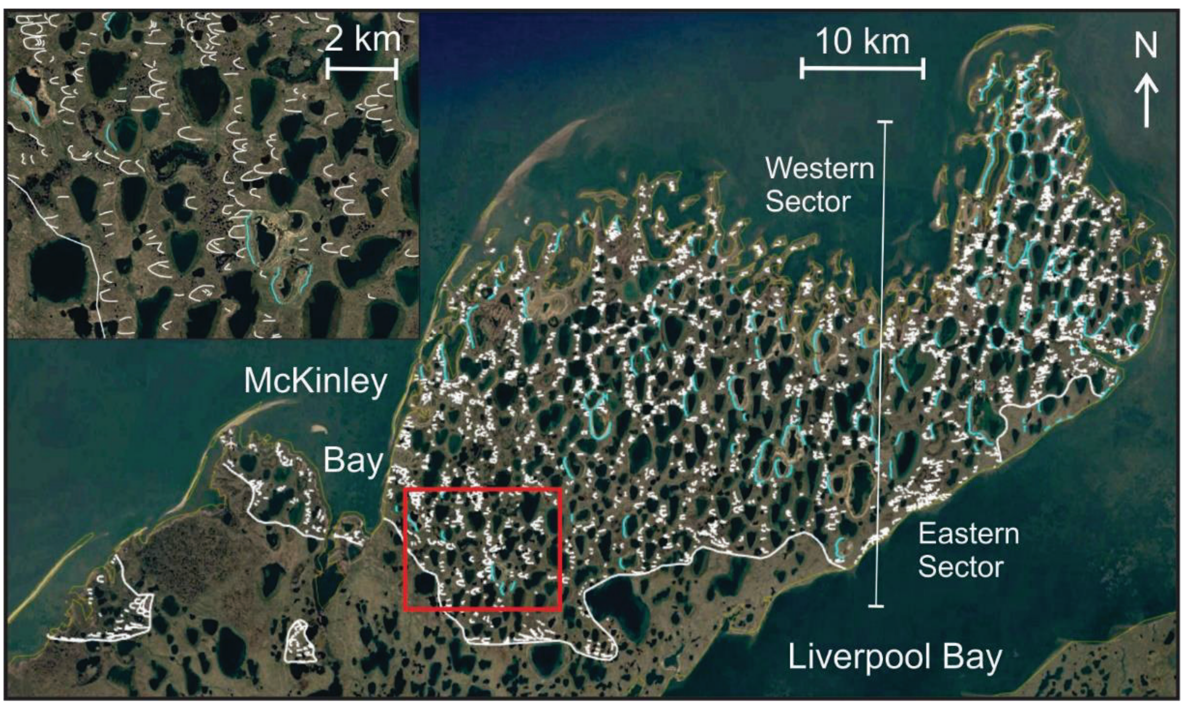

Figure S3-1. Eolian dune ridges on the northeastern McKinley Bay Coastal Plain. Active and stabilized lakeshore (and marineshore) dunes are outlined in blue. Stabilized lowland dunes ridges, representing parabolic dunes and related ridge features, are outlined in white. Solid white lines depict the limit of lowland dunes in the study area. Red box depicts limit of inset area. Image source Google Earth.

Several close associations between the lowland dune ridges and other lake basin and lowland features are notable and indicative of co-evolution (Fig.

S3-2). First, open-ended parabolic dunes occupying lowland terrain commonly occur in abundance downwind of the oriented-lake basins (Fig. S3-1 inset). This suggests that sediment, deflated from these upwind basin areas, was translocated downwind across the lowland terrain. These eolian processes occurred at a time when the lake basin areas were smaller than at present, as many stabilized dune ridges are truncated by the expanded lake shorelines. Second, small, shallow lake basins also have parabolic dunes on the downwind side, suggesting that eolian deflation may be responsible for the formation of small basins, which today are occupied by small lakes. Third, ice-wedge polygonal terrain occupies much of the lowland areas where eolian dune deposits are absent. This low-lying terrain likely represents areas of eolian erosion or non-deposition, and has favoured wetland development.

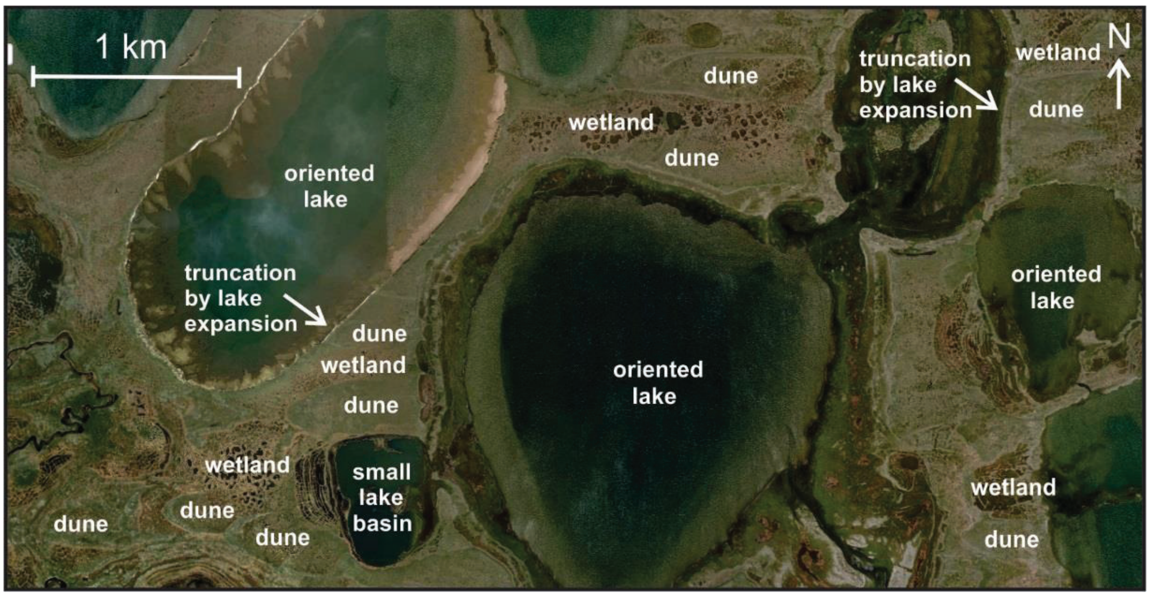

Figure S3-2. Relationships between eolian dunes and other terrain features in the study area. Stabilized dunes located downwind of oriented lakes and small lake basins. Stabilized parabolic dunes truncated by expansion of lake shorelines. Wetland polygonal terrain occupying low-lying areas between eolian dune deposits. Image source Google Earth.

We examined parabolic dune orientations in two sectors (Fig. S3-1) to determine the formative net sediment transport directions and to compare these against any differences in relation to lake orientations. Mean azimuth is approximately 89.2° in the western sector, based on 1638 observations, and 87.6° in the eastern sector, based on 1623 observations. This is equivalent to a net sediment transport direction toward 269.2° in the western sector and 267.6° in the eastern sector. Although this difference is small (Fig. S3-3), it is statistically significant under a two-tail t-test at 0.01 level of significance.

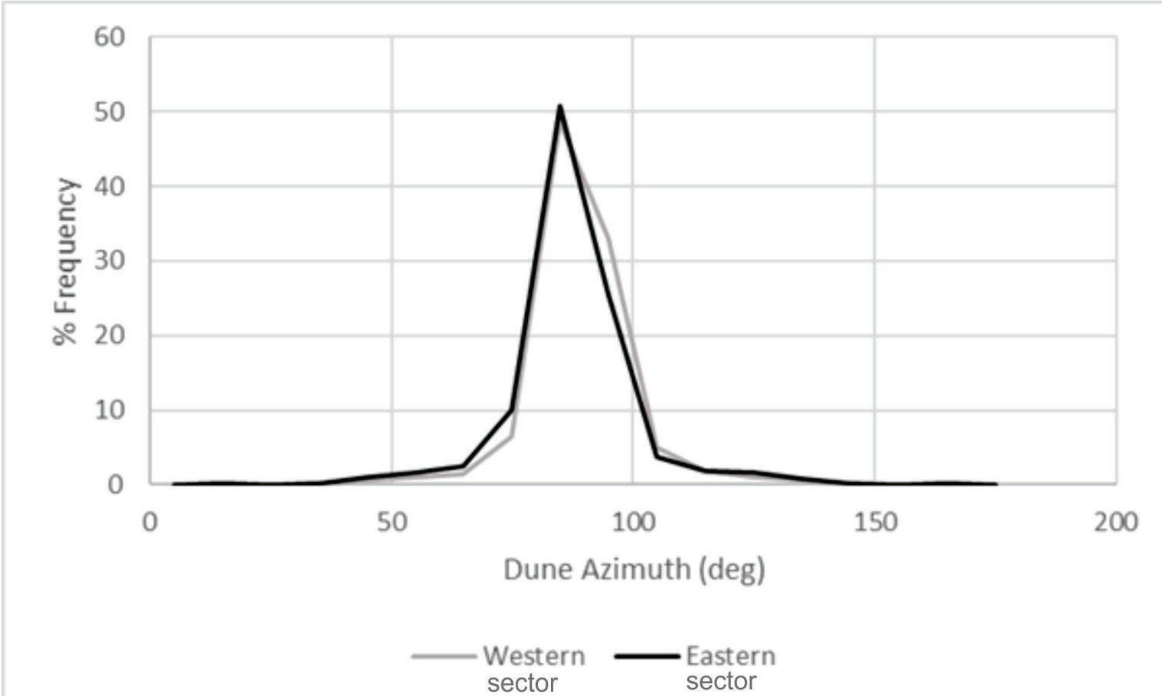

Figure S3-3. Frequency distribution of stabilized parabolic dune orientations (azimuths) for western and eastern sectors of the McKinley Bay Coastal Plain.

Lake basins and drainages

Oriented lake basins and drainages (streams and channels) mapped on the northeastern McKinley Bay Coastal Plain are shown in Fig. S3-4. We mapped 907 oriented lake basins and 240 drainages in the study area. Oriented lakes are most concentrated in the northeastern McKinley Bay Coastal Plain and are less abundant south of McKinley Bay. Conversely, streams and drainage channels are shorter where lakes are concentrated and longer where they are less abundant.

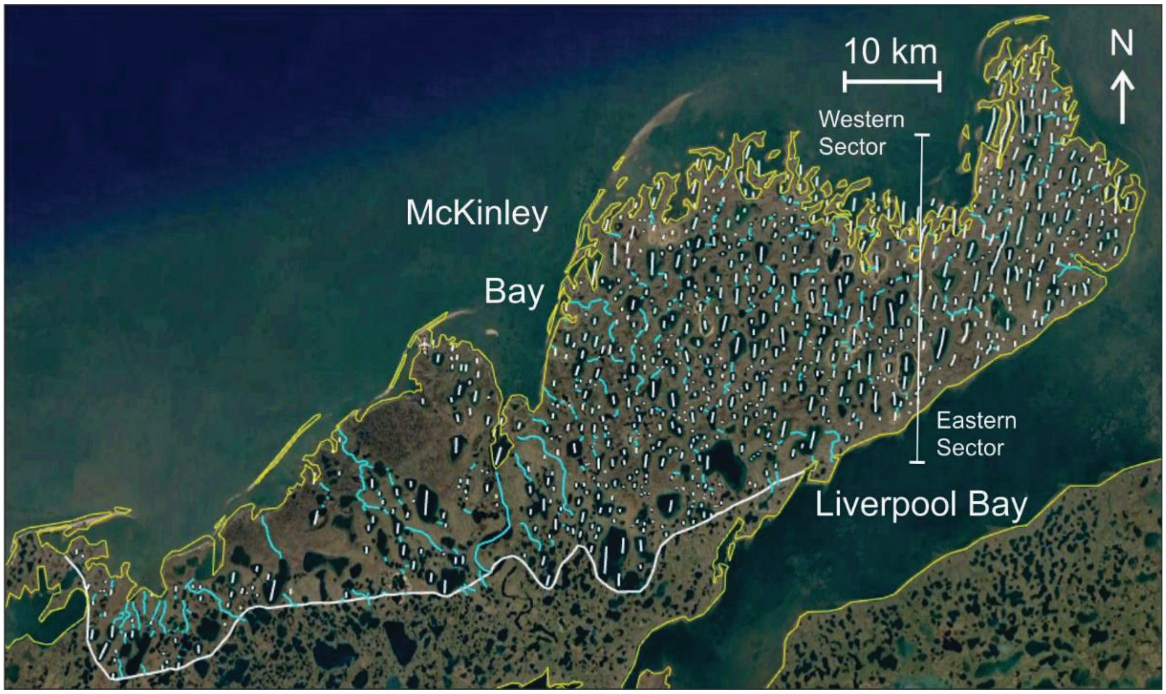

Figure S3-4. Oriented lake basins and drainages on the McKinley Bay Coastal Plain. Orientations of lake basins are shown by white lines, with solid white line marking the southern limit of oriented lakes depicted by Mackay (1963). Blue lines depict drainages connecting lakes.

Inspection of the lake orientations in the study area indicates differences in azimuths across the McKinley Bay Coastal Plain, with a distinctive eastern and western sector (Fig. S3-4). Mackay (1963) reported an eastward, clockwise, shift in axial trend, based on analysis of 88 lakes in the area, which vary from 2° (i.e. N 2° E) in the west (27 lakes), to 5° in the centre (30 lakes) and 11° in the east (31 lakes). We examined lake azimuths in the two sectors in Fig. S3-4 to compare them against those reported by Mackay (1963). Fig. S3-5 shows the frequency distributions of lake azimuths across both sectors. The mean azimuth is approximately 201° in the eastern sector, based on 220 observations, and 185.5° in the western sectors, based on 687 observations. This is equivalent to an axial trend of 21° in the eastern sector and 5.5° in the western sector. The difference of 15.5° (Fig. S3-5) is statistically significant under a two-tail t-test at 0.01 level of significance.

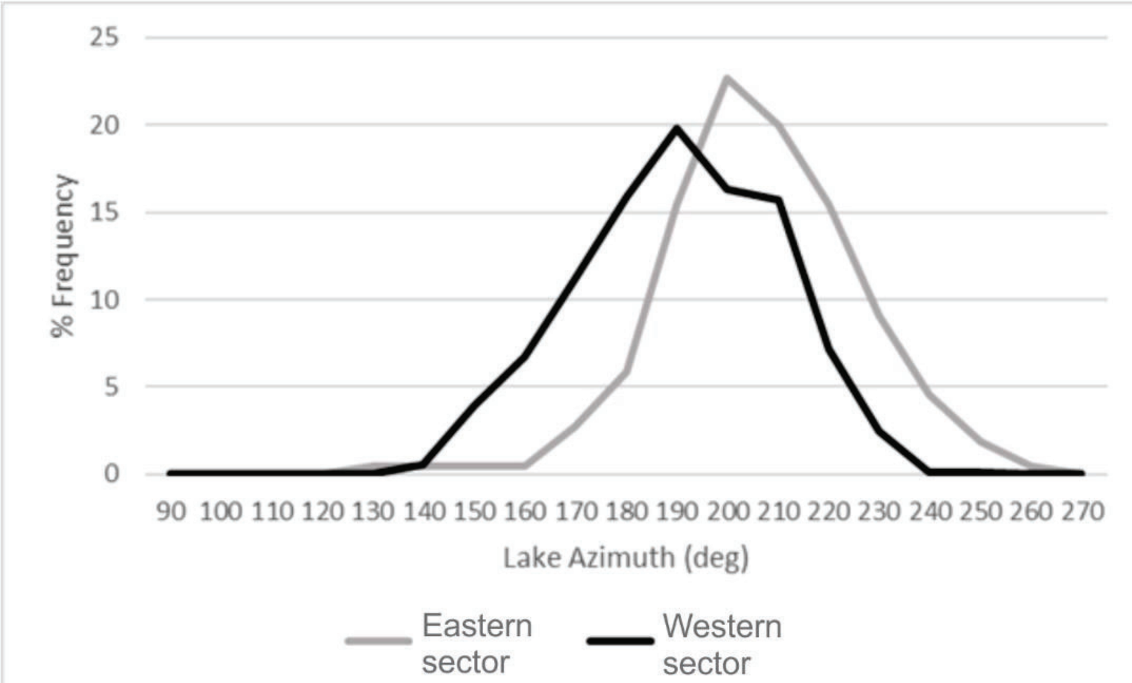

Figure S3-5. Lake orientations (azimuths) for eastern and western sectors of the McKinley Bay Coastal Plain.

Combined mapping

The combined extent of eolian dune ridges, oriented lakes and drainages in the study area is shown in Fig. S3-6. The solid white lines depict the limit of eolian dune ridges mapped in this study and the southern limit of oriented lakes as mapped by Mackay (1963). Several observations are evident. First, oriented lake basins are abundant where they occur in association with eolian dune ridges. Second, east of McKinley Bay and in a few other isolated areas eolian dunes and oriented lakes are co-located and in these areas drainage channels between lakes are short and less distinctive. Third, where eolian dunes are absent, oriented lakes are less abundant and drainage channels are long. These latter areas also closely correspond to terrain mapped by Rampton (1987) as underlain by glaciofluvial deposits.

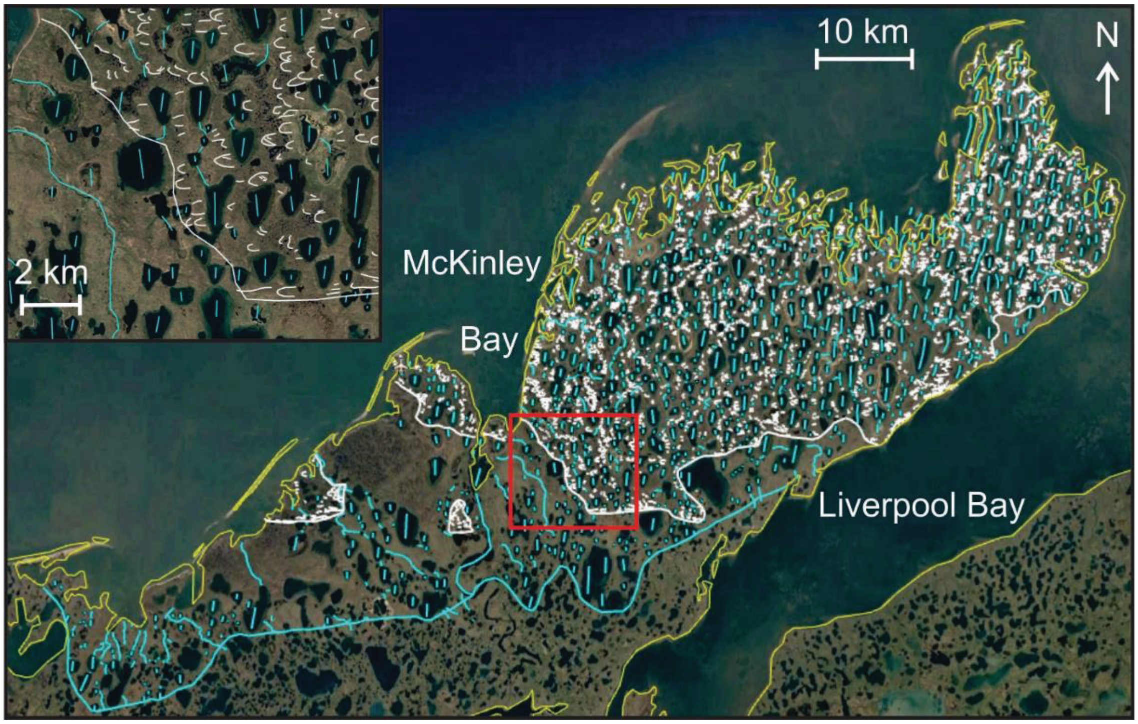

Figure S3-6. Eolian dune ridges, oriented-lake basins and drainages on the northeastern McKinley Bay Coastal Plain. White lines depict lines dune ridges and limit of eolian dune ridges as mapped in this study and blue lines depict lake orientations and drainages, and the southern limit of oriented lakes as mapped by (Mackay, 1963). Note, although some isolated oriented lakes occur south of this limit they are not mapped. Image source Google Earth.

S4. Arctic DEM results

Glacially-modified channel

Mackay (1963, figure 4) described the large abandoned river channel linking the Eskimo Lakes with McKinley Bay. This area is reproduced in Fig. 4-1 from the Arctic DEM. Mackay (1963) suggested that the southern half of the channel shows glacial modifications, whereas the northern half is seemingly unmodified. The transition in channel width occurs across the glaciofluvial outwash plain north of the Toker Point limit. This channel, which disappears to the south at the Toker Point Stade limit, is defined by a narrow (ca. 500 m wide) glacially-modified winding channel within hilly terrain, which transitions northward at about 69.73° N into a broad (≤7 km wide) channel with multiple terraces across flat terrain. This transition is only about 5 km north of the Toker Point limit as mapped by Rampton (1987).

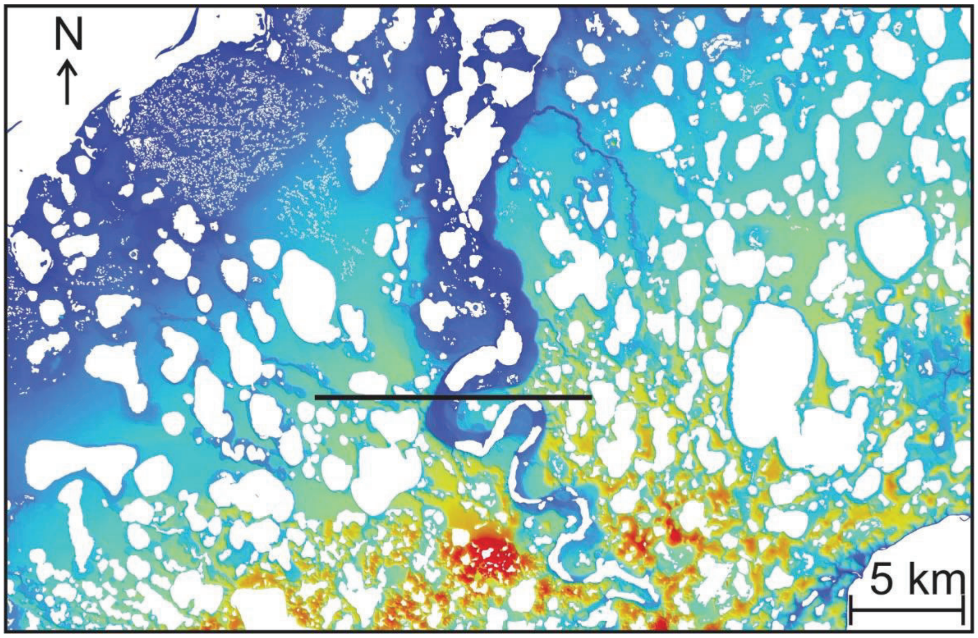

Figure S4-1. Abandoned river channel between the Eskimo Lakes and McKinley Bay. Black line denotes transition from a glacially confined to an unconfined channel.

References

Bateman, M.D. and Murton, J.B., 2006. The chronostratigraphy of Late Pleistocene glacial and periglacial aeolian activity in the Tuktoyaktuk Coastlands, NWT, Canada. Quat. Sci. Rev. 25, 2552-2568. DOI: 10.1016/j.quascirev.2005.07.023

Bateman, M.D., Murton, J.B. and Boulter, C., 2010. The source of De variability in periglacial sand wedges: Depositional processes versus measurement issues. Quat. Geochron. 5, 250-256.

Mackay, J.R., 1963. The Mackenzie Delta Area, N.W.T. Memoir 8. Geographical Branch, Mines and Technical Surveys, Ottawa. 202 p.

Rampton, V.R., 1987. Surficial Geology, Tuktoyaktuk Coastlands, Northwest Territories. Geological Survey of Canada, Map 1647A.

Smith, I.R., 2015. Seismic shothole drillers' lithostratigraphic logs: unearthing a wealth of regional geoscience information in northwestern Canada. GeoResJ 6, 21-19.

Table 1. Summary of primary units and secondary feature observations following the generalized stratigraphic framework of Rampton (1988) with additional Holocene units observed in the McKinley Bay Coastal Plain.

Stratigraphic unit and thickness (m)	**Primary unit: sedimentology, stratigraphy and occurrence**	**Primary unit: interpretation and provisional age**	**Secondary features: structures and contacts**	**Secondary features: interpretation and provisional age**
Holocene units				
9. Near-surface sand (0.3–2.5)	Well-sorted fine-medium sand, commonly root-rich.	Localized eolian sand-sheet deposits from marine and lakeshore sources. Localized eolian erosion: ca. **2** ka		
8. Lower sand unit B (0.5–2.5)	Thick mottled sand to pebbly sand with detrital organic layers and discontinuous clay-silt layer. Foresets to 2.5 m. Lowland terrain in drained-lake basins. Underlain by CDS with erosional surface at contact.	Shallow lake sediments. Foresets marking front of shallow littoral shelf (i.e. riser) of an oriented lake basin. Lake expansion: **>6.6–0.9** ka	Underlying CDS and sand wedges truncated by erosional surface.	Lake expansion: **<8.4–0.9** ka
7. Organic material (0.3–1.0)	Humic organic layer. Northern part of McKinley Bay Coastal Plain in lowland terrain. Underlain by lower sand unit A.	Vegetation stabilization and accumulation. Organic cover initiation: **10.7–8.9** ka	Organic layers interstratified with eolian sands and mantling small eolian dunes	Vegetated dunes. Stabilization: **9.6–4.6** ka
6. Lower sand unit A (0.4–6.0)	Wavy to horizontally bedded; crinkly lamination and vegetation-free layers of pinstripe lamination. Thicker vegetation-rich layers. Underlain by Kittigazuit Fm or CDS and sand wedges.	Sand-sheet accumulation and migrating dunes. Cold-dry conditions: **12.8–10.7** ka; warmer-moist conditions with vegetation: **10.7–1.9** ka	Erosional contact defined by a granule–pebble layer with wind-polished pebbles at the base of the sand sheet.	Eolian erosion. **>8.4–5.3** ka.
Glacial units				
5. Gravel and Boulders (≤ 1)	Rounded gravel and cobble deposits. Southern boundary of McKinley Bay Coastal Plain in upland terrain. Underlain by diamicton or Kittigazuit Fm.	Glacial outwash (Turnabout Member)		
4. Diamicton (1–2)	Grey silty clay with pebbles and cobbles. Southern boundary of McKinley Bay Coastal Plain area in upland terrain. Underlain by Kittigazuit Fm.	Toker Point Till	Underlying CDS units deformed	Glaciotectonic deformation.
Preglacial and proglacial units				
3. Cape Dalhousie Sands (CDS) (> 4.0)	Light-medium grey, poorly sorted to well-sorted pebbly sand and sandy gravel; granules; rounded to angular cobbles (with granites) to 140 mm and occ. boulders 0.36 m; clast long axes parallel to strata. Planar parallel laminations, well-stratified, horizontal to steeply-dipping layers 2 mm**–**0.25 m; undulating parallel to sub-parallel fine sand, foresets and abundant granules. Wood fragments, coal and internally curved erosion surfaces. In lowland terrain where Kittigazuit Fm is absent.	Proglacial braided channel network developed on preglacial braidplain, transporting seasonal glacial meltwater. Deposition: >**18.6–14.3** ka	CDS and sand wedges truncated by erosional surface, overlain by a pebble lag contact with wind-polished pebble and eolian sand sheet (Lower sand unit A) Sand wedges ≤ 3 m wide, with strata steeply upturned adjacent to wedges. (sections JB05-02,03,05) CDS foresets overturned and overlain by a pebbly silt with evidence of a sheared horizon (sect. JB05-01)	Eolian erosion. **>8.4–5.3** ka. Antisyngenetic wedges. Thermal contraction and infilling: **17.6–5.3** ka. Glaciotectonic deformation.
2. Kittigazuit Fm (3–20)	Sub-horizontal stratification to steeply dipping sandy foresets with a range of dip directions. Southern part of McKinley Bay Coastal Plain.	Proglacial sand dunes on abandoned preglacial braidplain. Deposition: **43.4–14.5** ka	Sand veins and wedges ≤ 1.5 m wide (sect. 2.11, 2.14); strata upturned adjacent to wedges. Kittigazuit Fm and wedges truncated by erosional contact below an eolian sand sheet	Antisyngenetic sand wedges ca. **18.8–16.1** ka Erosion: **12.8–10.7** ka
1. Kidluit Fm	Light grey, wavy, horizontally laminated sand. Rarely exposed.	Preglacial alluvial braidplain of paleo-river. Deposition: 63.2 ka (**72–27** ka)	Small sand veins and ice-wedge pseudomorphs	